

Aus der Klinik und Poliklinik für Neurologie
der Universität Würzburg
Direktor: Professor Dr. med. Volkmann

**High-resolution ultrasound for the identification of pathological
patterns in patients with polyneuropathies and amyotrophic
lateral sclerosis**

**Hochauflösender Ultraschall zur Identifizierung von
pathologischen Mustern bei Patienten mit Polyneuropathien
und amyotropher Lateralsklerose**

Inaugural - Dissertation
zur Erlangung der Doktorwürde der
Medizinischen Fakultät
der
Julius-Maximilians-Universität Würzburg
vorgelegt von
Philipp Köberle
aus Crailsheim

Würzburg, Dezember 2020

Introduction

Referentin: Univ.-Prof. Dr. Nurcan Üçeyler

Korreferent bzw. Korreferentin:

Dekan: Univ.-Prof. Dr. Matthias Frosch

Tag der mündlichen Prüfung:

Der Promovend ist Arzt.

Table of Contents

Aus der Klinik und Poliklinik für Neurologie.....	1
1 Introduction.....	1
1.1 Neuropathy of the peripheral nervous system	1
1.1.1 Definition of neuropathy.....	1
1.1.2 Diagnostic approach to neuropathies	1
1.2 Amyotrophic lateral sclerosis (ALS)	2
1.2.1 Definition and clinical presentation of ALS.....	2
1.2.2 Diagnostic approach to ALS	3
1.3 High-resolution nerve ultrasound (HRUS)	3
1.3.1 Technical requirements and sonographic imaging with HRUS.....	3
1.3.2 Echotexture of nerves when assessed with HRUS	3
1.4 HRUS - nerve alterations in neuropathies and ALS.....	5
1.4.1 HRUS findings in patients with demyelinating neuropathy	5
1.4.2 HRUS findings in patients with axonal neuropathies.....	6
1.4.3 HRUS findings in patients with ALS	7
1.5 Hypothesis and research questions	7
2 Patients, Material, and Methods.....	8
2.1 Recruitment of patients and healthy controls.....	8
2.1.1 Healthy control cohort.....	8
2.1.2 Patient cohort	8
2.2 Neuropathies were diagnosed applying the following criteria:	8
2.2.1 Axonal neuropathies.....	8
2.2.2 Demyelinating neuropathies	10
2.2.3 Hereditary neuropathy	11
2.2.4 Neuropathy, of unknown etiology	12
2.2.5 ALS	12
2.3 Definition of inflammatory and non-inflammatory neuropathy	12
2.4 Neuropathy scores.....	12
□ Modified Toronto Clinical Neuropathy Score (mTCNS)	12
□ Modified Medical Research Council-Score (mMRC)	13
□ Overall Disability Sum Score (ODSS)	13

Introduction

2.5	Questionnaires.....	13
□	Neuropathic Pain Symptom Inventory (NPSI)	13
□	Graded Chronic Pain Scale (GCPS)	14
□	“Allgemeine Depressionsskala (ADS)”	14
2.6	Laboratory tests	14
2.7	Nerve conduction studies (NCS)	15
2.8	Nerve biopsy.....	15
2.9	HRUS	15
2.9.1	Ultrasound device and examiner	15
2.9.2	Ultrasound technique.....	16
2.9.3	Measuring technique and parameters determined.....	16
2.9.4	Study protocol	17
2.9.5	Image transfer and storage.....	18
2.9.6	Data extraction	18
2.10	Statistical analysis.....	18
3	Results.....	19
3.1	Characterization of the healthy control cohort and normative values.	19
3.2	Characterization of the patient cohort.....	23
3.2.1	Neuropathy scores and questionnaires	24
3.3	Results of HRUS measurement	25
3.3.1	Comparison between patients with neuropathy and healthy controls	
	25	
3.3.2	Comparison between patients with axonal and demyelinating	
	neuropathies	28
3.3.3	Comparison between patients with inflammatory and non-	
	inflammatory neuropathies	31
3.3.4	Comparison between patients with painful and painless	
	neuropathies	34
3.3.5	Characterization of the patient subgroup with NSVN	37
3.3.6	Characterization of the subgroup with CIDP	43
3.3.7	Characterization of the subgroup with MADSAM	49
3.3.8	Characterization of the subgroup with MMN	55

Introduction

3.3.9 Characterization of the subgroup with ALS.....	61
3.3.10 Analysis of the results of nerve biopsy in relation to HRUS data	67
3.3.11 Results of NCS in synopsis with HRUS measurements at sites of electric conduction block (CB)	74
4 Discussion.....	75
4.1 Study findings	75
4.1.1 Healthy control cohort and normative values	76
4.1.2 Patients with neuropathy	76
4.1.3 Patients with ALS	79
4.2 Limitations of this study.....	80
4.3 Strengths of this study	80
4.4 Perspective	81
5 Summary	82
5 Zusammenfassung	83
6 Bibliography.....	84
Appendix	91
I List of Abbreviation	91
II List of Figures	94
III List of Tables.....	98
IV Danksagung	99
V Curriculum vitae.....	100
V Lebenslauf.....	101
VI Publication & Congress participation	102

1 Introduction

1.1 Neuropathy of the peripheral nervous system

1.1.1 Definition of neuropathy

Neuropathies are a common neurological condition. The overall prevalence is estimated 2.400 cases per 100.000 in the general population excluding traumatic nerve injuries with an increase to 8.000 per 100.000 at > 55 years of age (England and Asbury 2004). Neuropathies can be classified as mononeuropathies, multiplex mononeuropathies or polyneuropathies. Mononeuropathy implies a (focal) lesion of one single peripheral nerve. Multiplex mononeuropathy describes a random, multifocal pattern with multiple separated nerves involved either simultaneously or serially (England and Asbury 2004). In the following, the term “neuropathy” includes mononeuropathy, mononeuritis multiplex, and polyneuropathy. The heterogeneous group of neuropathies can be further subdivided into acquired and hereditary neuropathies. Acquired neuropathies can be of diverse etiology such as metabolic, paraproteinemic, toxic, autoimmune-mediated or may be caused by malnutrition, or infections. The clinical presentation is characterized by temporal course, pattern of clinical manifestation, sensory and motor deficits, quality and distribution of neuropathic pain, trophic changes, muscular atrophy, and autonomic involvement (Hufschmidt 2017).

1.1.2 Diagnostic approach to neuropathies

Sensory symptoms (e.g. numbness, tingling), muscle weakness, autonomic symptoms, or neuropathic pain may indicate peripheral neuropathy. The detailed medical history should be obtained, together with a complete neurological examination. Electromyography (EMG) and nerve conduction studies (NCS) are used to confirm the diagnosis, exclude differential diagnoses, localize the area of pathology, confirm the modalities affected (sensory and/or motor), define whether the neuropathy is secondary to axonal loss or demyelination, and to estimate disease severity and prognosis (Watson and Dyck 2015). Basic laboratory examination should include (alphabetic order): Bence-Jones-proteins in urine, C-reactive protein, differential blood count, electrolytes, erythrocyte sedimentation

Introduction

rate, immunofixation, liver and kidney function tests, and the thyroid stimulating hormone. Laboratory tests should be extended individually depending on the suspected diagnosis. Additionally, the examination of cerebrospinal fluid is useful in the differential diagnosis of suspected inflammatory neuropathies (Heuß 2019). After adequate clinical, electrophysiological, and laboratory investigation nerve biopsy is often the final step in the diagnostic work-up of patients with neuropathies of unknown origin. These nerve biopsies should be performed, processed, and evaluated at specialized centers (Sommer et al. 2010). Imaging modalities such as high-resolution nerve ultrasound (HRUS) or magnetic resonance imaging (MRI) are promising novel methods detecting specific alterations in patients with neuropathies and are increasingly integrated in clinical routine.

1.2 Amyotrophic lateral sclerosis (ALS)

1.2.1 Definition and clinical presentation of ALS

ALS is a fatal, neurodegenerative disease of the motor system. According to population-based studies, the incidence of ALS in Europe is about 2.16 per 100.000 person years; men have a higher incidence than women. The overall population-based lifetime risk for ALS is estimated 1:350 for men and 1:400 for women. Up to 90% of patients diagnosed with ALS are classified as having a sporadic disease, whereas the remaining 10% are assumed to be genetic. The peak age of onset for sporadic disease is between 58 – 63 years and between 47 – 52 years for genetic variants (Kiernan et al. 2011). The key characteristic of ALS is an impairment of the first and second motor neuron. Neuropathologically, ALS is defined by a lesion in the corticospinal tract, the anterior motor horn cells of the spinal cord, and bulbar motor nuclei of the cranial nerves. Clinically, focally beginning atrophic paresis and indications for lesions of the corticospinal tract may be found. Generalized fasciculations and muscle cramps are also frequent, but unspecific signs. Pain and sensory disturbance are not primary symptoms of ALS, however, mild sensory involvement does not exclude the diagnosis (Devigili et al. 2011, Ludolph 2014).

Introduction

1.2.2 Diagnostic approach to ALS

ALS is diagnosed according to clinical criteria. Further basic diagnostics are NCS, EMG, measurements of weight and body mass index, lung capacity, and blood tests to exclude other diseases. In addition, lumbar puncture, muscle and nerve biopsy, neuropsychological tests, cranial and spinal MRI, extended blood and urine tests, pulmonary function analysis, and examination of bulbar functions such as swallowing are carried out. If the family history is positive for ALS, dementia or psychiatric diseases, genetic testing is recommended (Ludolph 2014). The implementation of new and reliable diagnostic tools and procedures are warranted in ALS, which is of importance in an early stage of disease to detect differential diagnoses such as neuropathies.

1.3 High-resolution nerve ultrasound (HRUS)

1.3.1 Technical requirements and sonographic imaging with HRUS

HRUS in clinical and research use requires specific hardware tools: For superficially located nerves (e.g. median nerve), high frequency linear probes usually up to 18 MHz are necessary; lower frequencies (5-15 MHz) are advantageous for nerves in deeper layers such as the sciatic nerve (Kerasnoudis et al. 2015). In some studies, the manual tracing method is preferred (Kerasnoudis et al. 2014), while in others the ellipse tool is used (Alshami et al. 2009). A combination of both measuring methods was reported as well. There is evidence that the usage of zoom could artificially increase the cross-sectional area (CSA) of measured nerves (Jelsing et al. 2015). The usage of color Doppler can prevent inadvertent overestimation of nerve size due to inclusion of blood vessels (Jang et al. 2014). Also, there is no standardized protocol of nerves that should be examined with HRUS when investigating patients with neuropathies and ALS.

1.3.2 Echotexture of nerves when assessed with HRUS

Normal peripheral nerves show a characteristic echotexture: nerves appear tubular with multiple hypoechoic bands in longitudinal and multiple round hypoechoic areas in the transverse plane which is generally described as a

Introduction

fascicular or honeycomb pattern (Goedee et al. 2013, Suk et al. 2013). Figure 1A illustrates the typical presentation of the median nerve situated at the wrist in cross section. The nerve is shown with its hyperechoic rim and fascicular intrinsic structure surrounded by the tendons and blood vessels of the distal forearm. Figure 1B illustrates median nerve in longitudinal plane. In longitudinal section the upper and lower rim of the nerve is hyperechoic, and the fascicular intrinsic structure can be seen equally.

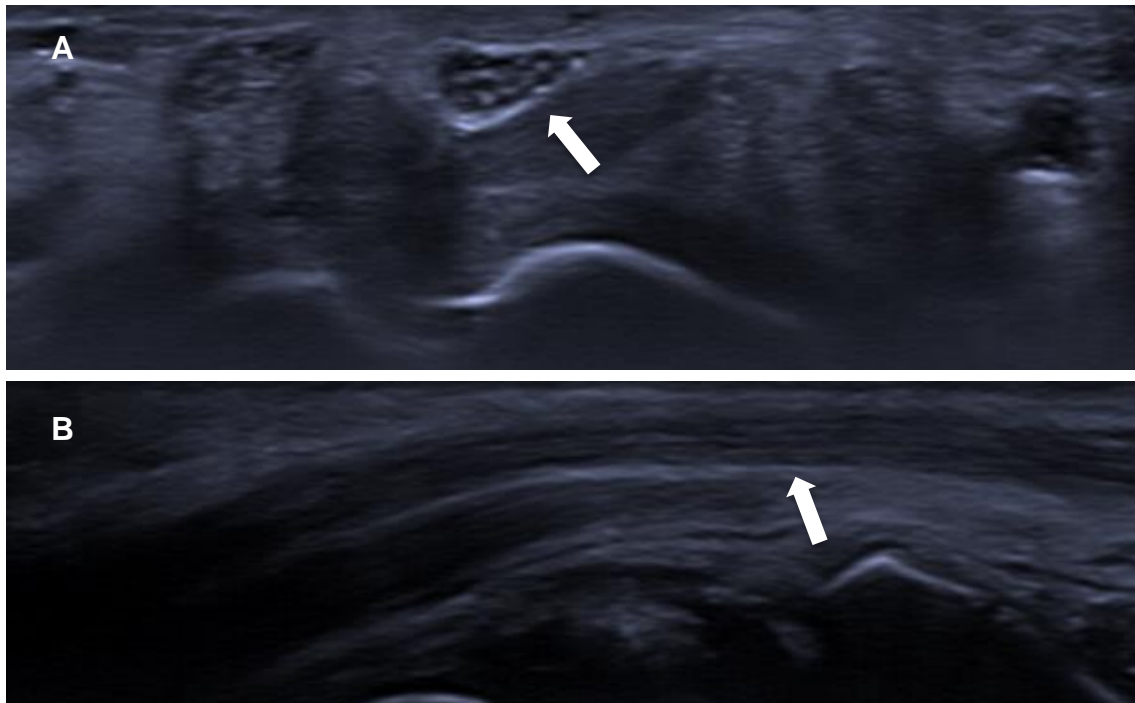


Figure 1: Median nerve at wrist of healthy control – cross-section and longitudinal section
A) Median nerve at wrist, cross section (arrow) B) Median nerve at wrist, longitudinal section (arrow)

HRUS is a relatively low-cost and widely available technique with short acquisition time. HRUS provides the advantage of dynamic imaging examination of peripheral nerves (Decard et al. 2018). It allows peripheral nerves to be visualized with an excellent resolution and has proven to be reliable, effective, non-invasive, and is tolerated well by patients. The resolution of sonography has improved considerably in the last decade. As many peripheral nerves run a superficial course, they are easy to access with sonography and can be examined over a long distance in a few minutes. Even very small nerves such as the sural nerve and fascicular patterns can be studied (Goedee et al. 2013). One drawback of HRUS is the intra- and interrater reliability, which very much depends on the examiner's experience (Decard et al. 2018). Furthermore, nerves can be

Introduction

difficult to visualize when they are located deeply or surrounded by fatty tissue and they may become invisible beneath bones because of acoustic shadowing. The field of view is relatively narrow, which can partially be overcome by applying panoramic view (Goedee et al. 2013).

1.4 HRUS - nerve alterations in neuropathies and ALS

Several studies have been published on HRUS in patients with mainly autoimmune inflammatory neuropathies reporting alterations in size and echotexture of the investigated nerves. Some neuropathy subtypes such as multifocal motor neuropathy (MMN), chronic inflammatory demyelinating polyneuropathy (CIDP), hereditary neuropathy with liability to pressure palsies (HNPP), and Charcot-Marie-Tooth (CMT) disease have been described in detail. Several examination strategies were developed to describe and measure patterns of nerve enlargement in CMT, CIDP, and other inflammatory and immune-mediated neuropathies. These patterns were mostly derived from reports of relatively small numbers of patients and different imaging protocols were used. Therefore this pattern need to be validated before used in routine diagnostics (Telleman et al. 2018). Little literature is available comparing neuropathies among each other and to ALS in single center studies with homogeneous recruitment and examination procedures. Most studies included one type of neuropathy comparing HRUS findings to clinical examination and NCS. Hardly any data exists on the correlation of sonography results and histological findings in nerve biopsies (Goedee et al. 2013, Grimm et al. 2014, Scheidl et al. 2014, Loewenbruck et al. 2016).

1.4.1 HRUS findings in patients with demyelinating neuropathy

The majority of neurosonographic studies of inflammatory neuropathies were performed in patients with demyelinating neuropathies and investigated alterations of the CSA at different nerve sites compared to both healthy and disease controls. In patients with CIDP, focal enlargement of the CSA was shown, partly with hypoechoic or heterogeneous hypo- and hyperechoic fascicles (Imamura et al. 2009, Padua et al. 2014, Di Pasquale et al. 2015). Additionally, a hypertrophy of cervical nerve roots was seen in most patients (Matsuoka et al.

Introduction

2004). In a pattern analysis, widely distributed nerve enlargement in particular at non-entrapment sites and in proximal regions was found in comparison to healthy controls (Jang et al. 2014). In patients with multifocal acquired demyelinating sensory and motor neuropathy (MADSAM) focal nerve enlargement was detected at multiple sites (Scheidl et al. 2012). HRUS examination of patients with MMN showed inhomogeneous, focal to multifocal enlargement of CSA, with weak correlation to NCS findings: alterations were seen in patients with and without electric conduction blocks. Increased CSA of nerves was detected in both electrophysiologically and clinically affected and unaffected nerves (Beekman et al. 2005, Kerasnoudis et al. 2015, Rattay et al. 2017). For CMT-1A, CMT-1B, and CMT-2A, an enlargement of the CSA was reported, whereas no nerve enlargement was found in patients with CMT-X (Heinemeyer and Reimers 1999, Martinoli et al. 2002, Cartwright et al. 2009, Zaidman et al. 2009, Schreiber et al. 2013). For patients with HNPP, the highest rate of enlargement of the CSA was seen at entrapment points such as the ulnar sulcus and at the fibular head. Additional nerve enlargement was also found at non-entrapment sites (Padua et al. 2018). Neurosonographic nerve enlargement was also found in the proximal median nerve and brachial plexus especially in chronic inflammatory neuropathies such as CIDP, MADSAM, and MMN (Goedee et al. 2016).

1.4.2 HRUS findings in patients with axonal neuropathies

It was described that nerve enlargement was more often seen in vasculitic neuropathies than in other axonal neuropathies, but was less frequent than in demyelinating neuropathies (Grimm et al. 2014). Enlargement of nerves at the upper extremity detected with HRUS proximal to sites of nerve compression with the exception of the brachial plexus may indicate a characteristic pattern of vasculitic neuropathy (Goedee et al. 2016). At the lower extremity, nerve enlargement could be detected for the CSA and the LD compared to disease controls with non-immune-mediated neuropathies and healthy controls (Üçeyler et al. 2016). Inconsistent data exist on the distribution of nerve alteration in patients with vasculitic neuropathy. Patients with systemic vasculitic neuropathy are mostly not distinguished from those with non-systemic vasculitic neuropathy

Introduction

(NSVN) and nerve biopsy was not always performed to ensure definite diagnosis of vasculitis (Scheidl et al. 2014).

1.4.3 HRUS findings in patients with ALS

Nerve size in patients with ALS was compared to those in patients suffering from MMN and to healthy controls. No difference of CSA was found between the ALS and the control group, whereas median values of the CSA distinguished between ALS and MMN, and between MMN and controls (Grimm et al. 2015). Consecutively, a high diagnostic accuracy of discrimination between MMN and ALS was confirmed suggesting high sensitivity and specificity (Loewenbruck et al. 2016). It is of note, that nerve enlargement was found at common sites of nerve compression and nerves of the lower extremity in patients with ALS compared to disease controls from a cohort of patients in outpatient clinics (Goedee et al. 2016). There is a lack of studies investigating large patient cohorts.

1.5 Hypothesis and research questions

HRUS is a complementary method in the diagnostic procedure of peripheral neuropathies. The objective of our study was to examine its diagnostic utility for the differentiation between subtypes of both axonal and demyelinating neuropathies by investigating clinical, electrophysiological, histological data, and sonological records. Additionally, patients with ALS were included to investigate potential sonographic differences between patients diagnosed with neuropathy and patients diagnosed with ALS. We hypothesized:

- 1) Neuropathy causes enlargement of peripheral nerves compared to healthy controls. ALS does not cause enlargement of peripheral nerves compared to healthy controls.
- 2) Enlargement of peripheral nerves can be detected by measurement of CSA and LD. Both types of measurements deliver comparable results.
- 3) Axonal and demyelinating neuropathies show distinct patterns of nerve enlargement. The subtypes of axonal and demyelinating neuropathies can be identified by HRUS.
- 4) Histological findings show corresponding measurement alterations in HRUS.

2 Patients, Material, and Methods

2.1 Recruitment of patients and healthy controls

The Würzburg Medical Faculty Ethics Committee approved our study (AZ 9/15). Recruitment took place between February 2015 and February 2018. All study participants gave written informed consent before inclusion.

2.1.1 Healthy control cohort

We enrolled 30 healthy volunteers. Controls were recruited from among relatives and acquaintances of patients. To exclude controls with any suspect of neuropathy, motor neuron disease, and nerve pathology, a standardized medical history and neurological examination was performed.

2.1.2 Patient cohort

We prospectively recruited patients with suspected neuropathy or ALS. Patients were enrolled as in- or out-patients at the Department of Neurology, University of Würzburg. Patients were excluded if neither a neuropathy nor ALS was diagnosed after diagnostic assessment. A medical history was taken, neurological examination, NCS, blood tests, and examination of cerebrospinal fluid were conducted. In addition, standardized scores and questionnaires were applied for the assessment of neuropathic pain, depression, disability, paresis and sensory impairment due to neuropathy. If the etiology remained unclear, nerve biopsy was performed respectively.

2.2 Neuropathies were diagnosed applying the following criteria:

2.2.1 Axonal neuropathies

- Vasculitic neuropathy: The diagnostic group of vasculitic neuropathies contains two subgroups: neuropathies as organ manifestation during systemic vasculitic neuropathy (SVN) and NSVN. SVN may occur secondary to disorders such as rheumatoid arthritis or viral infections. The International Chapel Hill Consensus Conference classification is the most accepted classification (Gwathmey et al. 2014). NSVN is diagnosed according to consensus recommendations (Collins et al. 2010) and the

Patients, Material, and Methods

diagnostic criteria developed by the Brighton Collaboration in 2015. The predominant clinical manifestations are asymmetric paresis, sensory disturbance, and pain. In the neurological examination, most patients present with sensorimotor signs. In nerve conduction studies reduced compound muscle action potential is shown. Nerve biopsy reveals transmural inflammatory infiltrations and is the diagnostic gold standard (Collins and Hadden 2017).

- Progressive idiopathic axonal neuropathy (PIAN): Patients were diagnosed following published criteria (Vrancken et al. 2004). Clinically, these patients show a rapid or subacute onset and a continuously or intermittent progressive course of disease with a distally symmetric distribution of sensory and motor symptoms. Neurological examination reveals both proximal and distal weakness, sometimes involvement of the cranial nerves, and often distal sensory impairment. NCS show reduced compound muscle action potentials. Sural nerve biopsy indicates axonal degeneration (Vrancken et al. 2004).
- Chronic idiopathic axonal polyneuropathy (CIAP): Diagnostic criteria were published in 1993 (Notermans et al. 1993). Neuropathy shows a slow disease onset and develops gradually over months and years. Clinically, a symmetrical distribution of both sensory and motor impairment of the limbs with a distal distribution can be observed. Neurological examination reveals sensory symptoms such as paresthesia, numbness, and burning pain. Typical motor symptoms are cramps, bilateral foot drop, and gait disturbance. NCS show a reduction of both the sensory nerve action potential amplitude and the compound muscle action potential amplitude. Nerve conduction block is not found in these patients. Nerve biopsy shows axonal degeneration and no signs of demyelination, inflammation, vasculitis, or amyloidosis were found (Notermans et al. 1993).
- Acute motor and sensory axonal neuropathy (AMSAN): Diagnosis was made following published criteria (Feasby et al. 1993). The clinical course often shows severe motor and sensory impairment with rapid progress after onset including limb weakness and severe autonomic symptoms.

Patients, Material, and Methods

Neurological examination reveals distal loss of pinprick and vibration sense, areflexia, facial weakness, and limb weakness, which can range up to tetraplegia. Nerve conduction studies show reduced compound muscle action potential amplitudes. Nerve biopsy reveals severe axonal degeneration without inflammation (Feasby et al. 1993, Trojaborg 1998).

- Diabetic neuropathy: The Diabetic Neuropathy Study Group of the European Association for the Study of Diabetes published respective diagnostic criteria (Tesfaye et al. 2010). The most common clinical manifestation of diabetic neuropathy is a distally symmetrical polyneuropathy, but other patterns such as small fiber predominant neuropathy, radiculoplexopathy, and autonomic neuropathy can occur as well. Clinical examination reveals motor weakness, areflexia, allodynia, hyperalgesia, and impaired vibration sense, beginning at the feet with symmetric, predominantly sensory symptoms. (Callaghan et al. 2012). Nerve conduction studies typically show a length-dependent, axonal, and sensorimotor neuropathy (Russell and Zilliox 2014) Sural nerve biopsy is not part of the diagnostics of diabetic neuropathy.
- Axonal neuropathy of unknown etiology: In respective patients signs of axonal impairment were found in NCS and/or nerve biopsy, but a more specific diagnose could not be made at time of inclusion.

2.2.2 Demyelinating neuropathies

- Chronic inflammatory demyelinating polyradiculoneuropathy (CIDP): The diagnosis of CIDP was made according to the Inflammatory Cause and Treatment (INCAT) criteria (Sander and Latov 2003). The classical clinical pattern evolves over more than two months with a sensory and motor neuropathy. A typical clinical finding in neurological examination is a symmetrical motor predominant peripheral neuropathy that produces both distal and proximal weakness as well as generalized areflexia. Nerve conduction studies show slowed conduction velocities, temporal dispersion, and conduction block. In nerve biopsy, segmental demyelination can be found along with onion bulb formation and endoneurial inflammation (Dyck and Tracy 2018)

Patients, Material, and Methods

- Multifocal acquired demyelinating sensory and motor neuropathy (MADSAM): The diagnosis of MADSAM is based on the description by Lewis and Sumner (Lewis et al. 1982) MADSAM clinically presents as asymmetric sensorimotor neuropathy, which shows focal affection of individual nerves focused at the upper extremities. Nerve conduction studies show multifocal conduction blocks. Nerve biopsy reveals signs of demyelination and remyelination with varying degree of fiber loss (Rajabally and Chavada 2009).
- MMN: The diagnosis is made according to the EFNS/PNS guideline (van Schaik et al. 2006, Hadden et al. 2010) . MMN is a asymmetric neuropathy with predominantly distal weakness and without sensory impairment of two or more peripheral nerves, without signs of an affection of the upper motor neuron. Among motor impairment, neurological examination can reveal decreased or absent tendon reflexes, cramps or fasciculations. Neurophysiological assessment typically reveals demyelination with conduction blocks (Van den Bergh et al. 2010). Sural nerve biopsy is not part of MMN diagnostics.
- IgM paraproteinemic demyelinating neuropathy (PDN): The diagnosis is made according to the EFNS/PNS guideline 2010. Patients with IgM PDN often show predominantly distally symmetric neuropathy. Neurological examination shows a slow progression with sensory impairment, ataxia, relatively mild weakness and often tremor. Typically, uniform symmetric and predominantly distally reduced conduction velocity without conduction block may be found. Nerve biopsy may show complement deposit or IgM deposits on myelin. Electron microscopy may show widely spaced myelin (Hadden et al. 2010).
- Demyelinating neuropathy of unknown etiology: In respective patients signs of demyelination were found in NCS and/or nerve biopsy, but a more specific diagnose could not be made at inclusion time.

2.2.3 Hereditary neuropathy

Hereditary neuropathies are assumed, if there is an early and slow onset of symptoms with a progressive course over several years. Symptoms are

Patients, Material, and Methods

predominantly distally located with both sensory and motor impairment. Hereditary neuropathies are often associated with structural foot and ankle deformities such as pes cavus, hammer toes, and calf atrophy. A family history of neuropathy is typical. Diagnosis is confirmed by genetic testing (Watson and Dyck 2015).

2.2.4 Neuropathy, of unknown etiology

Study participants who could not be diagnosed according to the subgroups detailed above were assessed to this group.

2.2.5 ALS

The diagnosis of ALS is supported by the revised El Escorial criteria (Brooks et al. 2000) and the electrodiagnostic criteria for diagnosis of ALS published in 2008 (de Carvalho et al. 2008). The clinical course starts insidiously with focal weakness and spreads to involve most muscles including the diaphragm. Neurological examination reveals muscular weakness, spasticity, fasciculations, atrophy and bulbar affection with difficulty in chewing, speaking, and swallowing (Brown and Al-Chalabi 2017). NCS are essential in the diagnostic process to eliminate other motor neuron disorders that may resemble ALS (de Carvalho et al. 2008). Sural nerve biopsy is not part of ALS diagnostics.

2.3 Definition of inflammatory and non-inflammatory neuropathy

The definition of inflammatory neuropathy was based on clinical diagnosis. The following neuropathies were classified as inflammatory: vasculitic neuropathy, PIAN, CIDP, AMSAN, MADSAM neuropathy, MMN, and paraproteinemic neuropathy. All other neuropathies were classified as non-inflammatory.

2.4 Neuropathy scores

- Modified Toronto Clinical Neuropathy Score (mTCNS)

The Toronto Clinical Neuropathy Score (TCNS) was used for the classification of sensory symptoms and signs in patients with diabetic neuropathy. The TCNS includes clinical findings of tactile discrimination, thermal and tactile sensitivity, vibration sense, and position sense, pain, numbness, tingling and ataxia. Each of

Patients, Material, and Methods

these modalities is scored from 0 (not present) to 3 (severe symptoms, which affect negatively both wellbeing and everyday activities). If one of these symptoms is present in the arms, this is recorded as well. A total score of 33 can be reached (Bril et al. 2009).

- Modified Medical Research Council-Score (mMRC)

For the standardized evaluation of muscle weakness, the modified Medical Research Council-Score (mMRC-score) was used (Merkies et al. 2003). The following muscle groups were scored: shoulder abductors, arm flexors, arm extensors, hand extensors, finger extensors, finger spreader, hip flexors, knee extensors, foot flexors, foot sinkers, toe lifters, toe extensors. Each group is provided with a defined score reaching from 0 (plegia) to 5 (full strength). The highest reachable sum score was 60.

- Overall Disability Sum Score (ODSS)

The Overall Disability Sum Score (ODSS) reflects the level of disability in patients with immune-mediated neuropathies. Therefore, performance of complex movements such as turning a key or using cutlery are recorded and the ability of walking, or the demand for crutches or a wheelchair are recorded. Arms are scored from 0 to 5, legs from 0 to 7. The sum scores reach from 0 (no disability) to 12 (maximum disability) (Merkies et al. 2002).

2.5 Questionnaires

- Neuropathic Pain Symptom Inventory (NPSI)

For the standardized assessment of the quality and intensity of current pain and pain within the last 24 hours, the Neuropathic Pain Symptom Inventory (NPSI) was used. The NPSI records distinct qualities of neuropathic pain and par-/dysesthesias on a scale ranging from 0 (no pain or par-/dysesthesias) to 1 (maximum pain or par-/dysesthesias). In addition, pain attacks and triggers of pain are recorded (Bouhassira et al. 2004, Sommer et al. 2011).

Patients, Material, and Methods

- Graded Chronic Pain Scale (GCPS)

The Graded Chronic Pain Scale (GCPS) records pain intensity and impairment due to pain at work and everyday life within the last 30 days. The GCPS results in pain intensity and impairment scores ranging from 0 (no pain/no disability) to 100 (maximum pain) (Von Korff et al. 2005). Patients were classified as having “painful” neuropathy, if current pain intensity, as determined by the GCSP, was $\geq 3/10$ on an eleven-point numeric rating scale (NRS) ranging from 0 to 10 points. If patients do not report pain, they were classified as painless neuropathy.

- “Allgemeine Depressionsskala (ADS)”

To detect potential depressive symptoms, we used the “Allgemeine Depressionsskala” (ADS; the German version of CES-D-Scale). The scale consists of a catalog of 20 standardized questions addressing depressive symptoms. It reaches a maximum score of 60 points. A total score of 23 hints to clinically relevant depressive symptoms in patients suffering from pain (Hautzinger M. 2012)

2.6 Laboratory tests

All patients underwent detailed laboratory studies including the following parameters: anti-nuclear antibodies (ANA), antibodies to extractable nuclear antigen (ENA), anti-neutrophil cytoplasmatic autoantibodies (ANCA), blood and differential cell counts, C-reactive protein, erythrocyte sedimentation rate, folid acid, glucose metabolism (HbA1c and oral glucose tolerance test), immunofixation, monoclonal immunoglobulins, rheumatoid factor, serology for borreliosis, serum electrolytes and renal and liver function tests, serum electrophoresis, thyroid function tests, and vitamin levels were performed. If serum was positive for a monoclonal immunoglobulin, urine analysis for Bence-Jones protein was performed. Most patients underwent tests of cerebrospinal fluid either at the Department of Neurology at University Würzburg including cell count and protein level or had undergone lumbar puncture prior to admission.

Patients, Material, and Methods

2.7 Nerve conduction studies (NCS)

All patients underwent electrophysiological examination as part of diagnostic work-up. NCS of the sural and tibial nerve were performed routinely, additionally the median nerve was assessed in most patients. The investigated side was chosen according to individual clinical manifestation. Further motor nerves (e.g. ulnar, radial or peroneal nerve) were examined as needed (Kimura 1984)

Conduction block was defined according to published criteria by a decrease in the size of compound muscle action potential on proximal versus stimulation of a nerve in absence of excess temporal dispersion of this potential (Feasby et al. 1985). In our department, a decrease of 50% of the size of compound muscle action potential amplitude between distal and proximal stimulation for the confirmation of a conduction block is mandatory.

2.8 Nerve biopsy

Diagnostic biopsy of the sural or radial nerve was performed when an inflammatory neuropathy was assumed, however, diagnosis could not be made applying all non-invasive tests detailed above. Biopsies were taken at the Department of Neurosurgery, University of Würzburg. Biopsy specimens were further processed for histopathological assessment. For data stratification in this thesis, we screened the diagnostic histological records for hints towards inflammation, demyelination, and edema. Edema was additionally classified semiquantitatively as mild, medium, and severe edema. Classification was carried out following written recordings of diagnostic histological assessment. Edema was classified mild if hints of edema or slight edema was described, medium edema was defined as visible edema but not in a strong manner, and severe edema was classified if strong or massive edema was found.

2.9 HRUS

2.9.1 Ultrasound device and examiner

For HRUS, a Siemens Acuson S1000 © (Eschborn, Germany) was used. The device was equipped with an 18 MHz linear-array probe. To guarantee

Patients, Material, and Methods

standardized data processing of images, the Siemens eSieScan® (Eschborn, Germany) software was used, which was installed on the ultrasound device.

All subjects were investigated by the same examiner. The examiner was trained in one basic and two advanced courses certified by “Deutsche Gesellschaft für Ultraschall in der Medizin” (DEGUM) for nerve ultrasound.

2.9.2 Ultrasound technique

HRUS was performed in B-imaging mode. Tendons were identified by anisotropy. For identification of blood vessels and for the discrimination between blood vessels and nerves the duplex mode was utilized. Lower permeability of bones allowed the detection of these structures. Nerves were identified at anatomical sites such as carpal tunnel, spiral groove or fibular head. For confirmation, nerves were identified both in cross section plane and longitudinal section plane and were tracked in proximal and distal directions. Epineurium and perineurium reflect more brightly than fascicles, which gives motor nerves and the brachial plexus a typical honey combed structure in the cross section. This can be observed in longitudinal section as fine septation.

2.9.3 Measuring technique and parameters determined

The CSA and the longitudinal diameter (LD) of the peripheral nerves were measured. For the brachial plexus and the spinal nerves, the CSA was determined. First, the nerve was identified by criteria described above. Then the probe was placed perpendicularly to the longitudinal axis of the respective extremity. Subsequently, the image was frozen under minimal pressure. The CSA was determined by manual tracing just within the hyperechoic rim of the epineurium. CSA measures were obtained three times each for every site. For the measurement in longitudinal plane, the probe was rotated 90° in the direction of anatomical longitudinal axis. The best plane for measurement was identified by minimal movements of the probe, then the image was frozen. LD was measured just inside the hyperechogenic reflection of the epineurium with a minimum of pressure. This procedure was performed three times per site. For each measured region three corresponding images without measurement traces were stored. Figure 2 illustrates the detected median nerve in cross section and

Patients, Material, and Methods

longitudinal section. Figure 2 also shows the measurement of the CSA via manual tracing and the measurement of the LD as a distance.

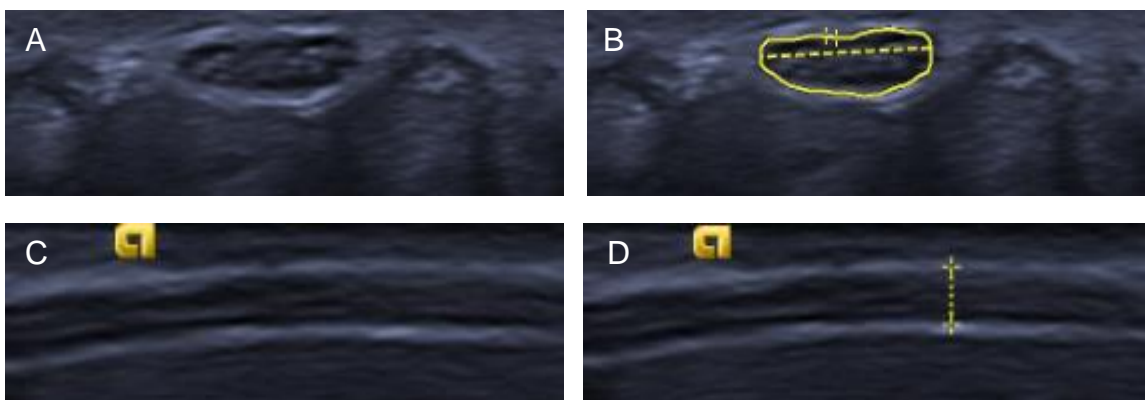


Figure 2 : Median nerve of healthy control – cross-section and longitudinal section
A) Median nerve at wrist in cross section; healthy control subject B) Median nerve at wrist in cross section with measurement of cross-sectional area (CSA); healthy control subject; CSA = 0.12 mm² C) Median nerve at wrist in longitudinal plane; control subject D) Median nerve at wrist in longitudinal plane with measurement of longitudinal diameter (LD); healthy control subject; LD = 1.8 mm

2.9.4 Study protocol

HRUS was performed at defined sites following a standardized study protocol for the left and the right body side, which was applied in patients and healthy controls. The following nerve sites were investigated:

Upper extremities

Median nerve at wrist, mid forearm, cubital fossa, mid upper arm.

Ulnar nerve at wrist, mid forearm, ulnar sulcus, mid upper arm.

Radial nerve at spiral groove.

Brachial plexus at clavicle and the scalene gap.

Spinal nerves C5, C6, C7.

Lower extremities

Sciatic nerve at the distal thigh.

Tibial nerve at the popliteal fossa, and at medial malleolus.

Common peroneal nerve at fibular head.

Deep peroneal nerve at instep.

Superficial peroneal nerve at mid lower leg.

Sural nerve at the calf.

Patients, Material, and Methods

2.9.5 Image transfer and storage

For data transfer and storage, Synedra DICOM viewer (version 15, Innsbruck, Austria) was used. After completing the protocol, data was saved in the internal storage system of the ultrasound device. In a second step, the protocol was opened again with the Synedra DICOM viewer. Then, the data file was stored at the intern server of our department before further processing.

2.9.6 Data extraction

Extraction of CSA and LD data was performed automatically via a software tool developed in collaboration with the Institute for Artificial Intelligence and Applied Computer Science, University of Würzburg (Reul et al. 2016).

2.10 Statistical analysis

Statistical analysis was performed with IBM SPSS 25® (IBM Germany GmbH, Ehningen, Germany). $P<0.05$ was assumed significant. Normal distribution was shown using Shapiro-Wilk-test. For group-wise comparison, t-test analysis was performed.

Pearson correlation coefficients were calculated. Graphs were generated with Microsoft Excel 2016® (Microsoft; Redmond, Washington, United States) and with IBM SPSS 25® (IBM Germany GmbH, Ehningen, Germany). Data points were connected by lines to show relation between the respective measurement sites of one nerve. Additional corresponding data such as the standard deviation and the level of significance are shown in a table which is attached to the graphs. The level of significance is additionally illustrated by transparent boxes within the respective figure. ROC-curves have been generated, if preceding data suggested necessity for further examination or specific clinical questions. Therefore, for example, data obtained from the brachial plexus was more extensively investigated than that of peripheral nerves such as median or sural nerve. For the investigation of peripheral nerves in patients with neuropathies, ROC analysis was performed for median, ulnar, and sciatic nerve in addition.

Results

3 Results

3.1 Characterization of the healthy control cohort and normative values

Our healthy control cohort consisted of 13/30 (43%) female and 17/30 (56%) male subjects. The median age was 47 years (18-75 years) in the whole cohort, 52 years (25-75 years) in the female, and 42 years (22-73 years) in the male subgroup. The comparison between male and female subjects (Figures 3,4; $p<0.05$), and between measurements on both body sides (not shown) revealed only single data points with intergroup differences. Hence, we pooled data of both sexes and body sides. Also, individual height, weight, and body-mass-index (BMI) data of our healthy controls inconsistently correlated with single HRUS data points and data were pooled (Table 1). Normative HRUS data derived from our data are shown in Table 2. Blue coloration shows significant correlation.

Table 1: Correlation of cross-sectional area (CSA) and longitudinal diameter (LD) with height, weight, and body-mass-index (BMI)

Blue coloration shows significant correlation. Abbreviations: BRA_IS = brachial plexus, inter-scalene muscles; BRA_SC = brachial plexus; supra-clavicular; CSA = cross-sectional area; ISC_DT = sciatic nerve, distal thigh; LD = longitudinal diameter; MED_CF = median nerve, cubital fossa; MED_MF = median nerve, mid forearm; MED_MU = median nerve, mid upper arm; MED_WR = median nerve, wrist; PER_FH = peroneal nerve, fibular head; PER_PP = peroneal nerve, profound peroneal nerve; PER_PS = peroneal nerve, superficial peroneal nerve; RAD_SG = radial nerve, spiral groove; SPI_C5 = spinal nerve; SPI_C6 = spinal nerve, sixth cervical nerve; SPI_C7= spinal nerve, seventh cervical nerve; SUR_IG = sural nerve, inter gastrocnemius muscle; TIB_MM = tibial nerve, medial malleolus; TIB_PF = tibial nerve, popliteal fossa; ULN_MF = ulnar nerve, mid forearm; ULN_MU = ulnar nerve, mid upper arm; ULN_US = ulnar nerve, ulnar sulcus; ULN_WR = ulnar nerve, wrist.

CSA correlation (Pearson) n = 30		MED_WR	MED_MF	MED_CF	MED_MU	ULN_WR	ULN_MF	ULN_US	ULN_MU	RAD_SG
with height	correlation significance	0,20 0,131	0,29 *0,027	0,10 0,428	0,27 *0,040	0,30 *0,021	0,23 0,075	-0,04 0,781	0,24 0,062	0,42 **0,001
with weight	correlation significance	0,43 ***0,001	0,37 **0,004	0,31 *0,018	0,38 **0,003	0,27 *0,036	0,54 ***0,000	0,37 *0,003	0,47 **0,000	0,29 **0,026
with BMI	correlation significance	0,38 *0,013	0,17 0,185	0,26 *0,045	0,22 0,090	0,07 0,621	0,42 **0,001	0,45 ***0,000	0,33 0,010	-0,01 0,957
Correlation (Pearson) n = 30		SPI_C5	SPI_C6	SPI_C7	BRA_SC	BRA_IS				
with height	correlation significance	0,14 0,297	0,23 0,077	0,18 0,208	0,24 0,062	0,18 0,185				
with weight	correlation significance	0,05 0,722	0,05 0,694	-0,15 0,289	0,16 0,223	-0,20 0,141				
with BMI	correlation significance	-0,05 0,719	-0,12 0,375	-0,32 *0,022	0,00 0,991	-0,36 *0,006				
Correlation (Pearson) n = 30		SUR_IG	PER_PS	PER_PP	PER_FH	TIB_MM	TIB_PF	SC_DT		
with height	correlation significance	0,02 0,882	0,03 0,854	-0,18 0,179	0,12 0,367	0,00 0,989	-0,05 0,692	-0,01 0,966		
with weight	correlation significance	0,05 0,708	0,03 0,835	-0,10 0,485	0,26 *0,045	-0,19 0,161	0,18 0,176	0,43 **0,001		
with BMI	correlation significance	0,04 0,752	0,01 0,930	-0,08 0,544	0,19 0,158	-0,21 0,104	0,23 0,077	0,44 **0,001		
LD correlation (Pearson) n = 30		MED_WR	MED_MF	MED_CF	MED_MU	ULN_WR	ULN_MF	ULN_US	ULN_MU	RAD_SG
with height	correlation significance	0,06 0,631	0,28 *0,027	0,08 0,539	0,10 0,441	0,30 *0,021	0,09 0,500	0,09 0,486	-0,15 0,281	-0,01 0,962
with weight	correlation significance	0,30 *0,020	0,37 **0,004	0,38 **0,003	0,33 **0,010	0,27 *0,040	0,26 *0,047	0,31 *0,017	0,21 0,103	0,27 *0,036
with BMI	correlation significance	0,28 0,031	0,00 0,976	0,43 ***0,001	0,27 *0,041	0,17 0,199	0,21 0,102	0,27 0,039	0,35 **0,006	0,30 *0,019
LD correlation (Pearson) n = 30		SUR_IG	PER_PS	PER_PP	PER_FH	TIB_MM	TIB_PF	SC_DT		
with height	correlation significance	-0,03 0,827	0,17 0,226	-0,18 0,179	0,05 0,714	-0,06 0,642	0,45 0,49	-0,04 0,18		
with weight	correlation significance	0,01 0,941	0,07 0,631	-0,20 0,144	0,32 *0,016	-0,11 0,932	0,49 ***0,000	0,18 0,202		
with BMI	correlation significance	-0,03 0,827	0,17 0,266	-0,67 0,579	0,30 *0,021	0,04 0,762	0,17 0,207	0,19 0,162		

Results

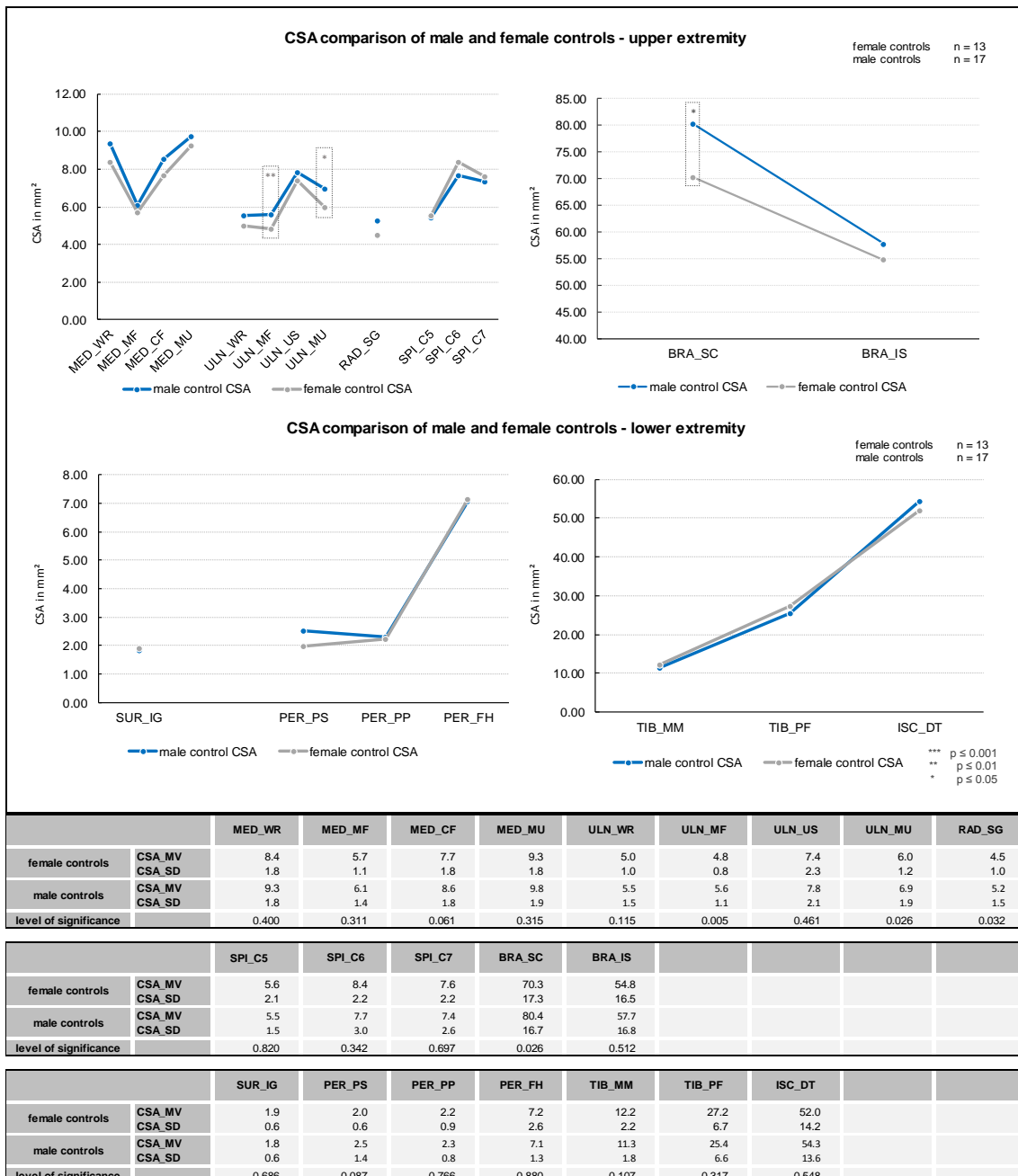


Figure 3: Cross-sectional area (CSA) comparison of male and female control subjects
Abbreviations: BRA_IS = brachial plexus, inter-scalene muscles; BRA_SC = brachial plexus; supra-clavicular; CSA = cross-sectional area; ISC_DT = sciatic nerve, distal thigh; MED_CF = median nerve, cubital fossa; MED_MF = median nerve, mid forearm; MED_MU = median nerve, mid upper arm; MED_WR = median nerve, wrist; PER_FH = peroneal nerve, fibular head; PER_PP = peroneal nerve, profound peroneal nerve; PER_PS = peroneal nerve, superficial peroneal nerve; RAD_SG = radial nerve, spiral groove; SPI_C5 = spinal nerve; SPI_C6 = spinal nerve, sixth cervical nerve; SPI_C7 = spinal nerve, seventh cervical nerve; SUR_IG = sural nerve, inter gastrocnemius muscle; TIB_MM = tibial nerve, medial malleolus; TIB_PF = tibial nerve, popliteal fossa; ULN_MF = ulnar nerve, mid forearm; ULN_US = ulnar nerve, ulnar sulcus; ULN_WR = ulnar nerve, wrist.

Results

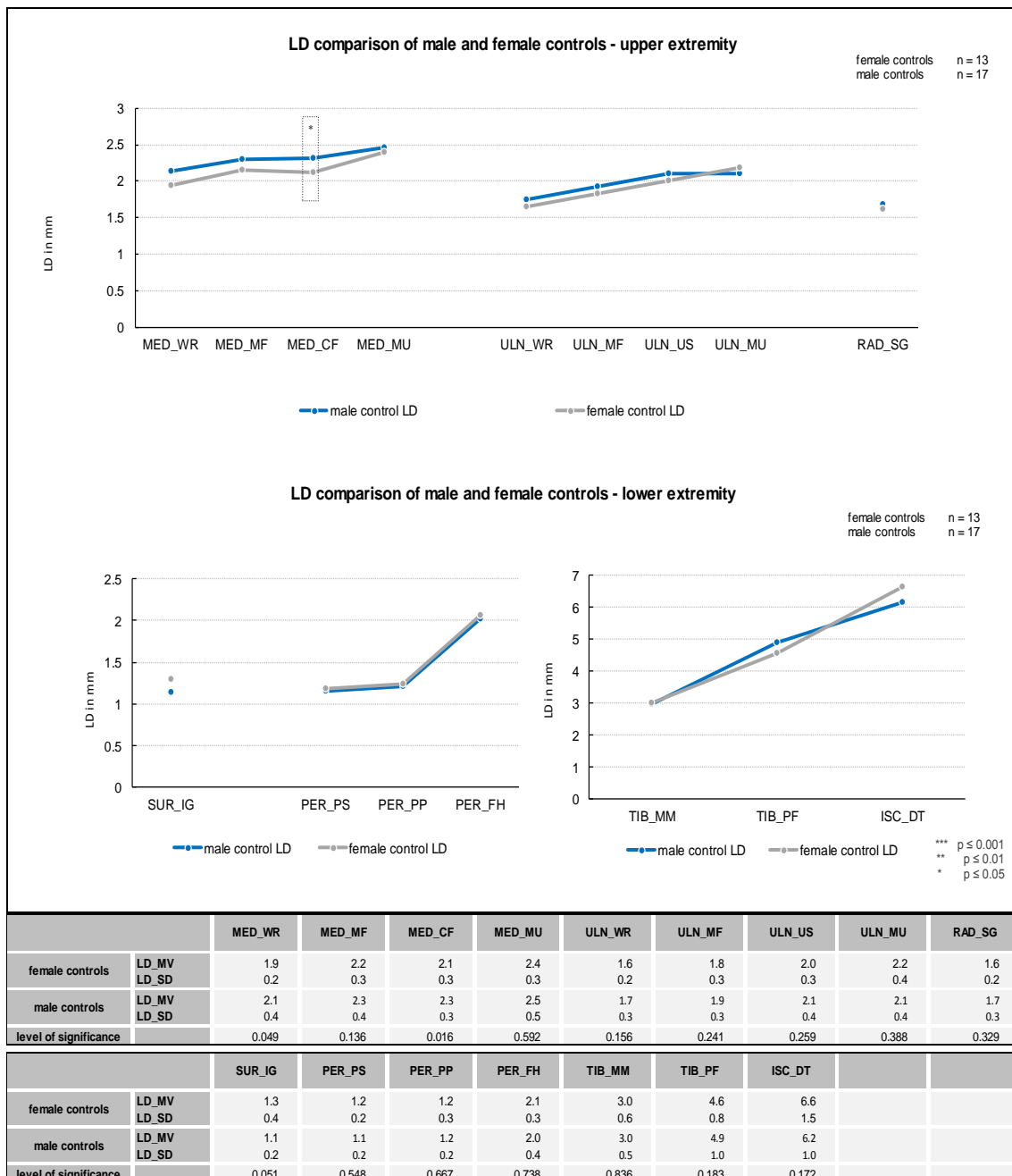


Figure 4: Longitudinal diameter (LD) comparison of male and female control subjects
 Abbreviations: ISC_DT = sciatic nerve, distal thigh; LD = longitudinal diameter; MED_CF = median nerve, cubital fossa; MED_MF = median nerve, mid forearm; MED_MU = median nerve, mid upper arm; MED_WR = median nerve, wrist; PER_FH = peroneal nerve, fibular head; PER_PP = peroneal nerve, profound peroneal nerve; PER_PS = peroneal nerve, superficial peroneal nerve; RAD_SG = radial nerve, spiral groove; SUR_IG = sural nerve, inter gastrocnemius muscle; TIB_MM = tibial nerve, medial malleolus; TIB_PF = tibial nerve, popliteal fossa; ULN_MF = ulnar nerve, mid forearm; ULN_MU = ulnar nerve, mid upper arm; ULN_US = ulnar nerve, ulnar sulcus; ULN_WR = ulnar nerve, wrist.

Results

Table 2: Normative values for cross-sectional area (CSA) and longitudinal diameter (LD) of upper and lower extremities

Abbreviations: CSA = cross-sectional area; LD = longitudinal diameter; mm = millimeter; C5/6/7 = fifth, sixth, seventh spinal nerve.

Upper extremity - control cohort n = 30					
Nerve	Site	CSA		LD	
		mean (mm ²)	SD (mm ²)	mean (mm)	SD (mm)
Median nerve	wrist	8.9	1.8	2.1	0.4
	mid forearm	5.9	1.3	2.2	0.4
	cubitital fossa	8.2	1.9	2.2	0.3
	mid upper arm	9.6	1.9	2.4	0.4
Ulnar nerve	wrist	5.3	1.3	1.7	0.3
	mid forearm	5.3	1.1	1.9	0.3
	ulnar sulcus	7.7	2.1	2.1	0.4
	mid upper arm	6.5	1.7	2.1	0.4
Radial nerve	spiral groove	4.9	1.3	1.7	0.2
Brachial plexus	supraclavicular	76	17.5	-	-
	scalenic gap	56.4	16.6	-	-
Spinal nerves	C5	5.5	1.7	-	-
	C6	8	2.7	-	-
	C7	7.5	2.4	-	-

Lower extremity - control cohort n = 30					
Nerve	Site	CSA		LD	
		mean (mm ²)	SD (mm ²)	mean (mm)	SD (mm)
Sciatic nerve	distal tigh	53.3	13.7	6.3	1.2
Tibial nerve	popliteal fossa	26.2	6.7	4.8	1
	medial malleoulus	11.7	2	3	0.5
Peroneal nerve	fibular head	7.1	1.9	2	0.4
	profound peroneal nerve	2.3	0.8	1.2	0.2
	superficial peroneal nerve	2.3	1.2	1.2	0.2
Sural nerve	proximal calf	1.9	0.6	1.2	0.3

Results

3.2 Characterization of the patient cohort

3.2.1 Patient recruitment and distribution of diagnoses

We initially recruited n=100 patients. After diagnostic re-assessment, eight patients had exclusion criteria, thus the final cohort consisted of 84/92 (91%) patients with neuropathies and 8/92 (9%) patients with ALS. Of these 28/92 (30%) were women. The median age of the study cohort was 57 years (20-80 years) and the median disease duration was 8 years (0.5-63 years). Figure 5 shows the distribution of diagnoses and neuropathy subgroups in the patient cohort.

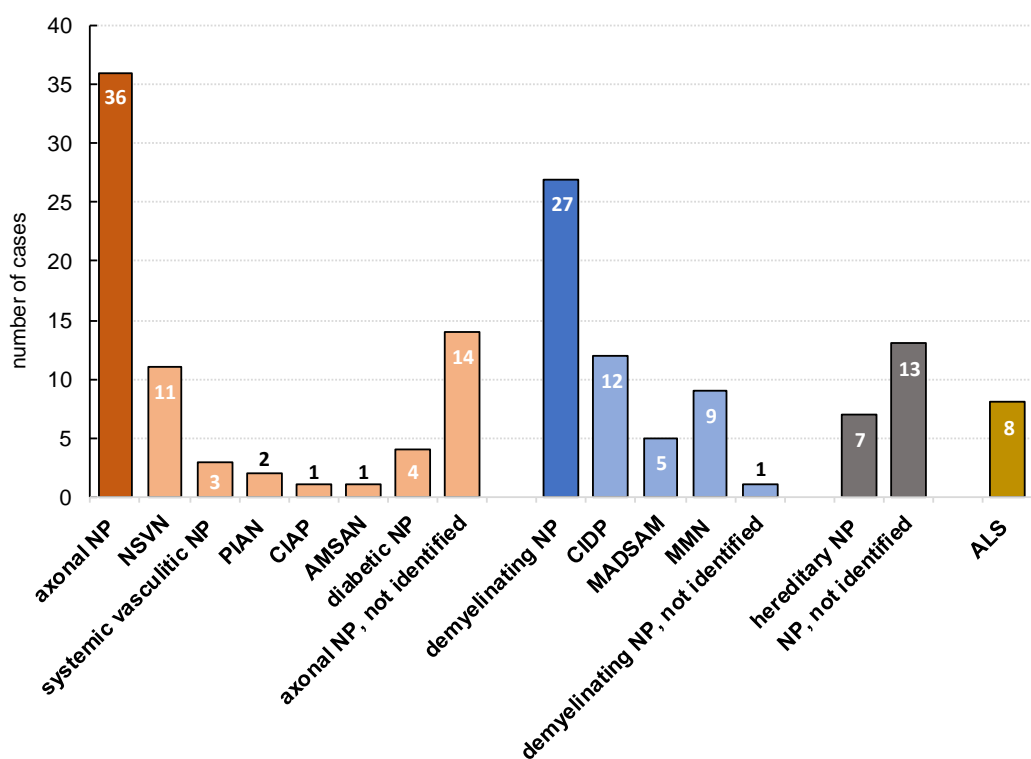


Figure 5: Distribution of diagnoses and subgroups of polyneuropathy and amyotrophic lateral sclerosis (ALS)
Abbreviations: ALS = amyotrophic lateral sclerosis; AMSAN = acute motor and sensory axonal neuropathy;
CIAP = chronic inflammatory axonal polyneuropathy; CIDP = chronic inflammatory demyelinating
polyneuropathy; MADSAM = multifocal acquired demyelinating sensory and motor neuropathy; MMN =
multifocal motor neuropathy; NP = neuropathy; NSVN = non-systemic vasculitic neuropathy.

Results

3.2.1 Neuropathy scores and questionnaires

Table 3A summarizes the results of neuropathy score assessment of patients distinguishing axonal and demyelinating neuropathies. No relevant intergroup difference was found. Table 3B displays the results of the questionnaire survey

Table 3: A) Results of neuropathy scores B) Results of questionnaires stratified for axonal and demyelinating neuropathies.

Level of significance: * p ≤ 0.05; ** p ≤ 0.01; *** p ≤ 0.001. Abbreviations: ADS = Allgemeine Depressionsskala; CIDP = chronic inflammatory demyelinating polyneuropathy; GCPS = Graded Chronic Pain Scale; MADSAM = multifocal acquired demyelinating sensory and motor neuropathy; MMN = multifocal motor neuropathy; mMRC = modified Medical Research Council-Score; mTCNS = Modified Toronto Clinical Neuropathy Score; NPSI = Neuropathic Pain Symptom Inventory; NSVN = non-systemic vasculitic neuropathy; ODSS = Overall Disability Sum Score.

A Results of neuropathy patient survey		Results of neuropathy scores		
		mTCNS	mMRC	ODSS
Neuropathy total N=84	median sumscore (min. - max.)	15,6 3.0-32.0	52,8 16.0-60.0	3,3 0.0-10.0
Axonal neuropathy total n=35	median sumscore (min. - max.)	16,1 3.0-32.0	55,5* 26-60.0	2,9 0.0-8.0
	NSVN median sumscore n=11 (min. - max.)	15,9 3.0-28.0	55,9 36.0-60.0	2,9 1.0-8.0
Demyelinating neuropathy total n=27	median sumscore (min. - max.)	15,3 3.0-31.0	46,3* 16.0-60.0	3,8 1.0-10.0
	CIPD median sumscore n=12 (min. - max.)	17,0 6.0-31.0	44,2 16.0-60.0	4,9 1.0-9.0
	MADSAM median sumscore n=5 (min. - max.)	15,4 9.0-21.0	51,8 48.0-58.0	3,0 2.0-4.0
	MMN median sumscore n=9 (min. - max.)	12,7 3.0-26.0	46,1 29.0-59.0	4,0 2.0-10.0
B Results of questionnaires		NPSI	GCPS	ADS
Neuropathy total N=84	median sumscore (min. - max.)	0.17 0.0-0.63	26 0.0-83.3	13.5 4.0-42.0
Axonal neuropathy total n=35	median sumscore (min. - max.)	0.23 0.0-0.63	34.3 0.0-83	14.2 4.0-36.0
	NSVN median sumscore n=11 (min. - max.)	0.23 0.0-0.63	31.3 0.0-83.3	15.5 4.0-36.0
Demyelinating neuropathy total n=27	median sumscore (min. - max.)	0.09 0.0-0.48	14.2 0.0-76.0	11.8 4.0-28.0
	CIPD median sumscore n=12 (min. - max.)	0.14 0.0-0.48	23.8 0.0-76.0	16 4.0-28.0
	MADSAM median sumscore n=5 (min. - max.)	0.08 0.0-0.2	0 0.0-0.0	7.8 4.0-12.0
	MMN median sumscore n=9 (min. - max.)	0.02 0.0-0.08	8.14 0.0-73.3	7.9 4.0-14.0

Results

of patients stratified for axonal and demyelinating polyneuropathies. An intergroup difference was only found for mMRC score ($p<0.05$).

3.3 Results of HRUS measurement

3.3.1 Comparison between patients with neuropathy and healthy controls

We first compared HRUS data of all patients with all healthy controls. Figure 6 shows ROCs of patients diagnosed with neuropathy at supraclavicular and interscalene brachial plexus versus healthy controls. The area under the curve (AUC) at supraclavicular brachial plexus was 0.67. The AUC for the interscalene brachial plexus was 0.59. Figure 7 shows data of CSA and Figure 8 of LD measurement in all patients diagnosed with neuropathy ($n = 84$) compared to the healthy control cohort ($n = 30$). CSA and LD were larger in patients with neuropathies compared to healthy controls at all investigated nerve sites of the upper and lower extremities ($p<0.05$ to <0.001) with few exceptions.

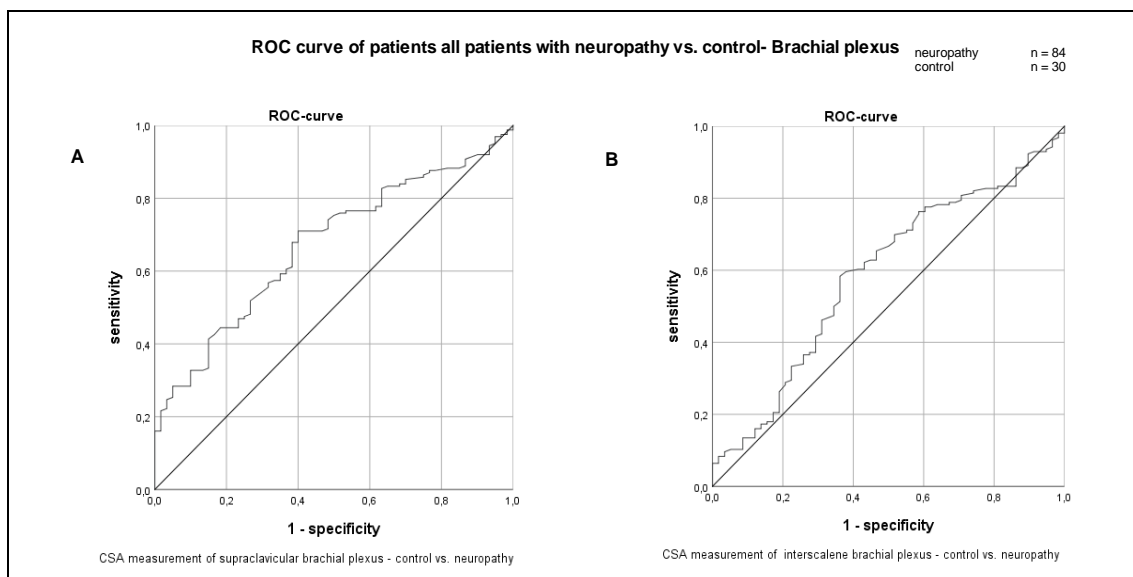


Figure 6: Receiver operating curve (ROC) patients with neuropathy vs. healthy controls – brachial plexus
A) supraclavicular and B) interscalene brachial plexus of patients in comparison to healthy controls
A) Area under the curve (AUC) 0.67; standard error 0.038; confidence interval (95%): lower limit 0.59; upper limit 0.75 B) AUC 0.59; standard error 0.044, confidence interval (95%): lower limit 0.50; upper limit 0.67.
Abbreviations: AUC = area under the curve; CSA= cross-sectional area, ROC = receiver operating characteristic

Results

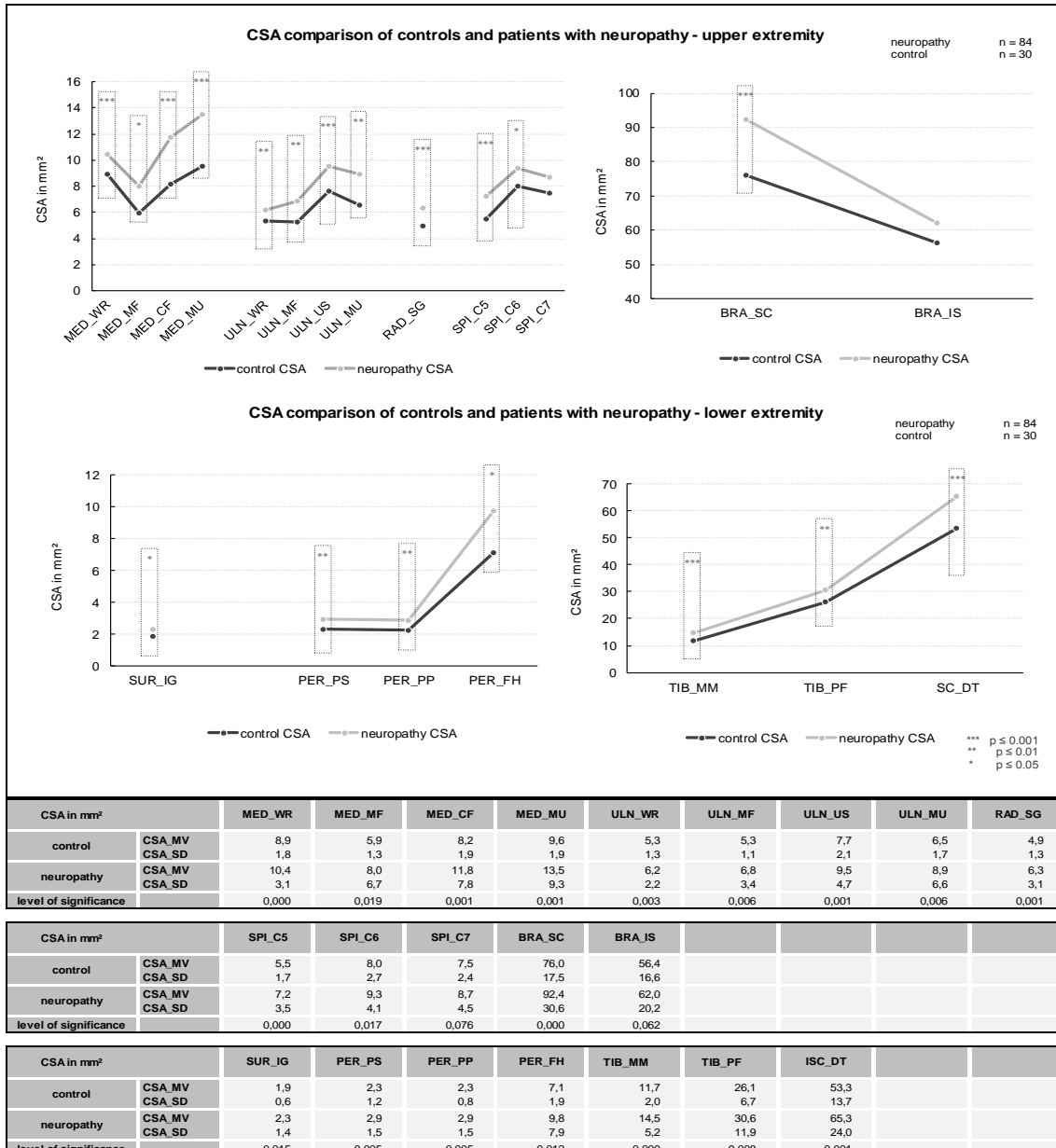


Figure 7: Cross-sectional area (CSA) comparison of patients with neuropathy and control subjects
 Abbreviations: BRA_IS = brachial plexus, inter-scalene muscles; BRA_SC = brachial plexus; supra-clavicular; CSA = cross-sectional area; ISC_DT = sciatic nerve, distal thigh; MED_CF = median nerve, cubital fossa; MED_MF = median nerve, mid forearm; MED_MU = median nerve, mid upper arm; MED_WR = median nerve, wrist; NP = neuropathy; PER_FH = peroneal nerve, fibular head; PER_PP = peroneal nerve, profound peroneal nerve; PER_PS = peroneal nerve, superficial peroneal nerve; RAD_SG = radial nerve, spiral groove; SPI_C5 = spinal nerve; SPI_C6 = spinal nerve, sixth cervical nerve; SPI_C7 = spinal nerve, seventh cervical nerve; SUR_IG = sural nerve, inter gastrocnemius muscle; TIB_MM = tibial nerve, medial malleolus; TIB_PF = tibial nerve, popliteal fossa; ULN_MF = ulnar nerve, mid forearm; ULN_MU = ulnar nerve, mid upper arm; ULN_US = ulnar nerve, ulnar sulcus; ULN_WR = ulnar nerve, wrist.

Results

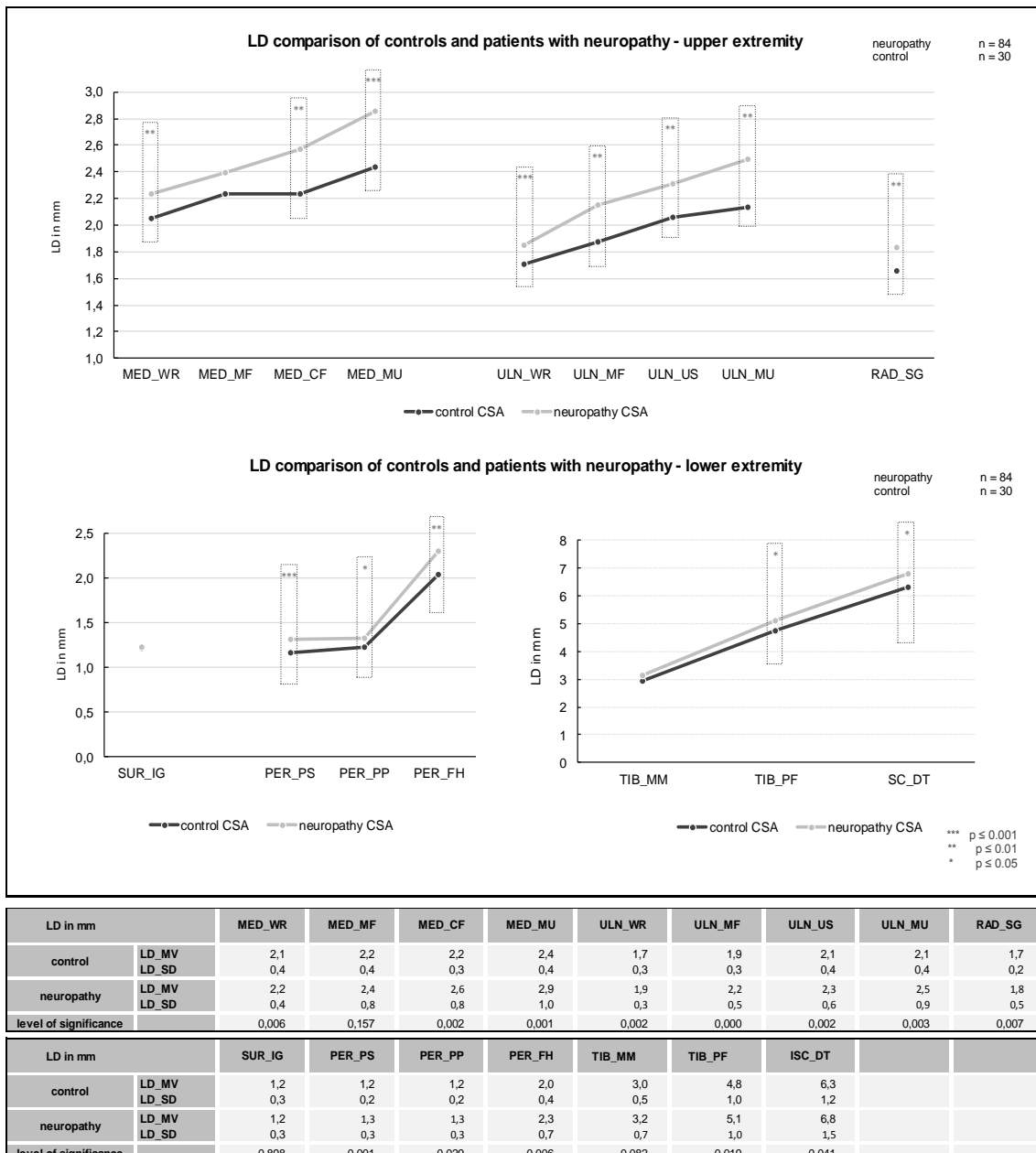


Figure 8: Longitudinal diameter (LD) comparison of patients with neuropathy and control subjects
 Abbreviations: ISC_DT = sciatic nerve, distal thigh; LD = longitudinal diameter; MED_CF = median nerve, cubital fossa; MED_MF = median nerve, mid forearm; MED_MU = median nerve, mid upper arm; MED_WR = median nerve, wrist; BRA PER_FH = peroneal nerve, fibular head; PER_PP = peroneal nerve, profound peroneal nerve; PER_PS = peroneal nerve, superficial peroneal nerve; RAD_SG = radial nerve, spiral groove; SUR_IG = sural nerve, inter gastrocnemius muscle; TIB_MM = tibial nerve, medial malleolus; TIB_PF = tibial nerve, popliteal fossa; ULN_MF = ulnar nerve, mid forearm; ULN_MU = ulnar nerve, mid upper arm; ULN_US = ulnar nerve, ulnar sulcus; ULN_WR = ulnar nerve, wrist.

Results

3.3.2 Comparison between patients with axonal and demyelinating neuropathies

As stated in 3.2.1, the cohort of patients diagnosed with neuropathies included 36/84 (43%) patients with axonal and 27/84 (32%) patients with demyelinating neuropathies. Figure 9 shows the receiver operating characteristic (ROC) for the measurement of CSA at supraclavicular and interscalene brachial plexus. Figure 10 shows HRUS data for the comparison of CSA between these subgroups. CSA enlargement of the demyelinating subgroup compared to the axonal subgroup was found at the median nerve (cubital fossa, mid-upper arm), the ulnar nerve (wrist), the radial nerve (spiral groove), the fifth spinal nerve, the brachial plexus (supraclavicular, interscalene), profound peroneal nerve and the tibial nerve (popliteal fossa) ($p<0.05$ each). At both measuring sites the AUC was > 0.5 . Figure 11 shows HRUS data comparing LD. Enlargement was found at the median nerve (cubital fossa, mid-upper arm), the ulnar nerve (wrist), the radial nerve (spiral groove), the tibial nerve (medial malleolus, popliteal fossa), and the sciatic nerve (distal thigh) ($p<0.05$ each).

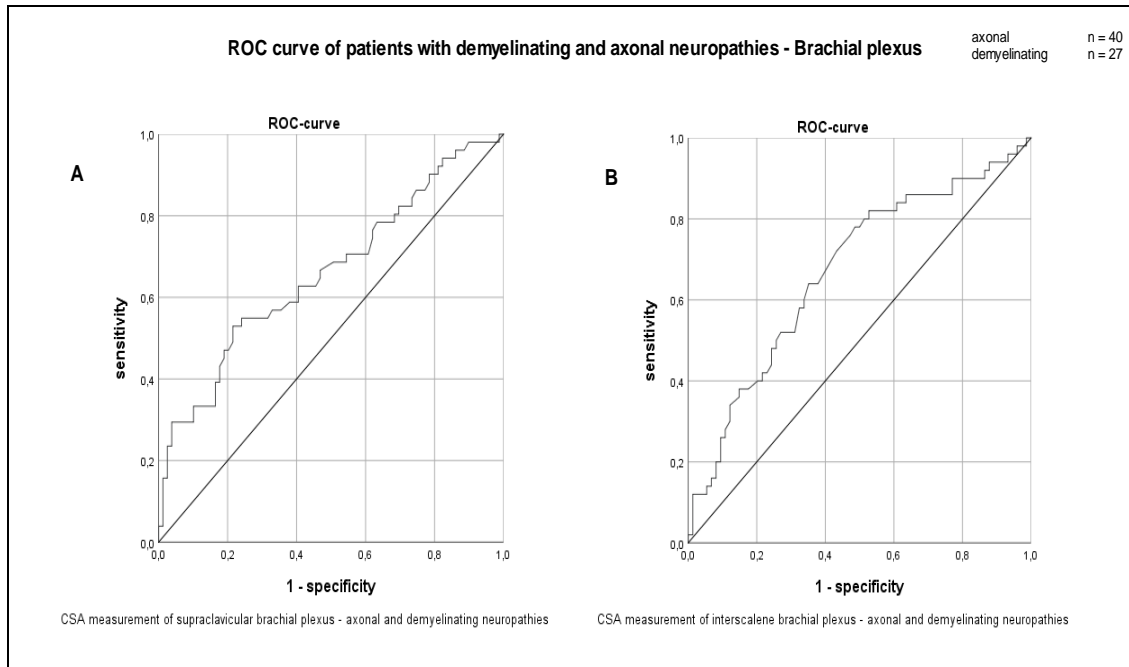


Figure 9: Receiver operating characteristic (ROC) of cross-sectional area (CSA) measurement at brachial plexus

A) ROC-curve of CSA measurement at supraclavicular brachial plexus AUC 0.66; standard error 0.50; confidence interval (95%): lower limit 0.562; upper limit 0.759 B) ROC-curve of CSA measurement at interscalene brachial plexus. AUC 0.67; standard error 0.50; confidence interval (95%): lower limit 0.573; upper limit 0.769 Abbreviations: AUC = area under the curve; CSA= cross-sectional area, ROC = receiver operating characteristic.

Results

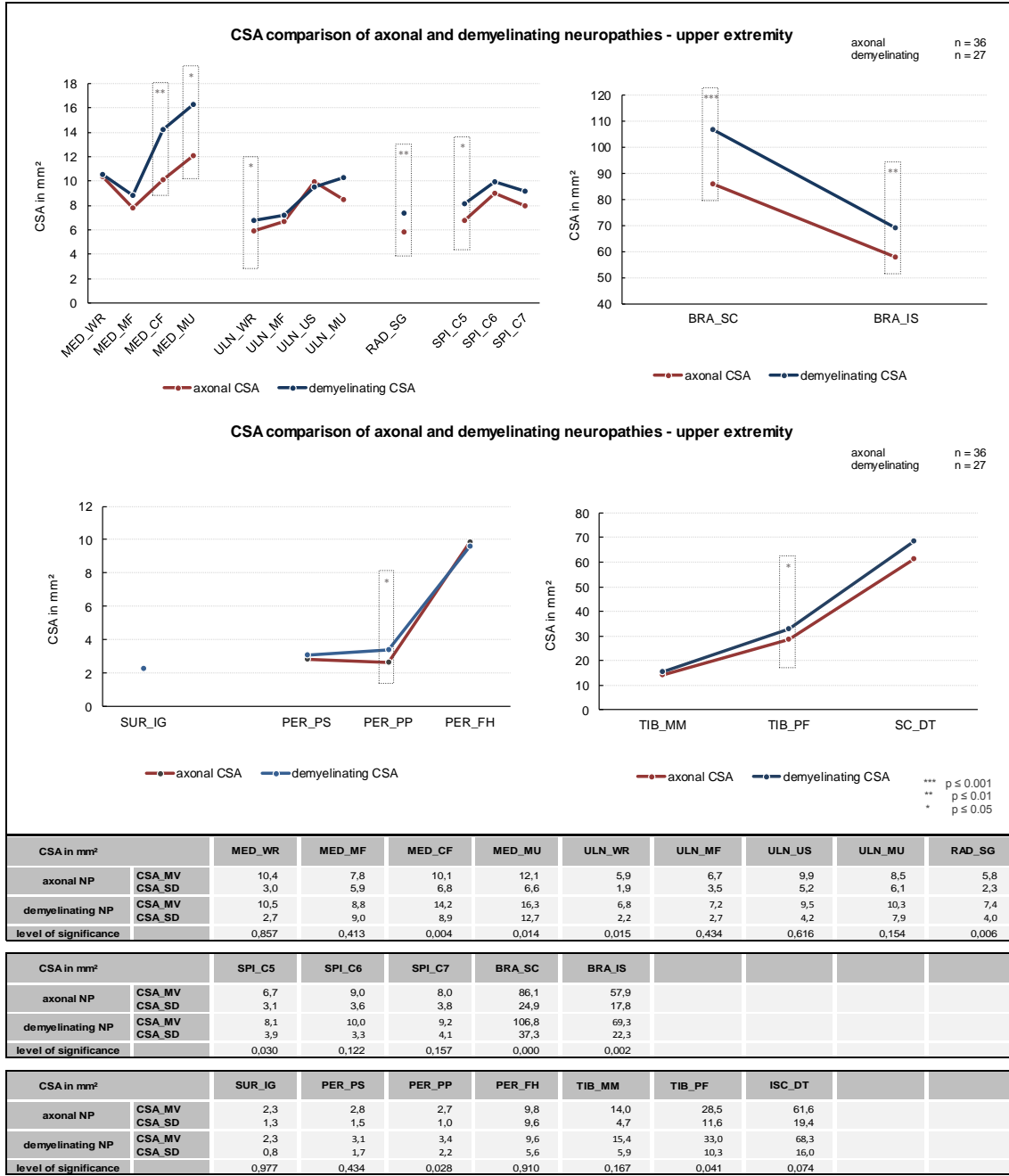


Figure 10: Cross-sectional area (CSA) comparison of patients with axonal and demyelinating neuropathies
 Abbreviations: BRA_IS = brachial plexus, inter-scalene muscles; BRA_SC = brachial plexus; supra-clavicular; CSA = cross-sectional area; ISC_DT = sciatic nerve, distal thigh; MED_CF = median nerve, cubital fossa; MED_MF = median nerve, mid forearm; MED_MU = median nerve, mid upper arm; MED_WR = median nerve, wrist; NP = neuropathy; PER_FH = peroneal nerve, fibular head; PER_PP = peroneal nerve, profound peroneal nerve; PER_PS = peroneal nerve, superficial peroneal nerve; RAD SG = radial nerve, spiral groove; SPI_C5 = spinal nerve; SPI_C6 = spinal nerve, sixth cervical nerve; SPI_C7= spinal nerve, seventh cervical nerve; SUR_IG = sural nerve, inter gastrocnemius muscle; TIB_MM = tibial nerve, medial malleolus; TIB_PF = tibial nerve, popliteal fossa; ULN_MF = ulnar nerve, mid forearm; ULN_MU = ulnar nerve, mid upper arm; ULN_US = ulnar nerve, ulnar sulcus; ULN_WR = ulnar nerve, wrist.

Results

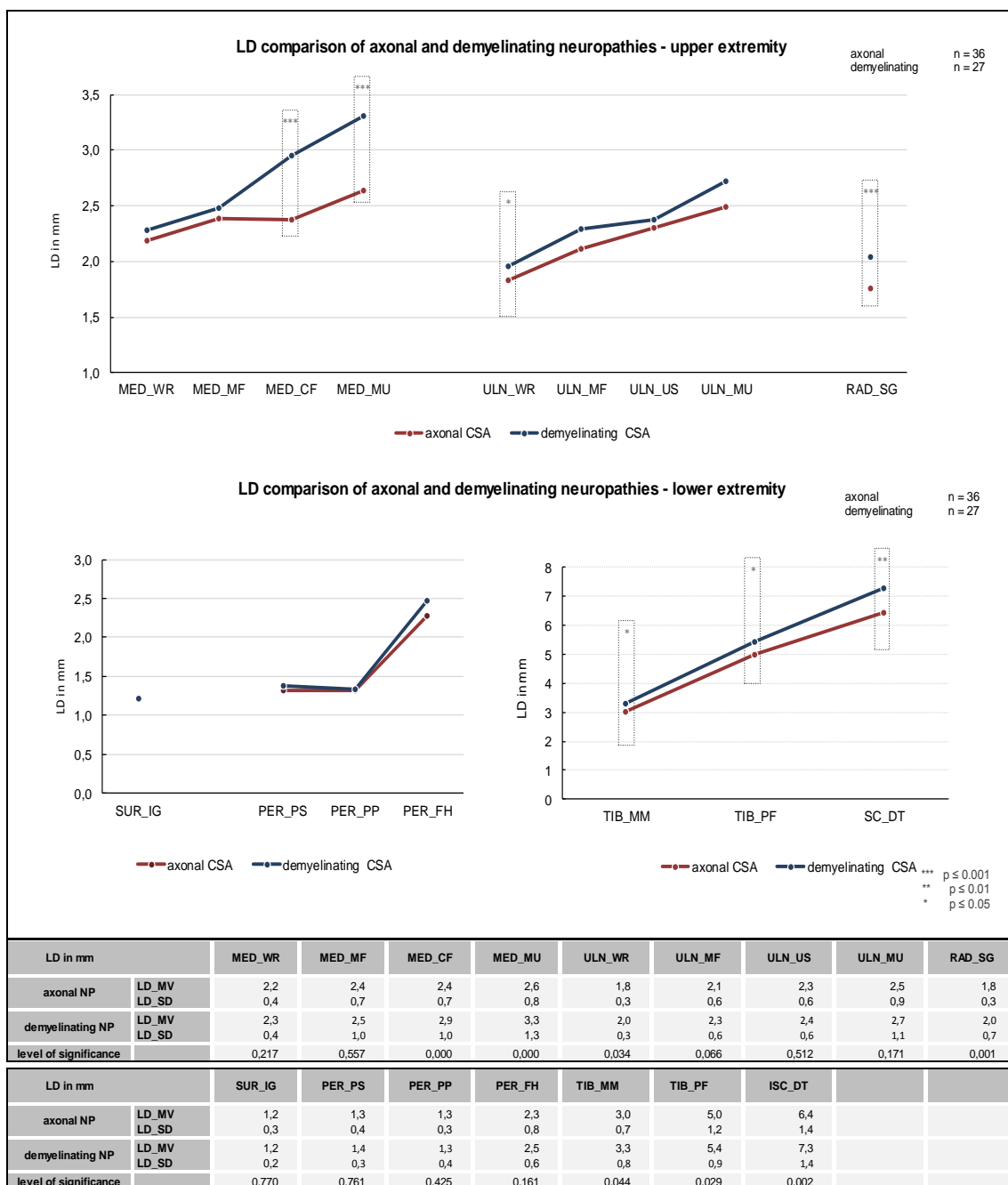


Figure 11: Longitudinal diameter (LD) comparison of patients with axonal and demyelinating neuropathies
 Abbreviations: ISC_DT = sciatic nerve, distal thigh; LD = longitudinal diameter; MED_CF = median nerve, cubital fossa; MED_MF = median nerve, mid forearm; MED_MU = median nerve, mid upper arm; MED_WR = median nerve, wrist; PER_FH = peroneal nerve, fibular head; PER_PP = peroneal nerve, profound peroneal nerve; PER_PS = peroneal nerve, superficial peroneal nerve; RAD_SG = radial nerve, spiral groove; SUR_IG = sural nerve, inter gastrocnemius muscle; TIB_MM = tibial nerve, medial malleolus; TIB_PF = tibial nerve, popliteal fossa; ULN_MF = ulnar nerve, mid forearm; ULN_MU = ulnar nerve, mid upper arm; ULN_US = ulnar nerve, ulnar sulcus; ULN_WR = ulnar nerve, wrist.

Results

3.3.3 Comparison between patients with inflammatory and non-inflammatory neuropathies

Following the criteria detailed in 2.3, 44/84 (52%) patients were classified as having inflammatory neuropathies and 12/84 (14%) patients as having non-inflammatory neuropathies. Figure 12 shows the intergroup comparison of CSA data. CSA at the ulnar nerve (wrist) was larger in patients with inflammatory neuropathies compared to non-inflammatory neuropathies ($p<0.05$). Also, the brachial plexus was larger in patients with inflammatory neuropathies compared to those with non-inflammatory neuropathies ($p<0.05$). The comparison of LD in both groups is shown in Table 13. LD did not differ between groups. Figure 12 shows the ROC of patients with inflammatory neuropathies in comparison to those without inflammatory neuropathies at supraclavicular and interscalene brachial plexus. At both sides the AUC for the detection of inflammation was > 0.5 .

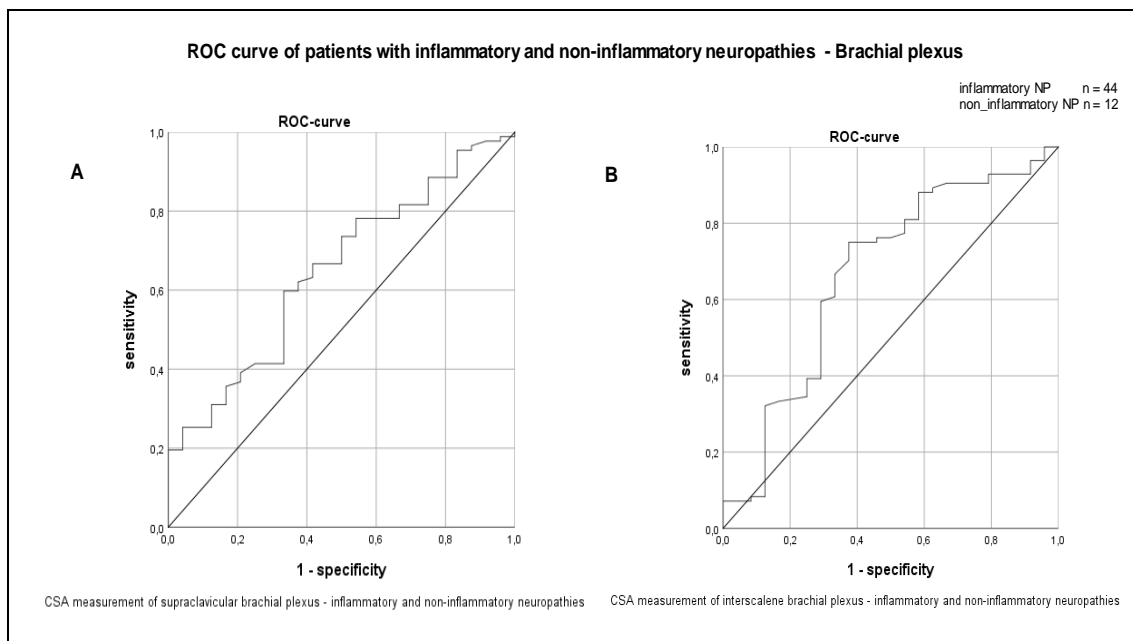


Figure 12: Receiver operating characteristic (ROC) of cross-sectional area (CSA) measurement at brachial plexus

A) ROC of supraclavicular brachial plexus AUC 0.647; standard error 0.61; confidence interval (95%): lower limit 0.528; upper limit 0.766. B) ROC of interscalene brachial plexus: AUC 0.66; standard error 0.67; confidence interval (95%): lower limit 0.534; upper limit 0.799.

Abbreviations: AUC = area under the curve; CSA= cross-sectional area, ROC = receiver operating characteristic.

Results

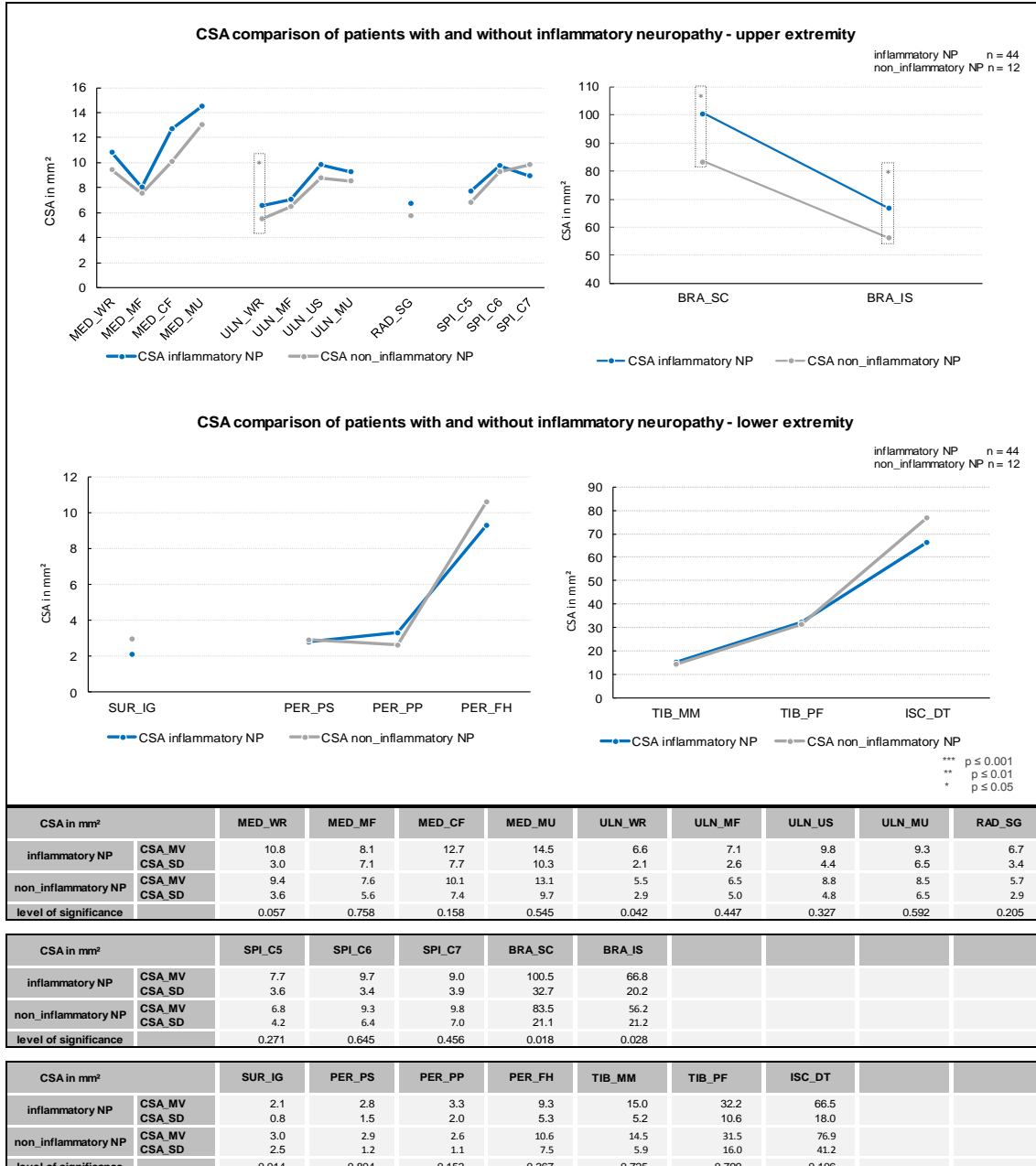


Figure 13: Cross-sectional area (CSA) comparison of patients with and without inflammatory neuropathy
Abbreviations: BRA_IS = brachial plexus, inter-scalene muscles; BRA_SC = brachial plexus; supra-clavicular; CSA = cross-sectional area; ISC_DT = sciatic nerve, distal thigh; MED_CF = median nerve, cubital fossa; MED_MF = median nerve, mid forearm; MED_MU = median nerve, mid upper arm; MED_WR = median nerve, wrist; NP = neuropathy; PER_FH = peroneal nerve, fibular head; PER_PP = peroneal nerve, profound peroneal nerve; PER_PS = peroneal nerve, superficial peroneal nerve; RAD SG = radial nerve, spiral groove; SPI_C5 = spinal nerve; SPI_C6 = spinal nerve, sixth cervical nerve; SPI_C7= spinal nerve, seventh cervical nerve; SUR_IG = sural nerve, inter gastrocnemius muscle; TIB_MM = tibial nerve, medial malleolus; TIB_PF = tibial nerve, popliteal fossa; ULN_MF = ulnar nerve, mid forearm; ULN_MU = ulnar nerve, mid upper arm; ULN_US = ulnar nerve, ulnar sulcus; ULN_WR = ulnar nerve, wrist.

Results

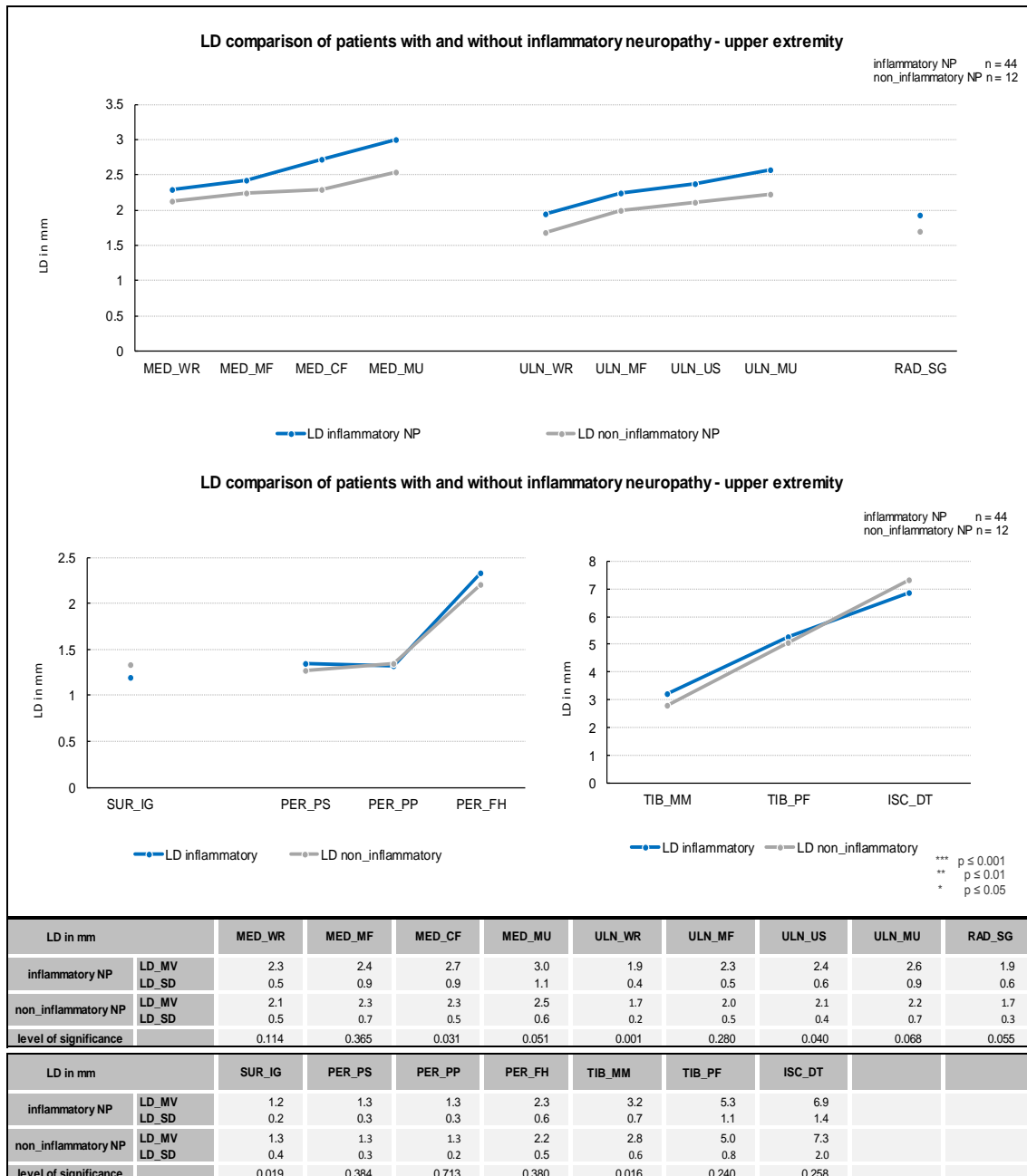


Figure 14: Longitudinal diameter (LD) comparison of patients with and without inflammatory neuropathy
 Abbreviations: ISC_DT = sciatic nerve, distal thigh; LD = longitudinal diameter; MED_CF = median nerve, cubital fossa; MED_MF = median nerve, mid forearm; MED_MU = median nerve, mid upper arm; MED_WR = median nerve, wrist; NP = nerve; BRA PER_FH = peroneal nerve, fibular head; PER_PP = peroneal nerve, profound peroneal nerve; PER_PS = peroneal nerve, superficial peroneal nerve; RAD_SG = radial nerve, spiral groove; SUR_IG = sural nerve, inter gastrocnemius muscle; TIB_MM = tibial nerve, medial malleolus; TIB_PF = tibial nerve, popliteal fossa; ULN_MF = ulnar nerve, mid forearm; ULN_MU = ulnar nerve, mid upper arm; ULN_US = ulnar nerve, ulnar sulcus; ULN_WR = ulnar nerve, wrist.

Results

3.3.4 Comparison between patients with painful and painless neuropathies

According to the definition given in 2.5, 51/84 (61%) patients reported painful neuropathy. Figure 15 shows the ROC for the investigation of pain for the supraclavicular plexus the AUC was < 0.5 and for the interscalene plexus the AUC was < 0.5 ($p > 0.05$). Figure 16 shows CSA data comparison between the two subgroups. CSA was larger in patients with painful neuropathy at the ulnar nerve (mid-forearm) and the sixth spinal nerve at upper extremity ($p < 0.05$ each) than in healthy controls. Similarly, the profound, superficial, and common peroneal nerve and the tibial nerve (popliteal fossa) were enlarged ($p < 0.05$ each) at the lower extremities. LD did not differ between groups (Figure 17).

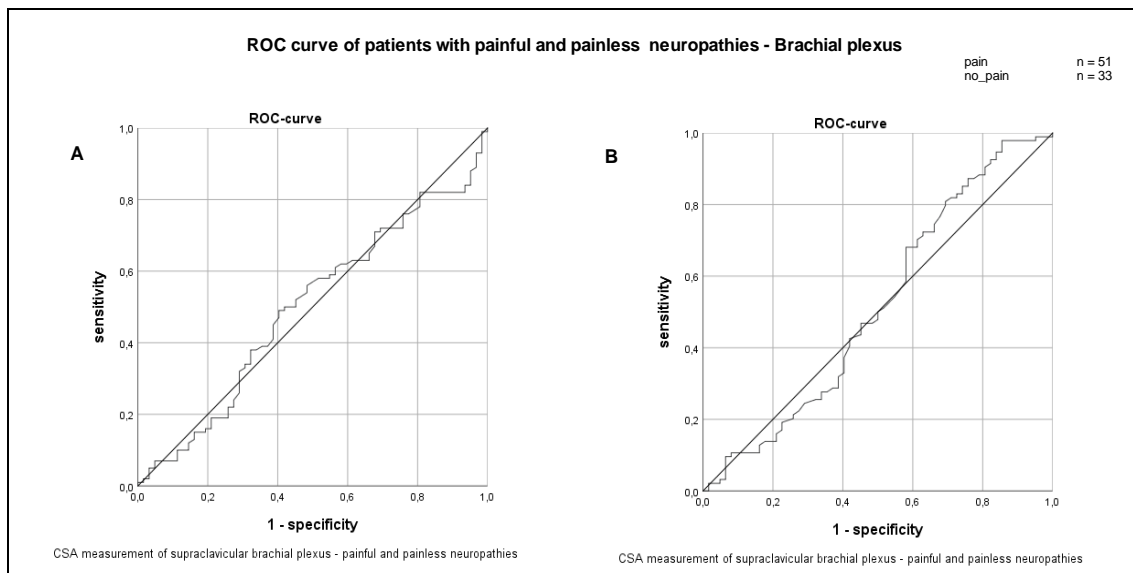


Figure 15: ROC of patients with painful and painless neuropathies – brachial plexus
 A) ROC-curve of CSA measurement at supraclavicular brachial plexus B) ROC-curve of CSA measurement at interscalene brachial plexus.
 A) AUC 0.497; standard error 0.047; confidence interval (95%): lower limit 0.405; upper limit 0.588 B) AUC 0.516; standard error 0.049; confidence interval (95%): lower limit 0.420; upper limit 0.613 Abbreviations:
 AUC = area under the curve; CSA= cross-sectional area, ROC = receiver operating characteristic.

Results

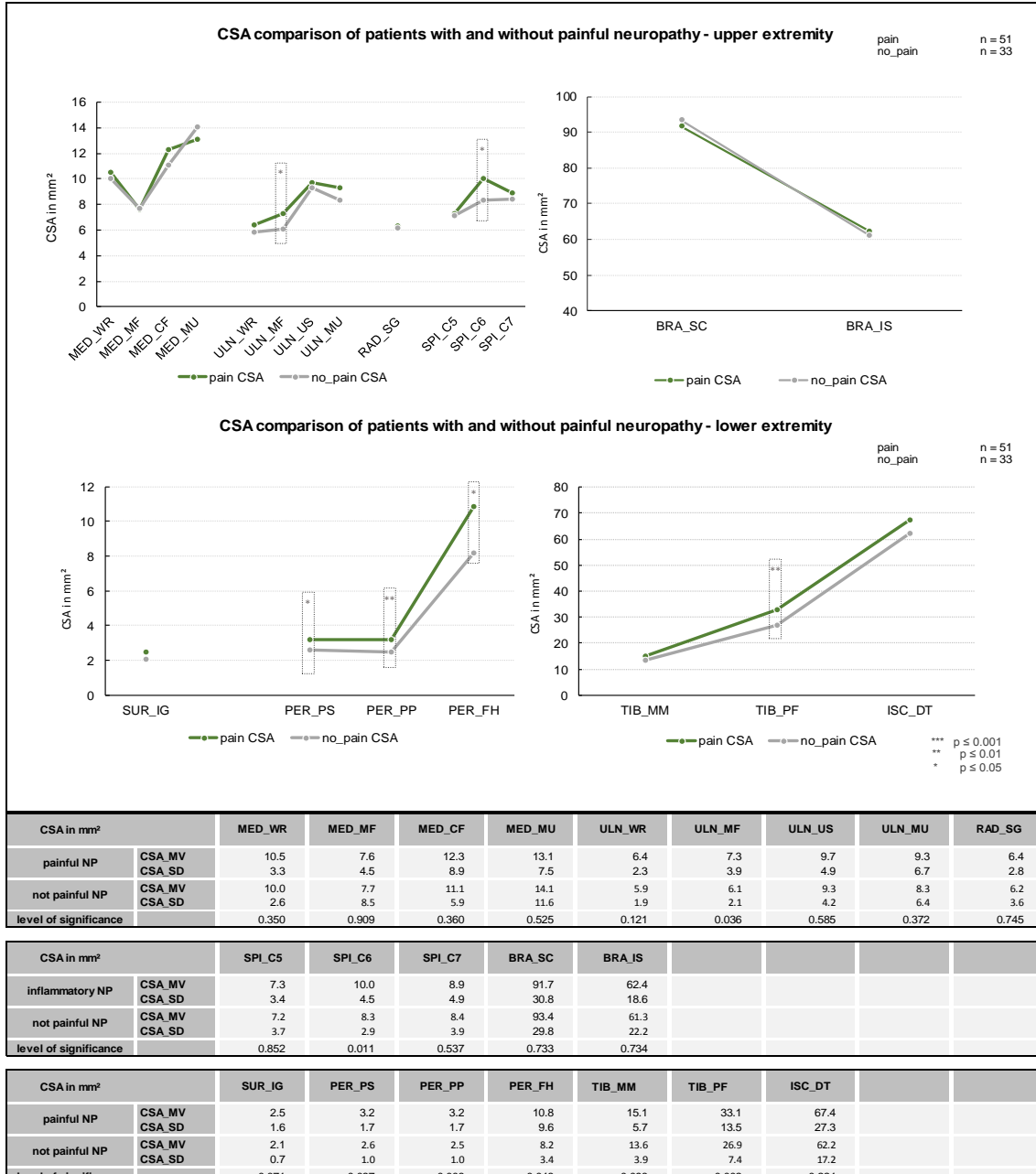


Figure 16: Cross-sectional area (CSA) comparison of patients with and without painful neuropathy
Abbreviations: BRA_IS = brachial plexus, inter-scalene muscles; BRA_SC = brachial plexus; supra-clavicular; CSA = cross-sectional area; ISC_DT = sciatic nerve, distal thigh; MED_CF = median nerve, cubital fossa; MED_MF = median nerve, mid forearm; MED_MU = median nerve, mid upper arm; MED_WR = median nerve, wrist; NP = neuropathy; PER_FH = peroneal nerve, fibular head; PER_PP = peroneal nerve, profound peroneal nerve; PER_PS = peroneal nerve, superficial peroneal nerve; RAD_SG = radial nerve, spiral groove; SPI_C5 = spinal nerve; SPI_C6 = spinal nerve, sixth cervical nerve; SPI_C7 = spinal nerve, seventh cervical nerve; SUR_IG = sural nerve, inter gastrocnemius muscle; TIB_MM = tibial nerve, medial malleolus; TIB_PF = tibial nerve, popliteal fossa; ULN_MF = ulnar nerve, mid forearm; ULN_MU = ulnar nerve, mid upper arm; ULN_US = ulnar nerve, ulnar sulcus; ULN_WR = ulnar nerve, wrist.

Results

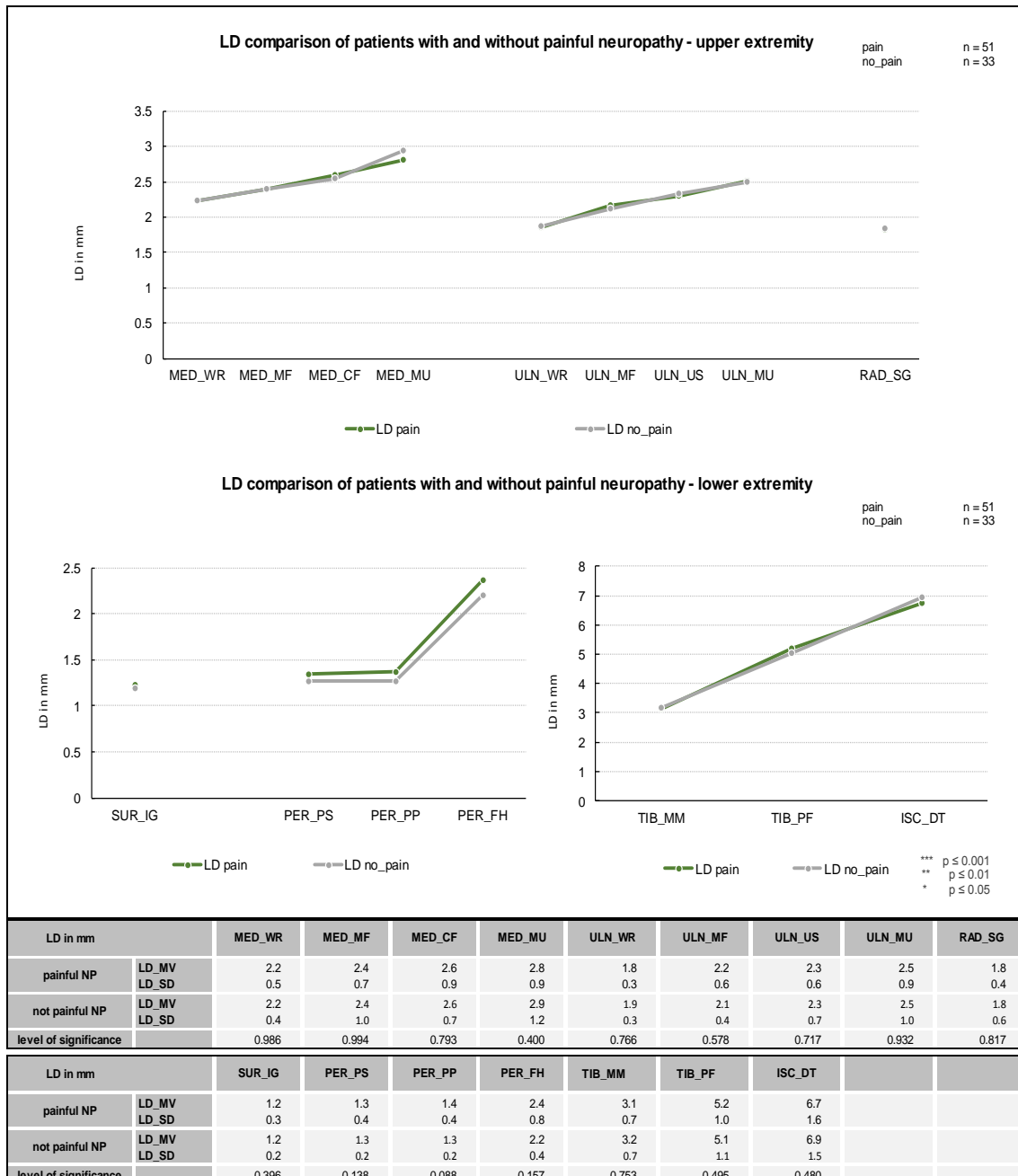


Figure 17: Longitudinal diameter (LD) comparison of patients with and with painless neuropathy

Abbreviations: ISC_DT = sciatic nerve, distal thigh; LD = longitudinal diameter; MED_CF = median nerve, cubital fossa; MED_MF = median nerve, mid forearm; MED_MU = median nerve, mid upper arm; MED_WR = median nerve, wrist; NP = neuropathy; PER_FH = peroneal nerve, fibular head; PER_PP = peroneal nerve, profound peroneal nerve; PER_PS = peroneal nerve, superficial peroneal nerve; RAD_SG = radial nerve, spiral groove; SUR_IG = sural nerve, inter gastrocnemius muscle; TIB_MM = tibial nerve, medial malleolus; TIB_PF = tibial nerve, popliteal fossa; ULN_MF = ulnar nerve, mid forearm; ULN_MU = ulnar nerve, mid upper arm; ULN_US = ulnar nerve, ulnar sulcus; ULN_WR = ulnar nerve, wrist.

Abbreviations: ISC_DT = sciatic nerve, distal thigh; LD = longitudinal diameter; MED_CF = median nerve, cubital fossa; MED_MF = median nerve, mid forearm; MED_MU = median nerve, mid upper arm; MED_WR = median nerve, wrist; NP = neuropathy; PER_FH = peroneal nerve, fibular head; PER_PP = peroneal nerve, profound peroneal nerve; PER_PS = peroneal nerve, superficial peroneal nerve; RAD_SG = radial nerve, spiral groove; SUR_IG = sural nerve, inter gastrocnemius muscle; TIB_MM = tibial nerve, medial malleolus; TIB_PF = tibial nerve, popliteal fossa; ULN_MF = ulnar nerve, mid forearm; ULN_MU = ulnar nerve, mid upper arm; ULN_US = ulnar nerve, ulnar sulcus; ULN_WR = ulnar nerve, wrist.

Results

3.3.5 Characterization of the patient subgroup with NSVN

We recruited eleven patients with NSVN. The median disease duration at inclusion was 5.1 (0.5-10 years) years. 7/11 (64%) had received immunomodulatory therapy before HRUS assessment. In 11/11 (100%) patients sural nerve biopsy was performed. As an example, Figure 18 shows HRUS images of CSA and LD of the median nerve at wrist of a patient diagnosed with NSVN. Figure 19 shows the results for the CSA of the cohort diagnosed with NSVN compared to healthy controls. At the upper extremities, CSA enlargement ($p<0.01$) was detected at all sites, except for the sixth and seventh spinal nerve and the interscalene brachial plexus. Also, at the lower extremities, all investigated nerve sites showed larger CSA in patients with NSVN compared to healthy controls ($p<0.01$ each), except for the sural nerve which was not different between groups. Figure 20 shows the results for the LD which was enlarged at most sites of median, ulnar, and radial nerves at the upper extremities ($p<0.05$ each). At the lower extremities, enlargement was only found at the superficial peroneal nerve ($p<0.001$) and the tibial nerve at the popliteal fossa ($p<0.05$). Figure 21 illustrates brachial plexus of a patient diagnosed with NSVN. CSA is enlarged with inhomogeneous distributed hypoechoogenic structures within the plexus structure. Figures 22 – 24 show ROCs of the brachial plexus and median, ulnar, and tibial nerve. AUC was > 0.6 for all measured nerves at all measuring sites for CSA and LD.

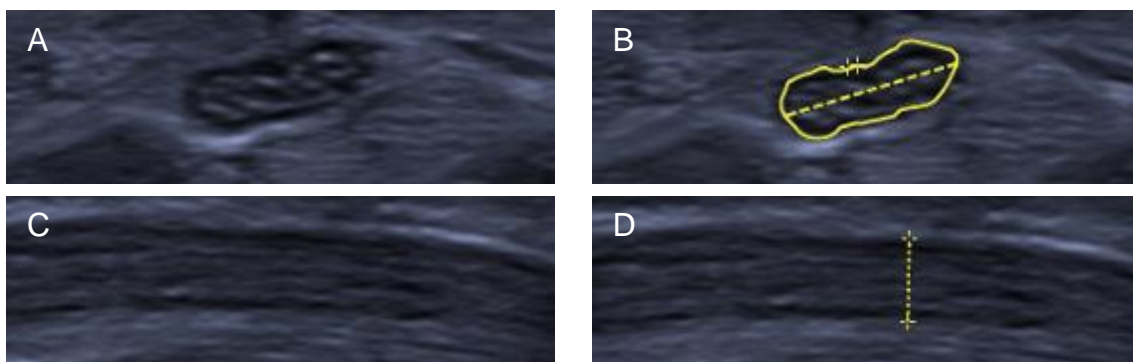


Figure 18: Median Nerve of patient with non-systemic vasculitic neuropathy (NSVN) – cross-section and longitudinal section

A) Median nerve at wrist in cross-section; patient with non-systemic vasculitic neuropathy (NSVN). B) Median nerve at wrist measurement of cross-sectional area; patient with NSVN; CSA = 14 mm² (control: mean 8.9 mm²; standard deviation 1.8 mm²) C) Median nerve at wrist in longitudinal section; patient with NSVN D) Median nerve at wrist measurement of longitudinal diameter; patient with NSVN; LD = 2.6 mm (control: mean 2.1 mm²; standard deviation 1.8 mm²).

Results

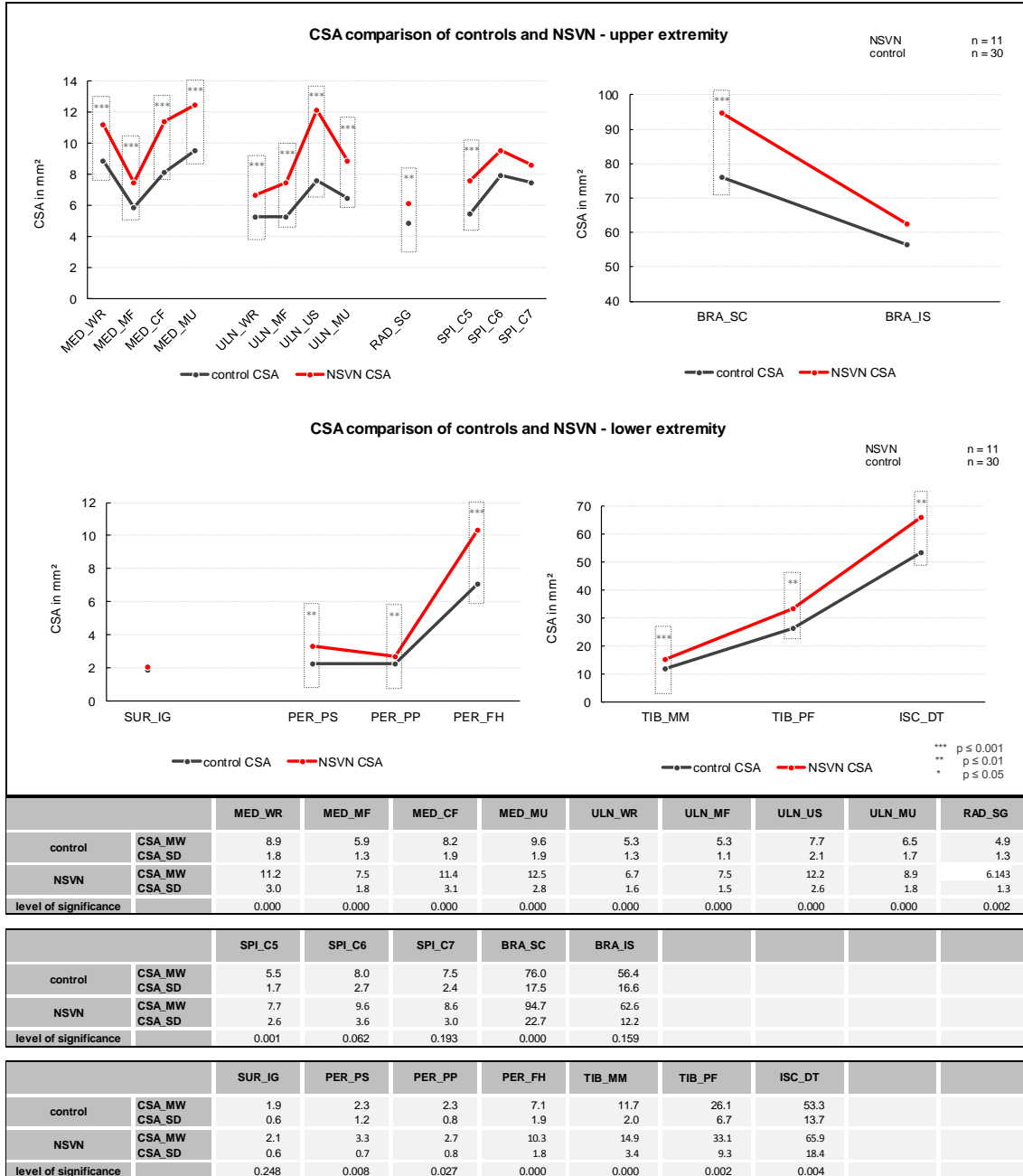


Figure 19: Cross-sectional area (CSA) comparison of control subjects and patients with non-systemic vasculitic neuropathy (NSVN)

Abbreviations: BRA_IS = brachial plexus, inter-scalene muscles; BRA_SC = brachial plexus; supraclavicular; CSA = cross-sectional area; ISC_DT = sciatic nerve, distal thigh; MED_CF = median nerve, cubital fossa; MED_MF = median nerve, mid forearm; MED_MU = median nerve, mid upper arm; MED_WR = median nerve, wrist; NSVN = non-systemic vasculitic neuropathy; PER_FH = peroneal nerve, fibular head; PER_PP = peroneal nerve, profound peroneal nerve; PER_PS = peroneal nerve, superficial peroneal nerve; RAD_SG = radial nerve, spiral groove; SPI_C5 = spinal nerve; SPI_C6 = spinal nerve, sixth cervical nerve; SPI_C7 = spinal nerve, seventh cervical nerve; SUR_IG = sural nerve, inter gastrocnemius muscle; TIB_MM = tibial nerve, medial malleolus; TIB_PF = tibial nerve, popliteal fossa; ULN_MF = ulnar nerve, mid forearm; ULN_MU = ulnar nerve, mid upper arm; ULN_US = ulnar nerve, ulnar sulcus; ULN_WR = ulnar nerve, wrist.

Results

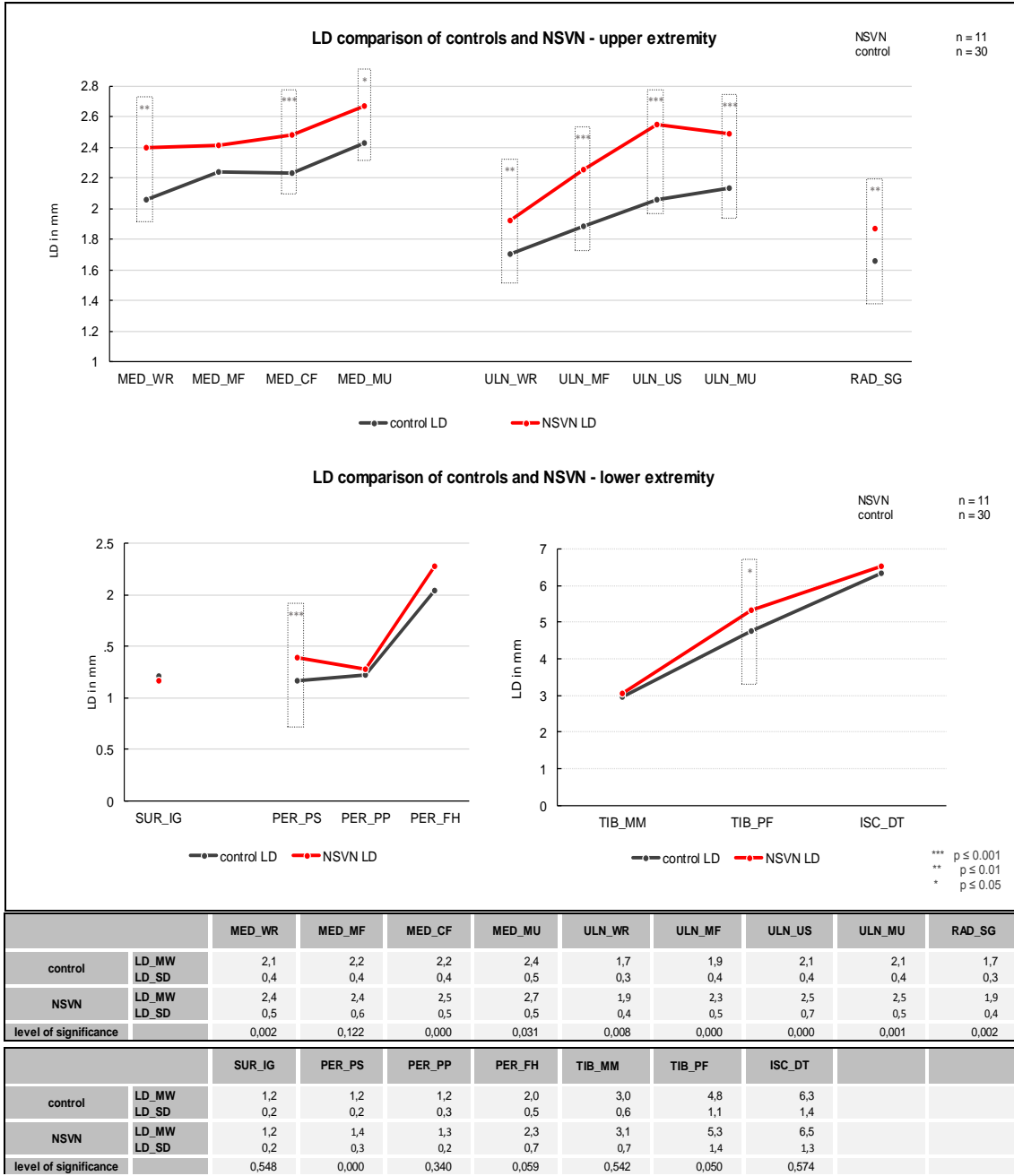


Figure 20: Longitudinal diameter (LD) comparison of healthy control subjects and patients with non-systemic vasculitic neuropathy (NSVN)

Abbreviations: ISC_DT = sciatic nerve, distal thigh; LD = longitudinal diameter; MED_CF = median nerve, cubital fossa; MED_MF = median nerve, mid forearm; MED_MU = median nerve, mid upper arm; MED_WR = median nerve, wrist; MV = median value; LD = longitudinal diameter; NSVN = non-systemic vasculitic neuropathy; PER_FH = peroneal nerve, fibular head; PER_PP = peroneal nerve, profound peroneal nerve; PER_PS = peroneal nerve, superficial peroneal nerve; RAD_SG = radial nerve, spiral groove; SD = standard deviation; SUR_IG = sural nerve, inter gastrocnemius muscle; TIB_MM = tibial nerve, medial malleolus; TIB_PF = tibial nerve, popliteal fossa; ULN_MF = ulnar nerve, mid forearm; ULN_US = ulnar nerve, ulnar sulcus; ULN_WR = ulnar nerve, wrist.

Results

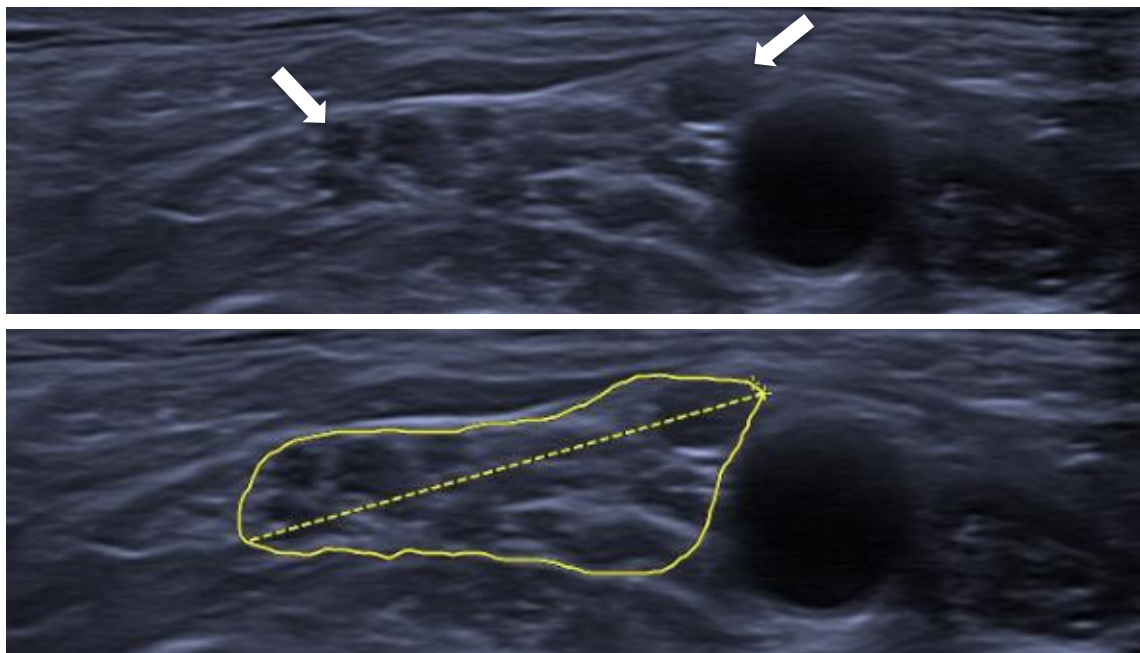


Figure 21: Supraclavicular Brachial plexus; patient with non-systemic vasculitic neuropathy (NSVN)
A) White arrows show hypoechoic fascicular structures within the plexus B) Measurement of CSA = 109 mm² (healthy control cohort: mean 76 mm² standard deviation 17,5 mm)
Abbreviations: CSA = cross-sectional area; mm = millimeter; NSVN = non-systemic vasculitic neuropathy.

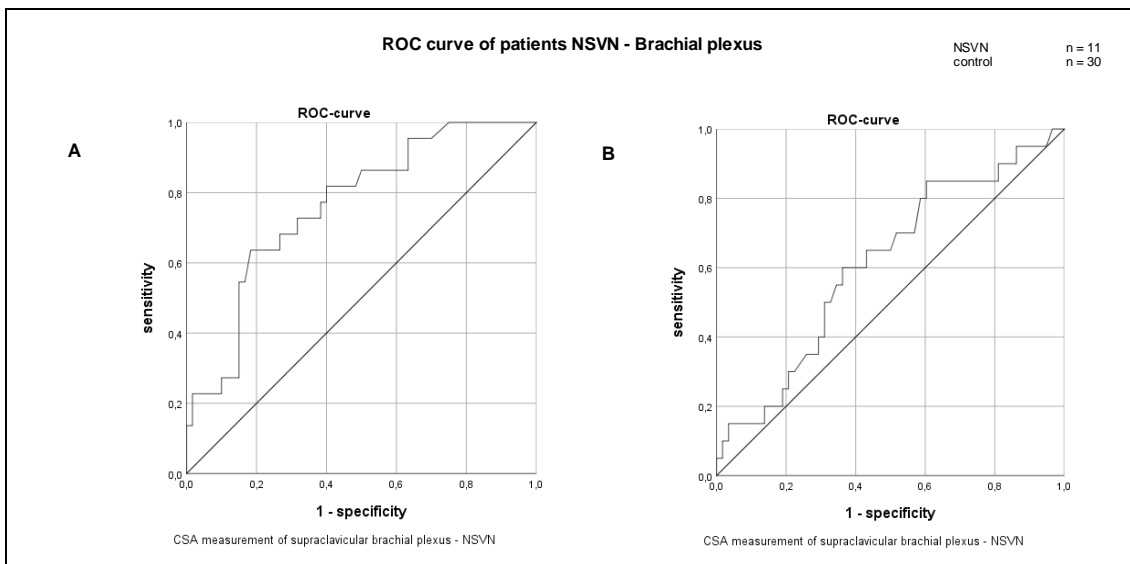


Figure 22: ROC of patients with non-systemic-vasculitic neuropathy (NSVN) – brachial plexus
A) Receiver operating characteristic (ROC) of cross-sectional area (CSA) measurement at supraclavicular brachial plexus. AUC 0.762; standard error 0.057; confidence interval (95%): lower limit 0.651; upper limit 0.874
B) ROC of CSA measurement at interscalene brachial plexus. AUC 0.612; standard error 0.072; confidence interval (95%): lower limit 0.470; upper limit 0.753
Abbreviations: AUC = area under the curve; CSA= cross-sectional area, NSVN = non-systemic vasculitic neuropathy; ROC-curve = receiver operating characteristic-curve.

Results

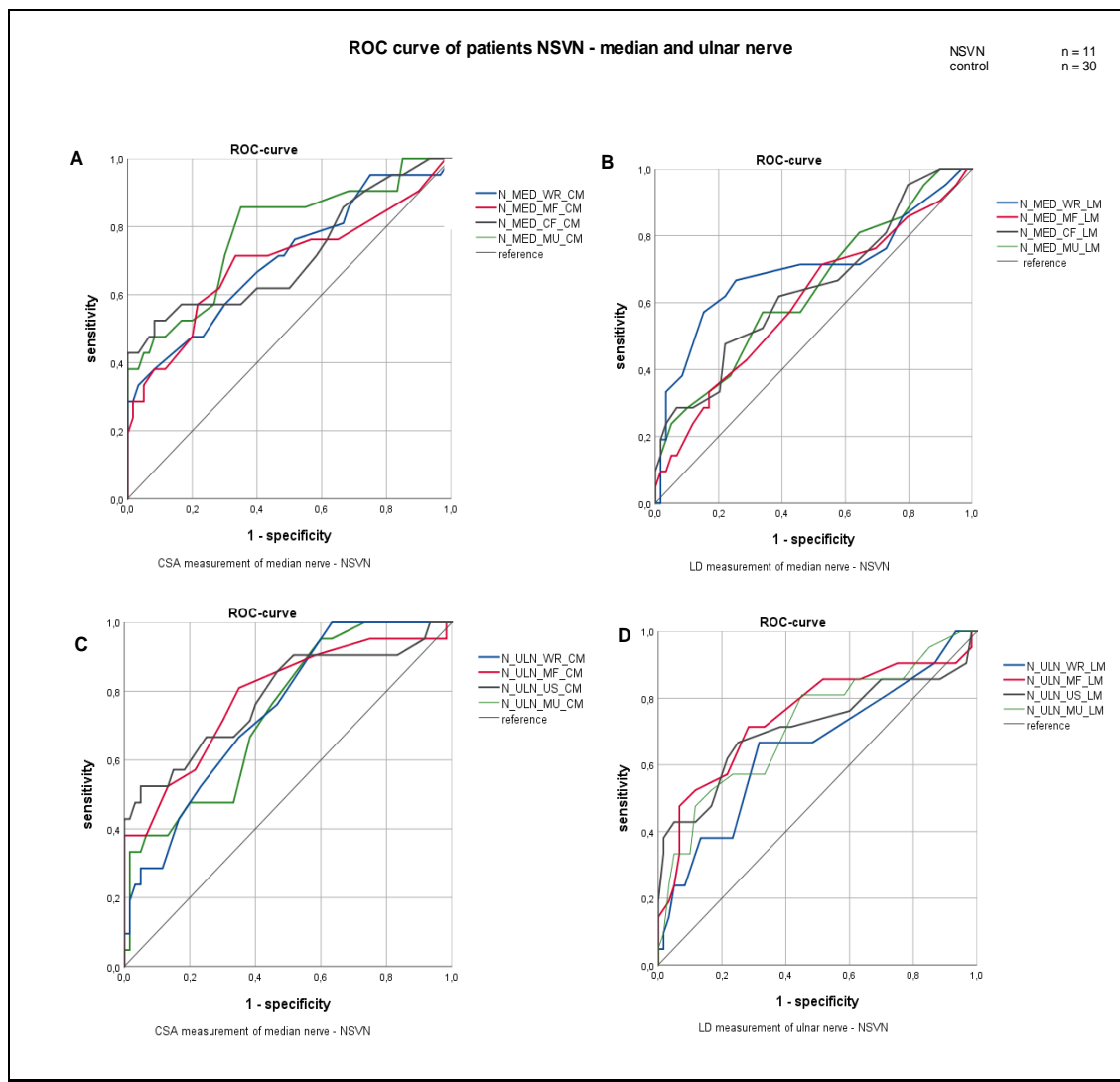


Figure 23: ROC of patients with non-systemic-vasculitic neuropathy (NSVN) – median and ulnar nerve

A) Receiver operating characteristic (ROC) of cross-sectional area (CSA) measurement median nerve in patients with non-systemic vasculitic neuropathy (NSVN) B) Receiver operating characteristic (ROC) of longitudinal diameter (LD) measurement median nerve in patients with non-systemic vasculitic neuropathy (NSVN) C) Receiver operating characteristic (ROC) of cross-sectional area (CSA) measurement ulnar nerve in patients with non-systemic vasculitic neuropathy (NSVN) D) Receiver operating characteristic (ROC) of cross-sectional area (CSA) measurement median nerve in patients with non-systemic vasculitic neuropathy (NSVN) E) data reference to A-D. Abbreviations: AUC = area under the curve; CSA= cross-sectional area, LD = longitudinal diameter; MED_CF = median nerve, cubital fossa; MED_MF = median nerve, mid forearm; MED_MU = median nerve, mid upper arm; MED_WR = median nerve, wrist; ROC-curve = receiver operating characteristic-curve; SE = standard error; ULN_MF = ulnar nerve, mid forearm; ULN_MU = ulnar nerve, mid upper arm; ULN_US = ulnar nerve, ulnar sulcus; ULN_WR = ulnar nerve, wrist.

Results

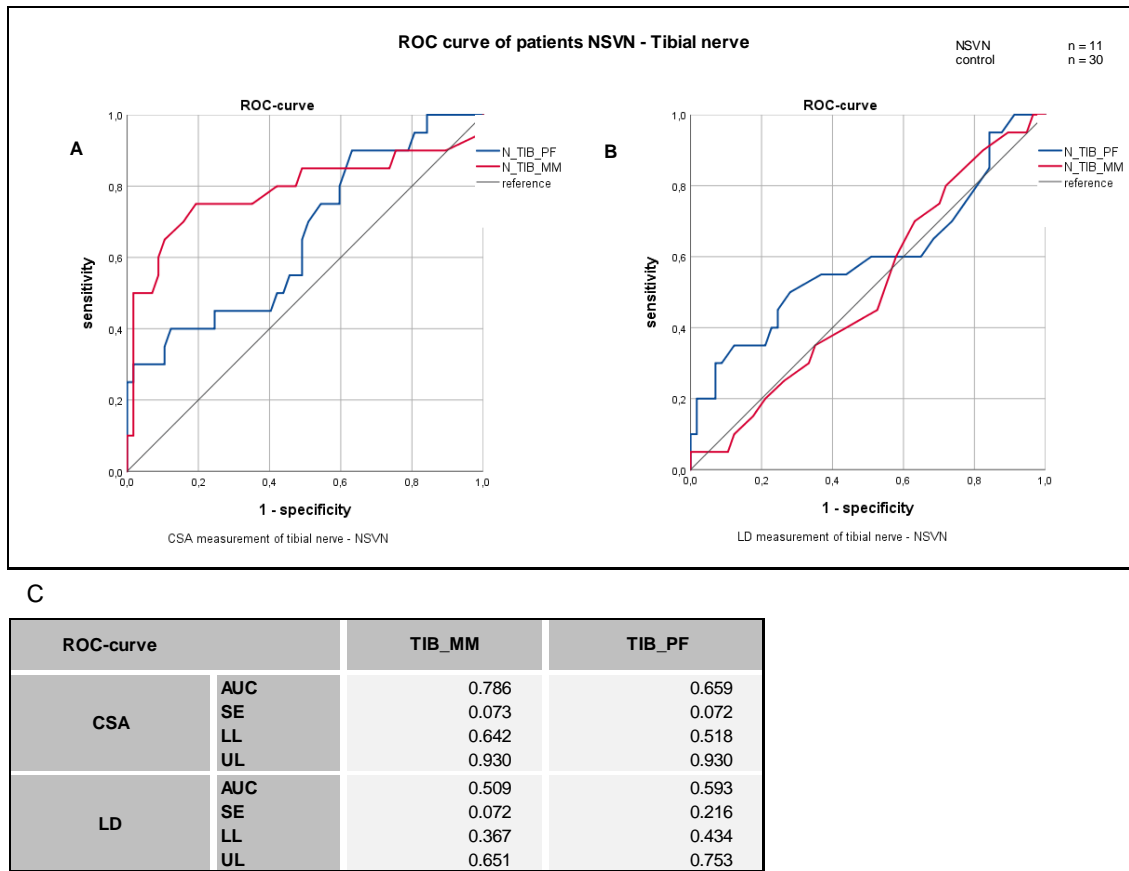


Figure 24: ROC of patients with non-systemic-vasculitic neuropathy (NSVN) – tibial nerve

A) Receiver operating characteristic (ROC) of cross-sectional area (CSA) measurement of tibial nerve in patients with non-systemic vasculitic neuropathy (NSVN) B) ROC of longitudinal diameter (LD) measurement of tibial nerve in patients with NSVN C) data reference to A-B

Abbreviations: AUC = area under the curve; CSA= cross-sectional area, LD = longitudinal diameter; NSVN = non-systemic vasculitic neuropathy; ROC-curve = receiver operating characteristic-curve; SE = standard error; TIB_MM = tibial nerve, medial malleolus; TIB_PF = tibial nerve, popliteal fossa. NSVN = non-systemic vasculitic neuropathy; ROC-curve = receiver operating characteristic-curve; SE = standard error; TIB_MM = tibial nerve, medial malleolus; TIB_PF = tibial nerve, popliteal fossa.

Results

3.3.6 Characterization of the subgroup with CIDP

Twelve patients were diagnosed with CIDP. Of these twelve patients, ten fulfilled the INCAT criteria (Sander and Latov 2003). Median disease duration was 12 years (0.5-25 years). Figure 25 shows the median nerve at the cubital fossa with enlarged CSA and LD. Figure 26 shows the CSA of patients diagnosed with CIDP compared to the cohort of healthy controls. Enlargement of the CSA ($p<0.05$) was found at all sites investigated except for the seventh spinal nerve. The entire median, ulnar, and radial nerves showed CSA enlargement ($p<0.01$) in patients with CIDP. This was also true for spinal nerves and the supraclavicular plexus ($p<0.001$). At the lower extremities, enlargement of the CSA was found in all nerves and at all nerve sites ($p<0.001$). LD results are shown in Figure 27 and correlate positively with the CSA ($p<0.05$). Figure 28 gives an example of a supraclavicular brachial plexus of a patient diagnosed with CIDP. One typical finding are hypoechoic segments within the plexus. Cross sectional area is often increased. Results of ROC- analysis of supraclavicular and interscalene plexus is shown in Figures 29-31. AUC reaches >0.6 for most measuring sites with exception of tibial nerve at malleolus medialis for LD. At many measuring sites AUC was >0.8 .

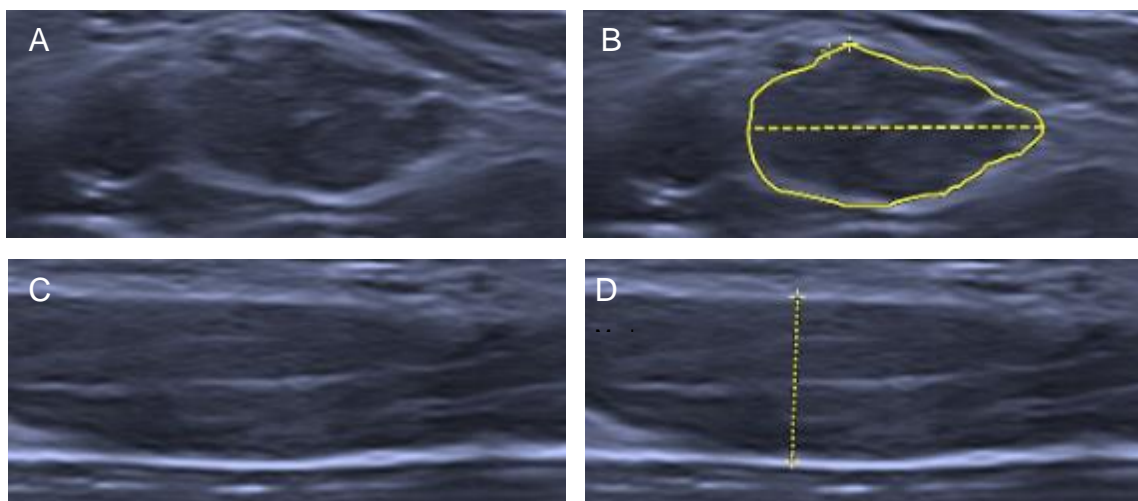


Figure 25: Median nerve at cubital fossa of a patient with chronic inflammatory demyelinating polyneuropathy (CIDP) – cross-section and longitudinal section

A) Median nerve at cubital fossa in cross section; patient with chronic inflammatory demyelinating polyneuropathy (CIDP). B) Median nerve at cubital fossa measurement of cross-sectional area (CSA); patient with CIDP; CSA = 47 mm² (healthy control cohort: mean 8.2 mm² standard deviation 1.9mm²) C) Median nerve at cubital fossa in longitudinal section- patient with CIDP. D) Median nerve at cubital fossa measurement of longitudinal diameter- patient with CIDP; LD = 6.1 mm (healthy control cohort: mean 2.2 mm, standard deviation 0.3mm).

Results

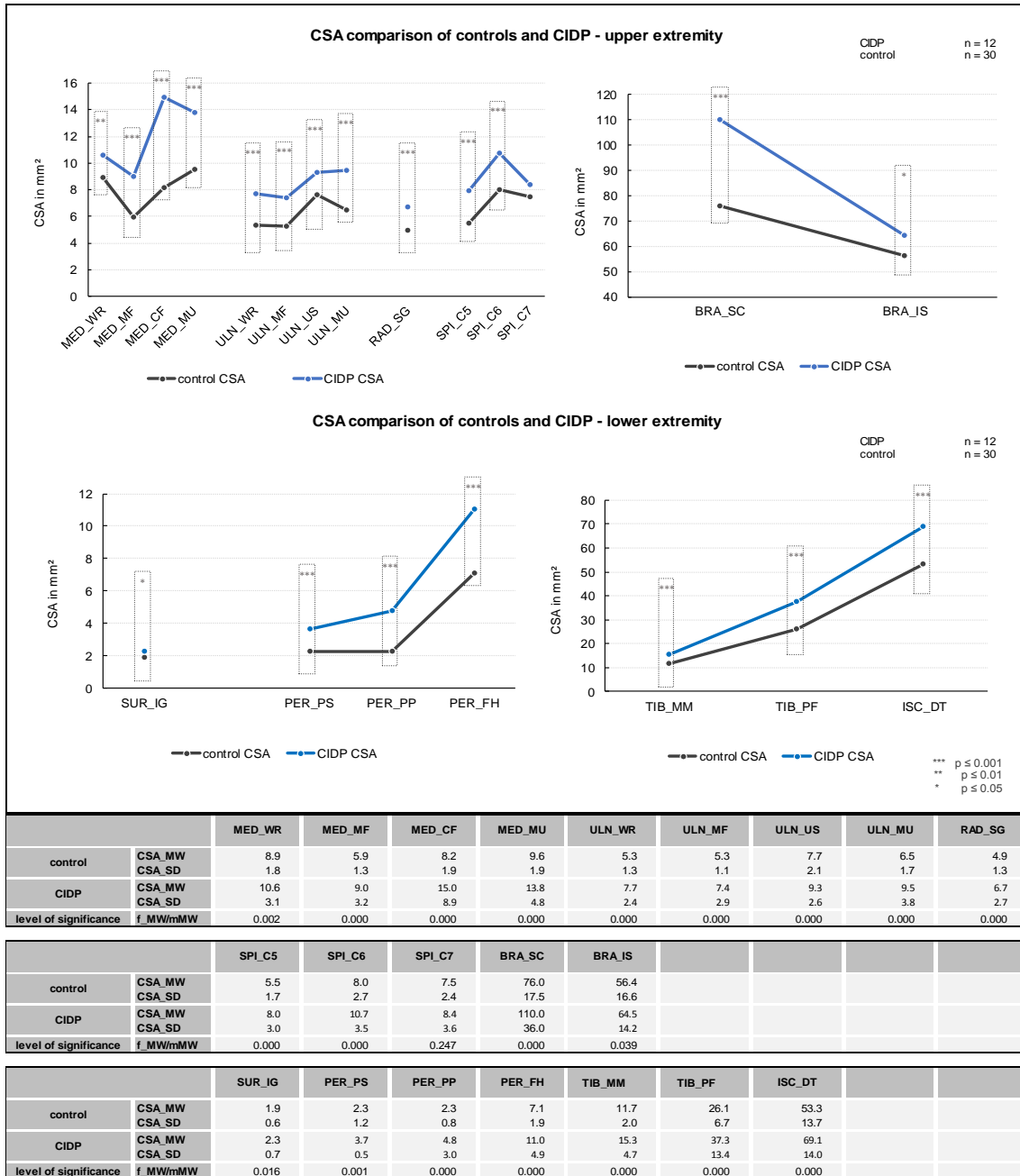


Figure 26: Cross-sectional area (CSA) comparison of healthy control subjects and patients with chronic inflammatory demyelinating polyneuropathy (CIDP)
BRA_IS = brachial plexus, inter-scalene muscles; BRA_SC = brachial plexus; CSA = cross-sectional area; CIDP = Chronic inflammatory demyelinating polyneuropathy; ISC_DT = sciatic nerve, distal thigh; MED_CF = median nerve, cubital fossa; MED_MF = median nerve, mid forearm; MED_MU = median nerve, mid upper arm; MED_WR = median nerve, wrist; PER_FH = peroneal nerve, fibular head; PER_PP = peroneal nerve, profound peroneal nerve; PER_PS = peroneal nerve, superficial peroneal nerve; RAD SG = radial nerve, spiral groove; SPI_C5 = spinal nerve; SPI_C6 = spinal nerve, sixth cervical nerve; SPI_C7 = spinal nerve, seventh cervical nerve; SUR_IG = sural nerve, inter gastrocnemius muscle; TIB_MM = tibial nerve, medial malleolus; TIB_PF = tibial nerve, popliteal fossa; ULN_MF = ulnar nerve, mid forearm; ULN_MU = ulnar nerve, mid upper arm; ULN_US = ulnar nerve, ulnar sulcus; ULN_WR = ulnar nerve, wrist.

Results

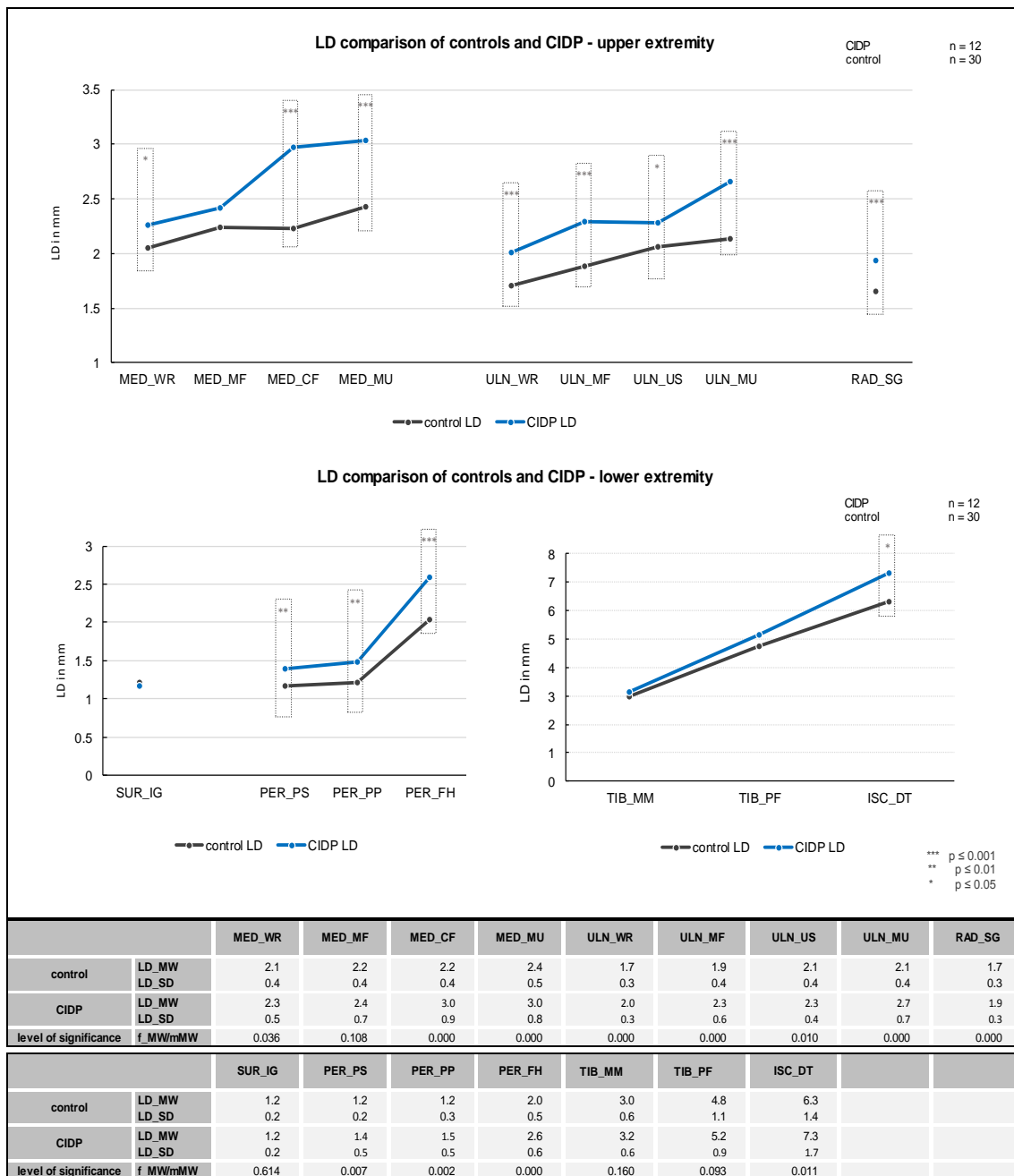


Figure 27: Longitudinal diameter (LD) comparison of healthy control subjects and chronic inflammatory neuropathy (CIDP)

Abbreviations: CIDP = chronic inflammatory demyelinating neuropathy; ISC_DT = sciatic nerve, distal thigh; LD = longitudinal diameter; MED_CF = median nerve, cubital fossa; MED_MF = median nerve, mid forearm; MED_MU = median nerve, mid upper arm; MED_WR = median nerve, wrist; PER_FH = peroneal nerve, fibular head; PER_PP = peroneal nerve, profound peroneal nerve; PER_PS = peroneal nerve, superficial peroneal nerve; RAD_SG = radial nerve, spiral groove; SUR_IG = sural nerve, inter gastrocnemius muscle; TIB_MM = tibial nerve, medial malleolus; TIB_PF = tibial nerve, popliteal fossa; ULN_MF = ulnar nerve, mid forearm; ULN_MU = ulnar nerve, mid upper arm; ULN_US = ulnar nerve, ulnar sulcus; ULN_WR = ulnar nerve, wrist.

Results

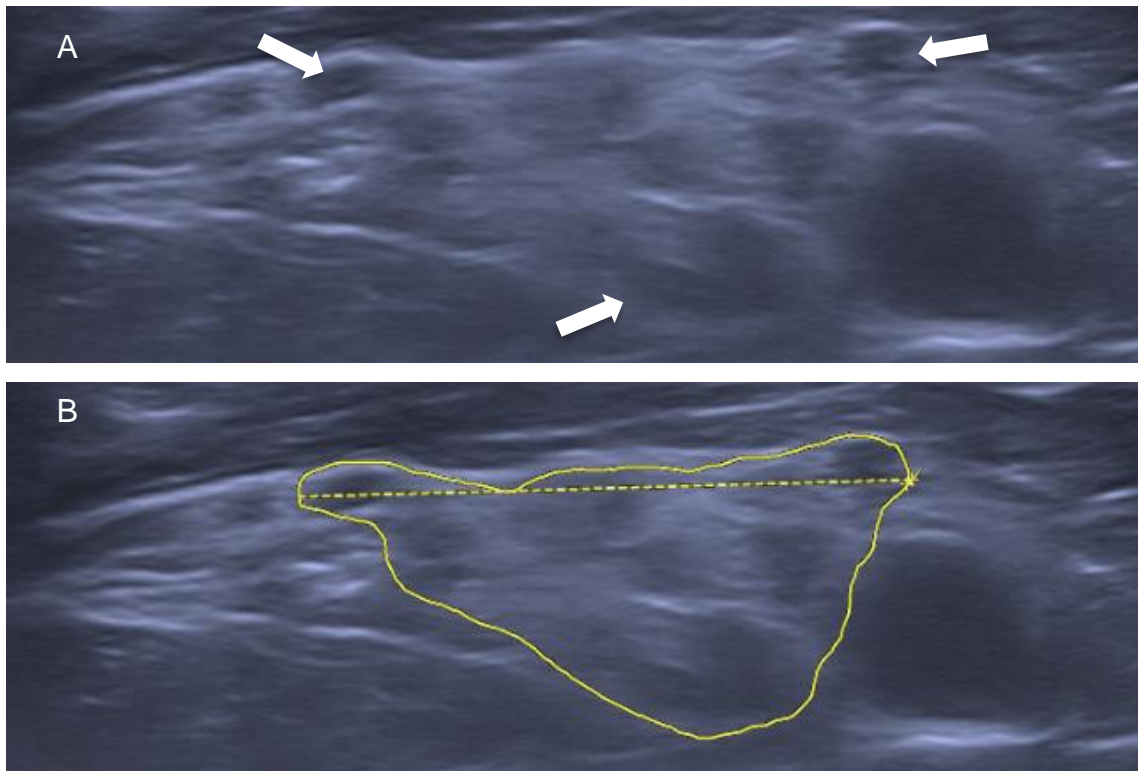


Figure 29: Supraclavicular Brachial plexus; patient with chronic inflammatory demyelinating polyneuropathy (CIDP) – cross-section

A) White arrows show hypoechoic fascicular structures within the plexus B) Measurement of cross-sectional area (CSA) = 200mm² (healthy control cohort: mean 76 mm² standard deviation 17.5 mm)

Abbreviations: CIDP = chronic inflammatory demyelinating polyneuropathy; CSA = cross-sectional area; mm = millimeter.

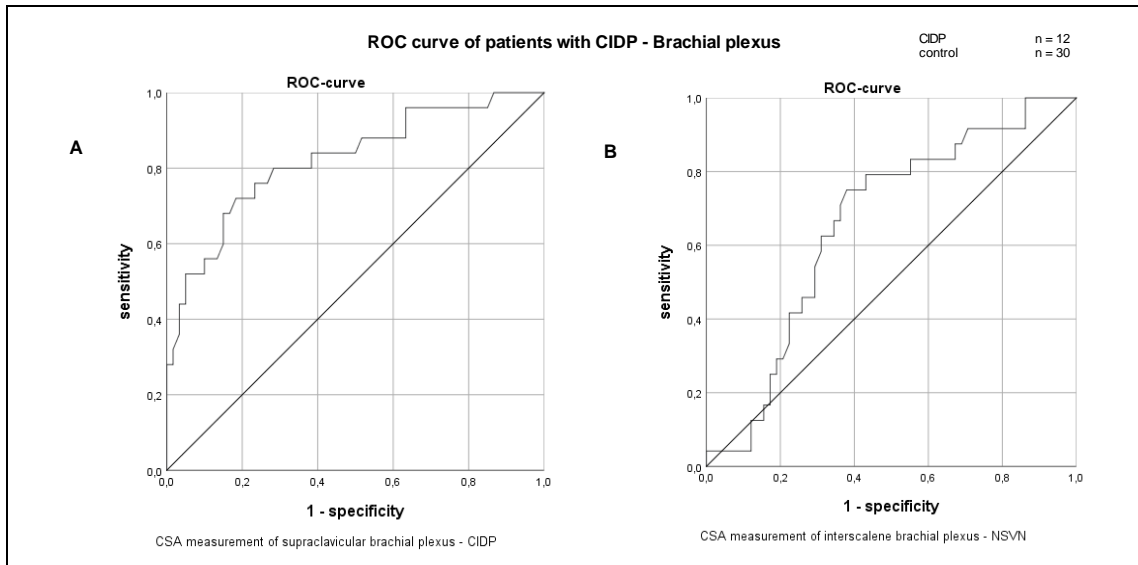


Figure 28: ROC of patients with chronic inflammatory demyelinating polyneuropathy (CIDP)– brachial plexus
A) Receiver operating characteristic (ROC) of cross-sectional area (CSA) measurement median nerve in patients with non-systemic vasculitic neuropathy (NSVN)

A) Receiver operating characteristic (ROC) of cross-sectional area (CSA) measurement at supraclavicular brachial plexus. AUC 0.82; standard error 0.053; confidence interval (95%): lower limit 0.72; upper limit 0.93
B) ROC of CSA measurement at interscalene brachial plexus. AUC 0.66; standard error 0.063; confidence interval (95%): lower limit 0.53; upper limit 0.78.

Abbreviations: AUC = area under the curve; CIDP = chronic inflammatory demyelinating polyneuropathy; CSA= cross-sectional area, ROC-curve = receiver operating characteristic-curve.

Results

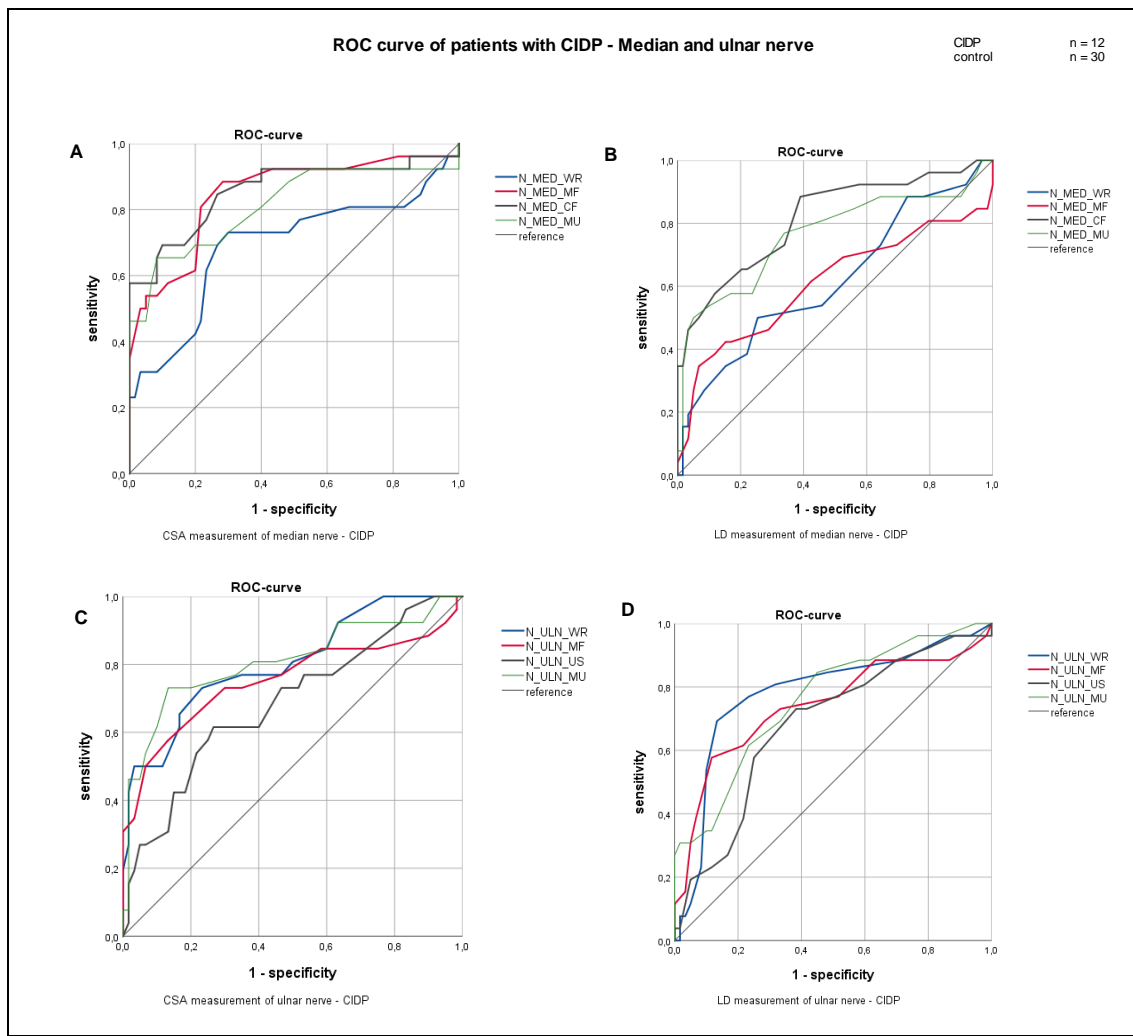


Figure 30: ROC of patients with chronic inflammatory demyelinating polyneuropathy (CIDP) -median and ulnar nerve

A) Receiver operating characteristic (ROC) of cross-sectional area (CSA) measurement median nerve in patients with chronic inflammatory demyelinating polyneuropathy (CIDP) B) ROC of longitudinal diameter (LD) measurement median nerve in patients with CIDP C) ROC-curve of CSA measurement ulnar nerve in patients with CIDP D) ROC-curve of CSA measurement median nerve in patients with CIDP E) data reference to A-D

Abbreviations: AUC = area under the curve; CIDP = chronic inflammatory demyelinating polyneuropathy; CSA= cross-sectional area, LD = longitudinal diameter; MED_CF = median nerve, cubital fossa; MED_MF = median nerve, mid forearm; MED_MU = median nerve, mid upper arm; MED_WR = median nerve, wrist; ROC-curve = receiver operating characteristic-curve; SE = standard error; ULN_MF = ulnar nerve, mid forearm; ULN_MU = ulnar nerve, mid upper arm; ULN_US = ulnar nerve, ulnar sulcus; ULN_WR = ulnar nerve, wrist.

Results

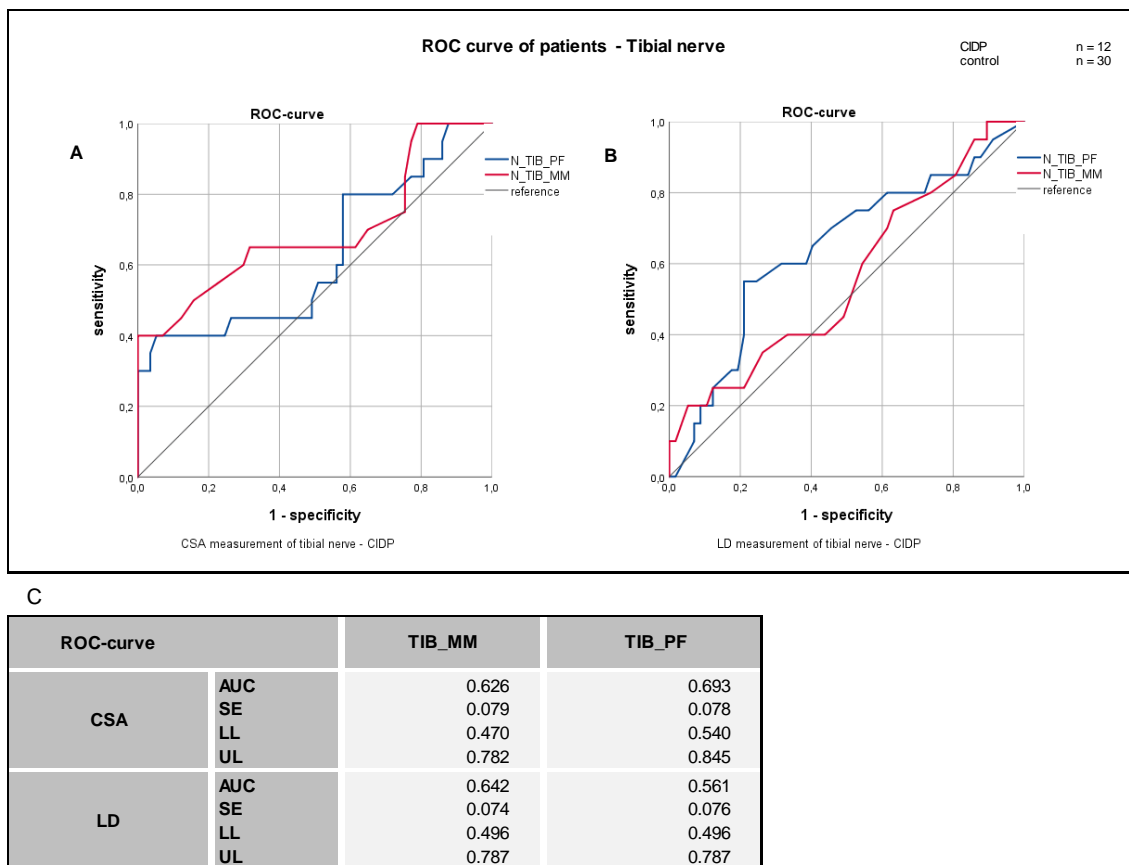


Figure 31: ROC of patients with chronic inflammatory demyelinating polyneuropathy (CIDP) -tibial nerve
A) Receiver operating characteristic (ROC) of cross-sectional area (CSA) measurement of tibial nerve in patients with chronic inflammatory polyneuropathy (CIDP) B) ROC of longitudinal diameter (LD) measurement of tibial nerve in patients with CIDP C) data reference to A-B
Abbreviations: AUC = area under the curve; CSA= cross-sectional area, CIDP = Chronic inflammatory demyelinating polyneuropathy LD = longitudinal diameter; ROC-curve = receiver operating characteristic-curve; SE = standard error; TIB_MM = tibial nerve, medial malleolus; TIB_PF = tibial nerve, popliteal fossa.

Results

3.3.7 Characterization of the subgroup with MADSAM

Five patients were diagnosed with MADSAM. Median disease duration was 12 years (0.5-33 years). Figure 32 shows an example with focal nerve enlargement of the median nerve at mid upper arm of a patient with MADSAM. Figure 33 shows CSA data comparing patients diagnosed with MADSAM with the cohort of healthy controls. Increased CSA ($p<0.05$) was found in all nerves at all measuring sites except for the profound peroneal nerve. Especially the proximal parts of the median, ulnar, and radial nerves showed enlargement ($p<0.01$). At the lower extremities CSA enlargement was found at the sciatic, tibial, peroneal, and sural nerves compared to healthy controls. Only the distal segments of the peroneal nerve were normal when comparing both groups. Figure 34 shows LD data. At the upper extremities, LD enlargement was found at the median, ulnar, and radial nerves ($p<0.05$). At the lower extremities, LD enlargement was found at the peroneal, tibial, and sciatic nerves. The sural nerve and the distal segments of the peroneal nerve did not show LD enlargement in the patient group compared to the group of healthy controls. Figure 35 shows supraclavicular plexus of a patient diagnosed with MADSAM. Figures 36 – 38 show ROCs of brachial plexus and median, ulnar and tibial nerve. AUC was >0.5 at all sites.

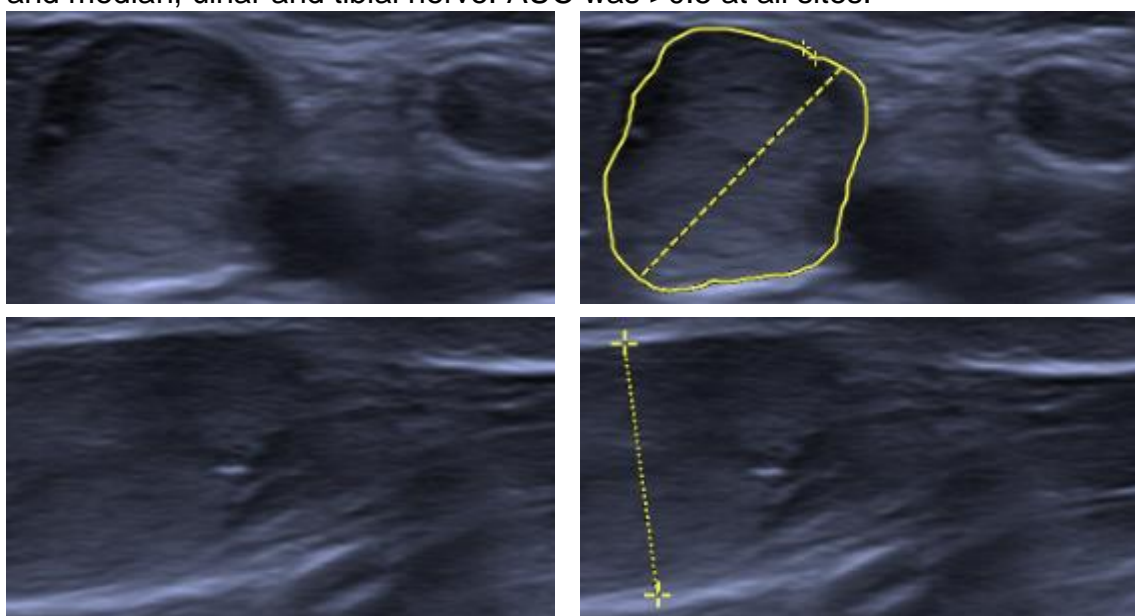


Figure 32: Supraclavicular Brachial plexus; patient with multifocal acquired demyelinating and sensory neuropathy (MADSAM)– cross-section

A) Median nerve at mid upper arm in cross section; patient with MADSAM B) Median nerve at mid upper arm measurement of cross-sectional area (CSA); patient with MADSAM; CSA = 80 mm²(healthy control cohort: mean 9.6 mm² standard deviation 1.9 mm²) C) Median nerve at mid upper arm in longitudinal section; patient with MADSAM D) Median nerve at mid upper arm measurement of LD; patient with MADSAM; LD = 9.9 mm (healthy control cohort: mean 2.4 mm; standard deviation 0.4 mm).

Results

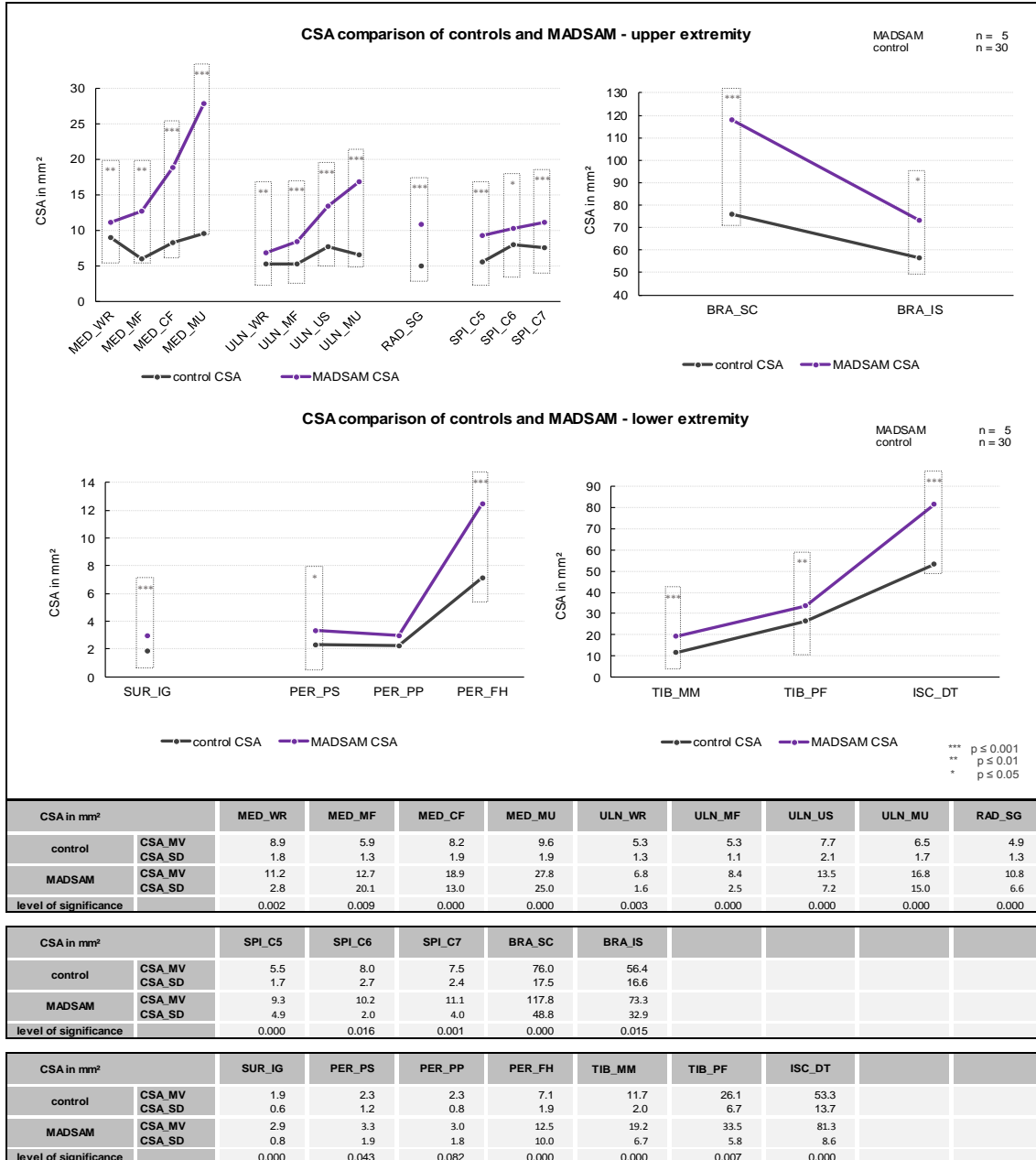


Figure 33: Cross-sectional area (CSA) comparison of healthy control subjects and multifocal acquired demyelinating sensory and motor neuropathy (MADSAM)

Abbreviations: BRA_IS = brachial plexus, inter-scalene muscles; BRA_SC = brachial plexus; supra-clavicular; CSA = cross-sectional area; ISC_DT = sciatic nerve, distal thigh; MADSAM = multifocal acquired demyelinating sensory and motor neuropathy; MED_CF = median nerve, cubital fossa; MED_MF = median nerve, mid forearm; MED_MU = median nerve, mid upper arm; MED_WR = median nerve, wrist; PER_FH = peroneal nerve, fibular head; PER_PP = peroneal nerve, profound peroneal nerve; PER_PS = peroneal nerve, superficial peroneal nerve; RAD_SG = radial nerve, spiral groove; SPI_C5 = spinal nerve; SPI_C6 = spinal nerve, sixth cervical nerve; SPI_C7 = spinal nerve, seventh cervical nerve; SUR_IG = sural nerve, inter gastrocnemius muscle; TIB_MM = tibial nerve, medial malleolus; TIB_PF = tibial nerve, popliteal fossa; ULN_MF = ulnar nerve, mid forearm; ULN_MU = ulnar nerve, mid upper arm; ULN_US = ulnar nerve, ulnar sulcus; ULN_WR = ulnar nerve, wrist.

Results

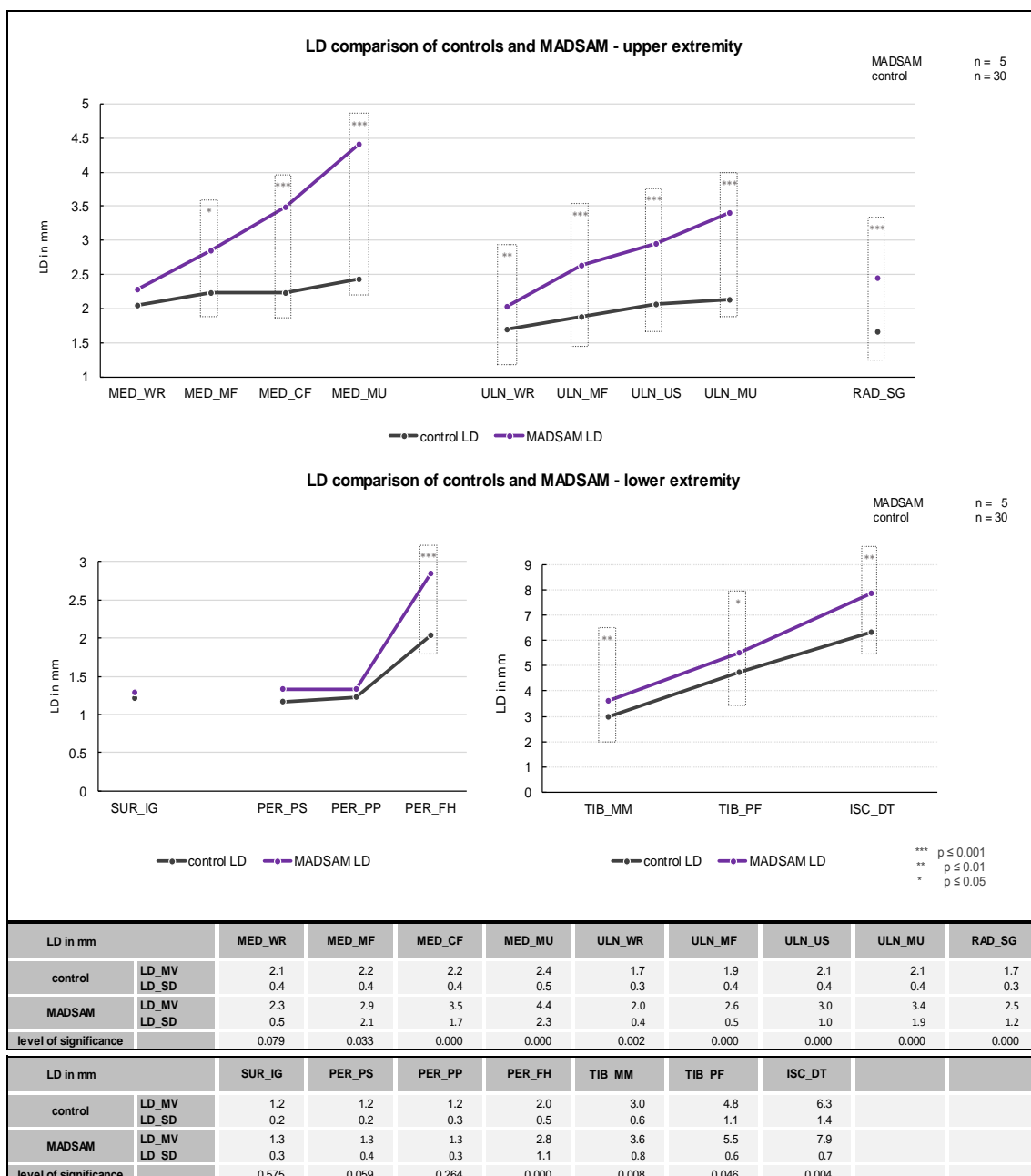


Figure 34: Longitudinal diameter (LD) comparison of healthy control subjects and patients with multifocal acquired demyelinating sensory and motor neuropathy (MADSAM)

Abbreviations: ISC_DT = Sciatic nerve, distal thigh; LD = longitudinal diameter; MADSAM = multifocal acquired demyelinating sensory and motor neuropathy; MED_CF = median nerve, cubital fossa; MED_MF = median nerve, mid forearm; MED_MU = median nerve, mid upper arm; MED_WR = median nerve, wrist; PER_FH = peroneal nerve, fibular head; PER_PP = peroneal nerve, profound peroneal nerve; PER_PS = peroneal nerve, superficial peroneal nerve; RAD_SG = radial nerve, spiral groove; SUR_IG = sural nerve, inter gastrocnemius muscle; TIB_MM = tibial nerve, medial malleolus; TIB_PF = tibial nerve, popliteal fossa; ULN_MF = ulnar nerve, mid forearm; ULN_MU = ulnar nerve, mid upper arm; ULN_US = ulnar nerve, ulnar sulcus; ULN_WR = ulnar nerve, wrist.

Results

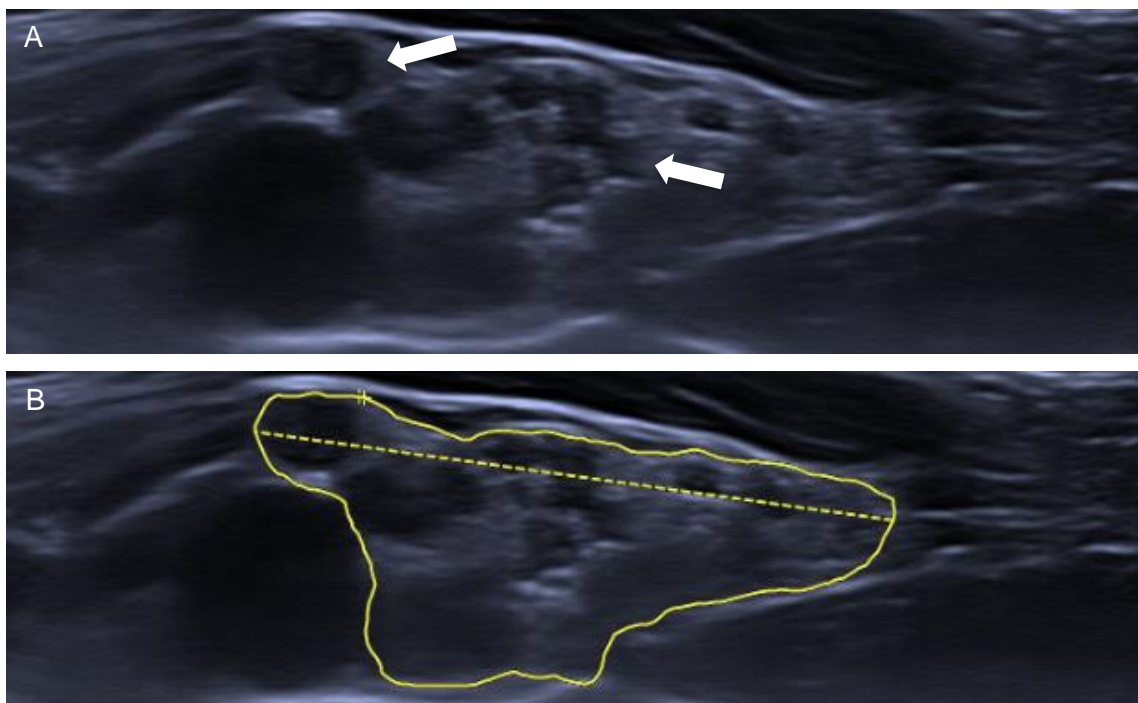


Figure 35: Supraclavicular brachial plexus; patient with multifocal acquired demyelinating sensory and motor neuropathy (MADSAM)

A) White arrows show hypoechoic fascicular structures within the plexus B) Measurement of CSA = 189 mm² (healthy control cohort: mean 76 mm² standard deviation 17,5 mm)

Abbreviations: MADSAM = multifocal acquired demyelinating sensory and motor neuropathy; CSA = cross-sectional area; mm = millimeter.

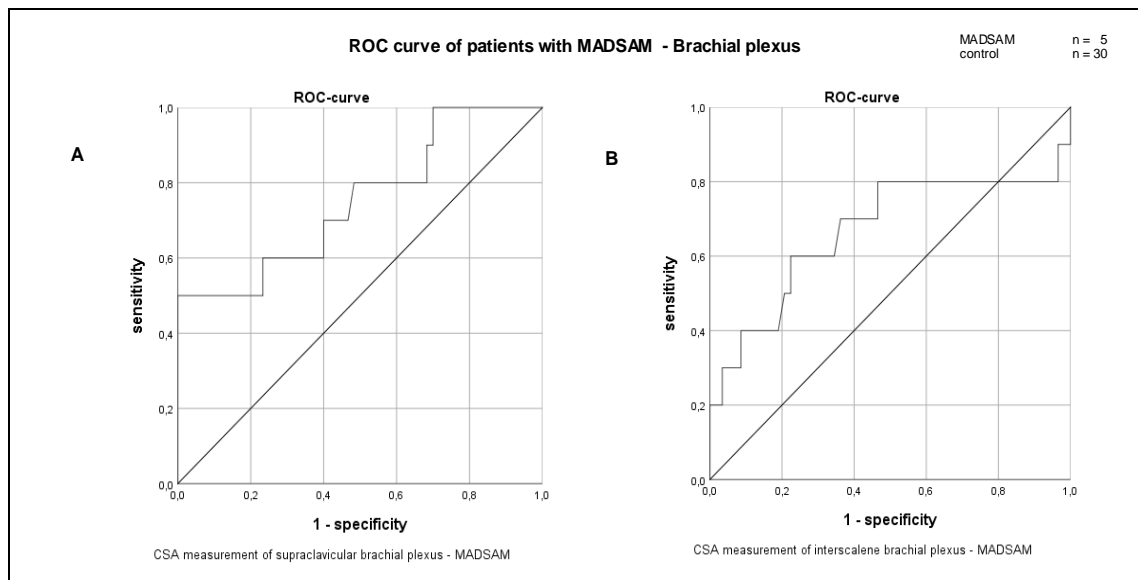


Figure 36: ROC of patients with multifocal acquired demyelinating sensory and motor neuropathy (MADSAM) -tibial nerve

A) Receiver operating characteristic (ROC) of cross-sectional area (CSA) measurement at supraclavicular brachial plexus. AUC 0.751; standard error 0.092; confidence interval (95%): lower limit 0.570; upper limit 0.932; B) ROC of CSA measurement at interscalene brachial plexus. AUC 0.667; standard error 0.116; confidence interval (95%): lower limit 0.441; upper limit 0.894

Abbreviations: AUC = area under the curve; MADSAM = multifocal acquired demyelinating sensory and motor neuropathy; CSA= cross-sectional area, ROC-curve = receiver operating characteristic.

Results

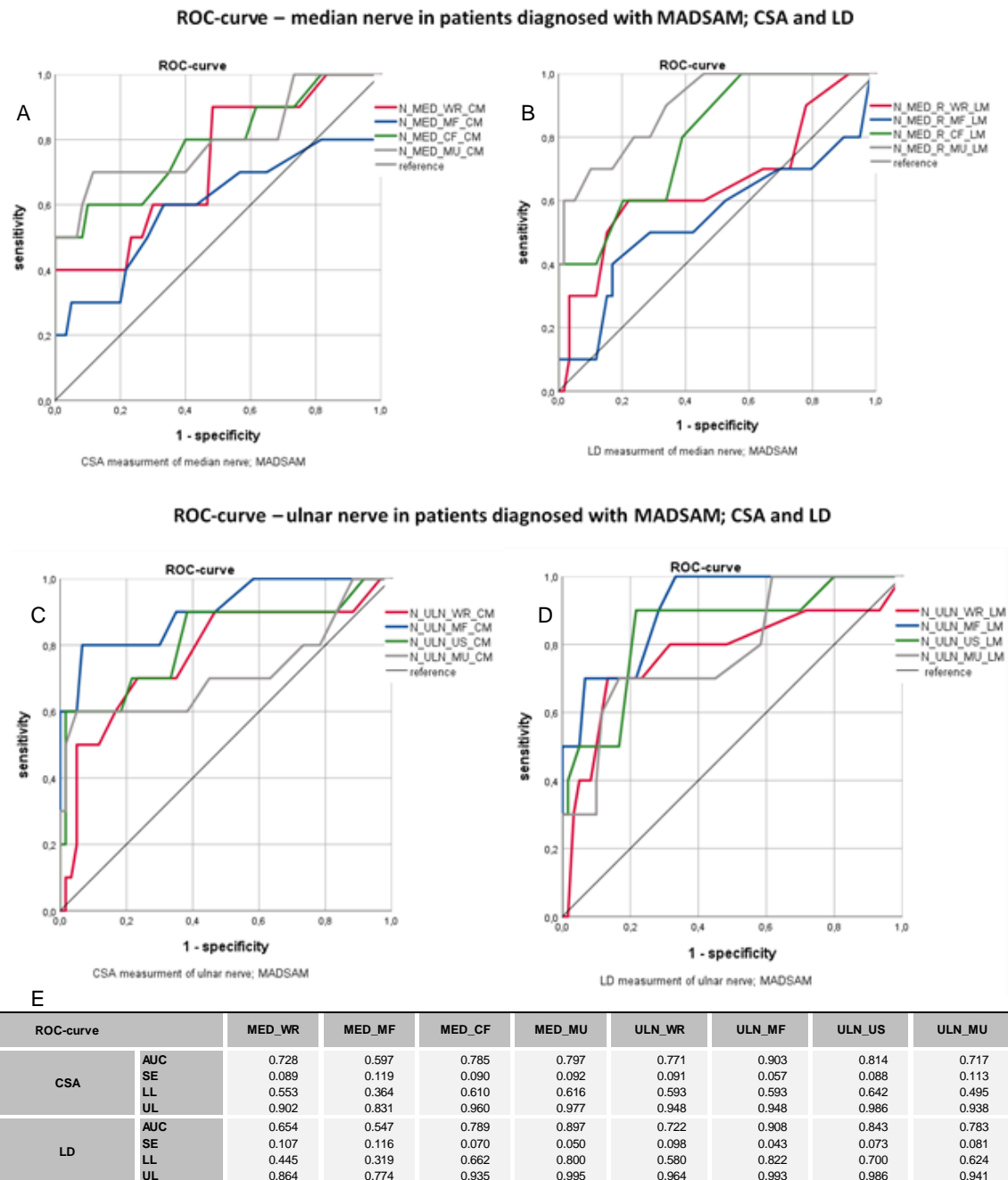


Figure 37: ROC of patients with multifocal acquired demyelinating sensory and motor neuropathy (MADSAM) -median and ulnar nerve

A) Receiver operating curve (ROC of cross-sectional area (CSA) measurement median nerve in patients with multifocal acquired demyelinating sensory and motor neuropathy (MADSAM) B) ROC of longitudinal diameter (LD) measurement median nerve in patients with MADSAM C) ROC of CSA measurement ulnar nerve in patients with MADSAM D) ROC of CSA measurement median nerve in patients with MADSAM E) data reference to A-D

Abbreviations: AUC = area under the curve; CSA= cross-sectional area, LD = longitudinal diameter; MADSAM = multifocal acquired demyelinating and sensory neuropathy; MED_CF = median nerve, cubital fossa; MED_MF = median nerve, mid forearm; MED_MU = median nerve, mid upper arm; MED_WR = median nerve, wrist; ROC-curve = receiver operating characteristic-curve; SE = standard error; ULN_MF = ulnar nerve, mid forearm; ULN_MU = ulnar nerve, mid upper arm; ULN_US = ulnar nerve, ulnar sulcus; ULN_WR = ulnar nerve, wrist.

Results

ROC-curve – tibial nerve in patients diagnosed with MADSAM; CSA and LD

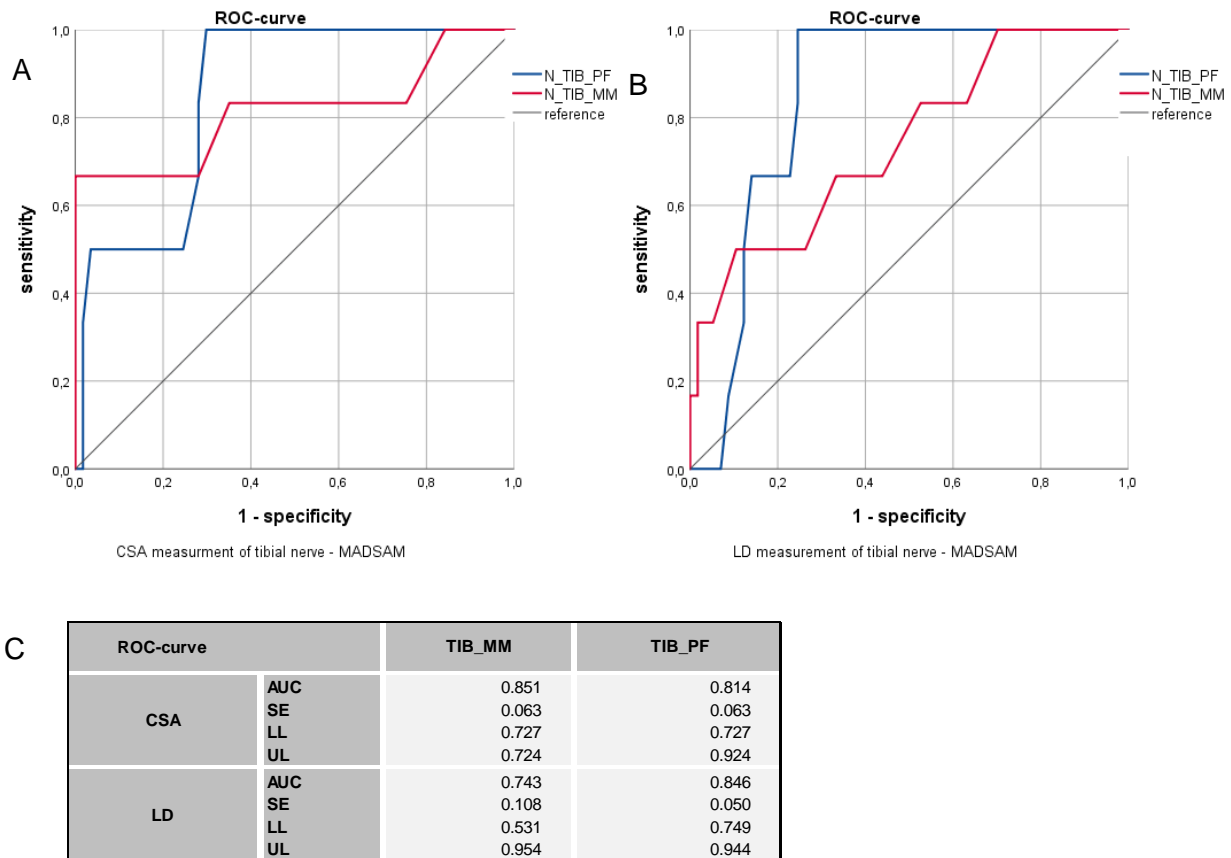


Figure 38: ROC of patients with multifocal acquired demyelinating sensory and motor neuropathy (MADSAM) – tibial nerve

A) Receiver operating characteristic (ROC) of cross-sectional area (CSA) measurement of tibial nerve in patients with multifocal acquired demyelinating sensory and motor neuropathy (MADSAM) B) ROC of longitudinal diameter (LD) measurement of tibial nerve in patients with MADSAM C) data reference to A-B
Abbreviations: AUC = area under the curve; CSA= cross-sectional area, LD = longitudinal diameter; MADSAM = multifocal acquired demyelinating polyneuropathy; ROC-curve = receiver operating characteristic-curve; SE = standard error; TIB_MM = tibial nerve, medial malleolus; TIB_PF = tibial nerve, popliteal fossa.

Results

3.3.8 Characterization of the subgroup with MMN

Nine patients were diagnosed with MMN. Median disease duration was 5 years (1-22 years). Figure 39 shows radial nerve at spiral groove of a patient diagnosed with MMN with enlargement of CSA in comparison to healthy controls. The intrinsic fascicular structure can be identified especially in the cross-section plane. Figure 40 shows the radial nerve of a patient diagnosed with MMN. CSA is also enlarged, but the intrinsic fascicular structure cannot be identified. Figure 41 shows HRUS results of patients with MMN compared to healthy controls. Increased CSA ($p<0.05$) was found at the median, radial, the fifth spinal nerves, the brachial plexus at the upper extremities, and at the tibial and sciatic nerves at the lower extremities. HRUS results of LD are shown in Figure 42 with an enlargement of the median, ulnar, radial, peroneal, tibial, and sciatic nerves of the cohort of patients compared to the cohort of healthy controls ($p<0.05$ each). Figure 43 shows enlarged supraclavicular brachial plexus. Figures 44 – 46 show ROCs of the brachial plexus and median, ulnar, and tibial nerve of patients diagnosed with MMN. The AUC was >0.5 at all measured sites.

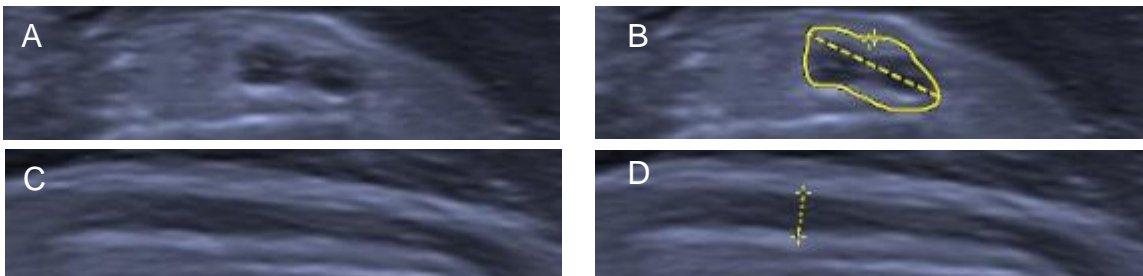


Figure 39 Radial nerve of patient with multifocal motor neuropathy (MMN)
A) Radial nerve at spiral groove in cross section; patient with (MMN) B) Radial nerve at spiral groove measurement of cross-sectional area (CSA); patient with MMN; CSA = 10 mm² (healthy control cohort: mean 4.9 mm²; standard deviation 1.3 mm²) C) Radial nerve at spiral groove in longitudinal section; patient with MMN D) Radial nerve at spiral groove measurement of longitudinal diameter; patient with MMN; LD = 1,7 mm (healthy control cohort: mean 1.7 mm; 0.2 mm).

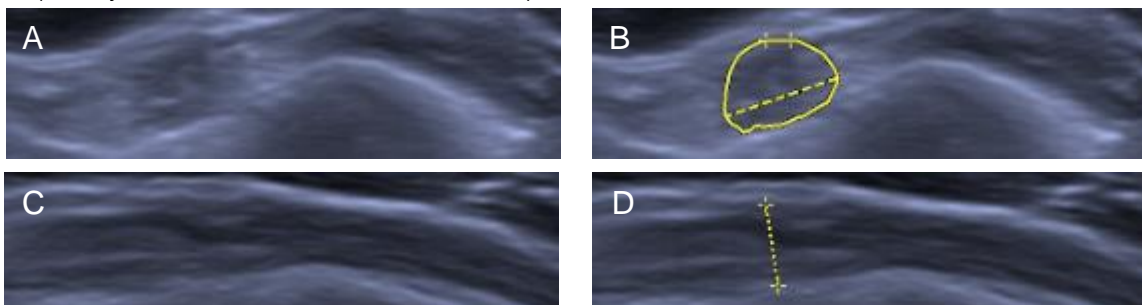


Figure 40: Radial nerve of second patient with multifocal motor neuropathy (MMN)
A) Radial nerve at spiral groove in cross section; patient with MMN B) Radial nerve at spiral groove measurement of cross-sectional area (CSA); patient with MMN; CSA = 11 mm² (healthy control cohort: mean 4.9 mm²; standard deviation 1.3 mm²) C) Radial nerve at spiral groove in longitudinal section; patient with MMN D) Radial nerve at spiral groove measurement of longitudinal diameter (LD); patient with MMN; LD = 3.1 mm (healthy control cohort: mean 1.7 mm; 0.2 mm).

Results

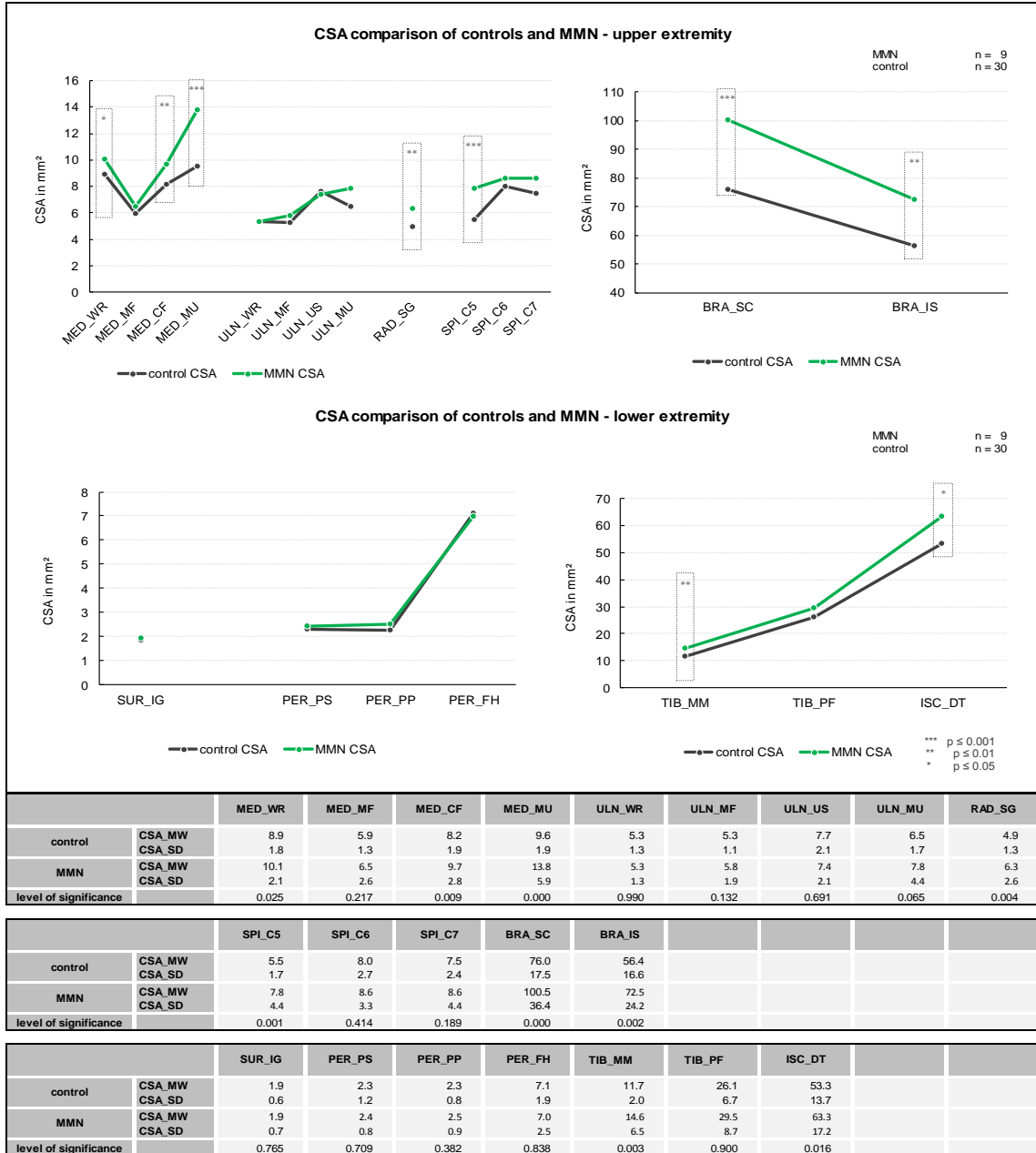


Figure 41: Cross-sectional area (CSA) comparison of healthy control subjects and multifocal motor neuropathy (MMN)

Abbreviations: BRA_IS = brachial plexus, inter-scalene muscles; BRA_SC = brachial plexus; supra-clavicular; CSA = cross-sectional area; ISC_DT = sciatic nerve, distal thigh; MED_CF = median nerve, cubital fossa; MED_MF = median nerve, mid forearm; MED_MU = median nerve, mid upper arm; MED_WR = median nerve, wrist; MMN = multifocal motor neuropathy; PER_FH = peroneal nerve, fibular head; PER_PP = peroneal nerve, profound peroneal nerve; PER_PS = peroneal nerve, superficial peroneal nerve; RAD SG = radial nerve, spiral groove; SPI_C5 = spinal nerve; SPI_C6 = spinal nerve, sixth cervical nerve; SPI_C7 = spinal nerve, seventh cervical nerve; SUR_IG = sural nerve, inter gastrocnemius muscle; TIB_MM = tibial nerve, medial malleolus; TIB_PF = tibial nerve, popliteal fossa; ULN_MF = ulnar nerve, mid forearm; ULN_MU = ulnar nerve, mid upper arm; ULN_US = ulnar nerve, ulnar sulcus; ULN_WR = ulnar nerve, wrist.

Results

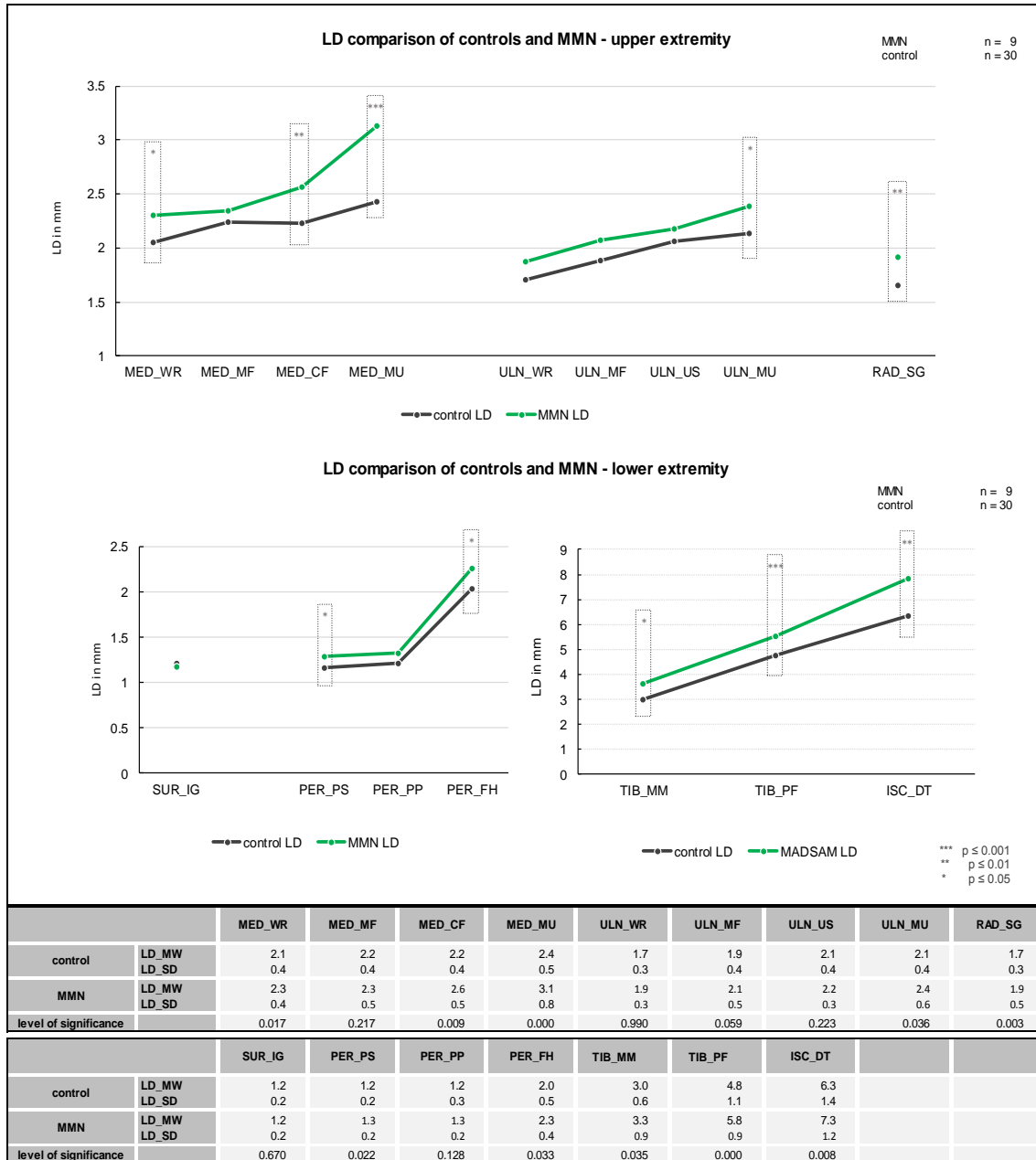


Figure 42: Longitudinal diameter (LD) comparison of healthy control subjects and patients with multifocal motor neuropathy (MMN)

Abbreviations: ISC_DT = sciatic nerve, distal thigh; LD = longitudinal diameter; MED_CF = median nerve, cubital fossa; MED_MF = median nerve, mid forearm; MED_MU = median nerve, mid upper arm; MED_WR = median nerve, wrist; MMN = multifocal motor neuropathy; PER_FH = peroneal nerve, fibular head; PER_PP = peroneal nerve, profound peroneal nerve; PER_PS = peroneal nerve, superficial peroneal nerve; RAD_SG = radial nerve, spiral groove; SUR_IG = sural nerve, inter gastrocnemius muscle; TIB_MM = tibial nerve, medial malleolus; TIB_PF = tibial nerve, popliteal fossa; ULN_MF = ulnar nerve, mid forearm; ULN_MU = ulnar nerve, mid upper arm; ULN_US = ulnar nerve, ulnar sulcus; ULN_WR = ulnar nerve, wrist.

Results

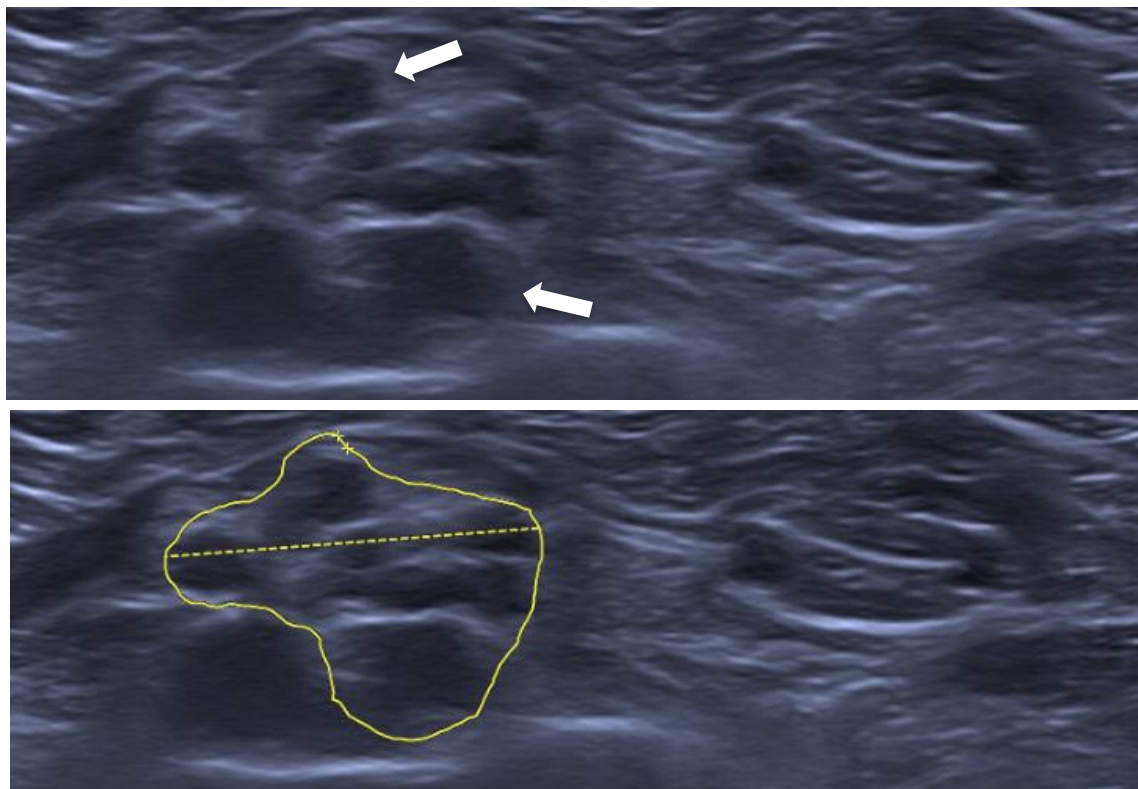


Figure 43 Supraclavicular brachial plexus; patient with multifocal motor neuropathy (MMN)
A) White arrows show hypoechoic fascicular structures within the plexus B) Measurement of cross-sectional area (CSA) = 160 mm² (healthy control cohort: mean 76 mm² standard deviation 17,5 mm)
Abbreviations: MMN = multifocal motor neuropathy; CSA = cross-sectional area; mm = millimeter.

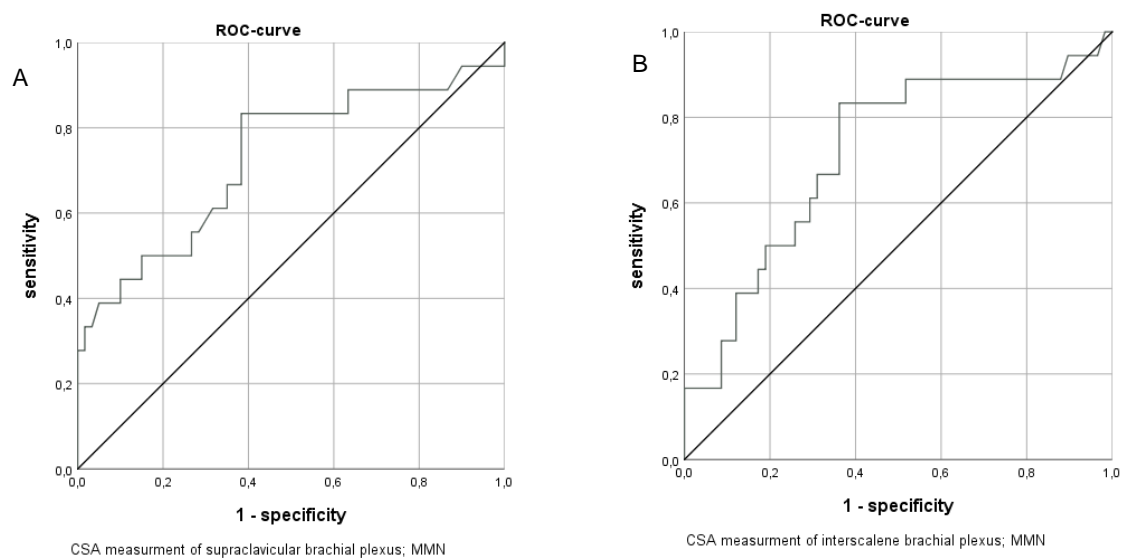


Figure 44: ROC of patients with multifocal motor neuropathy (MMN) - brachial plexus
A) Receiver operating curve (ROC) of cross-sectional area (CSA) measurement at supraclavicular brachial plexus. AUC 0.728; standard error 0.076; confidence interval (95%): lower limit 0.580; upper limit 0.876B)
ROC of CSA measurement at interscalene brachial plexus. AUC 0.716; standard error 0.072; confidence interval (95%): lower limit 0.441; upper limit 0.894
Abbreviations: AUC = area under the curve; MMN = multifocal motor neuropathy; CSA= cross-sectional area; ROC-curve = receiver operating characteristic-curve.

Results

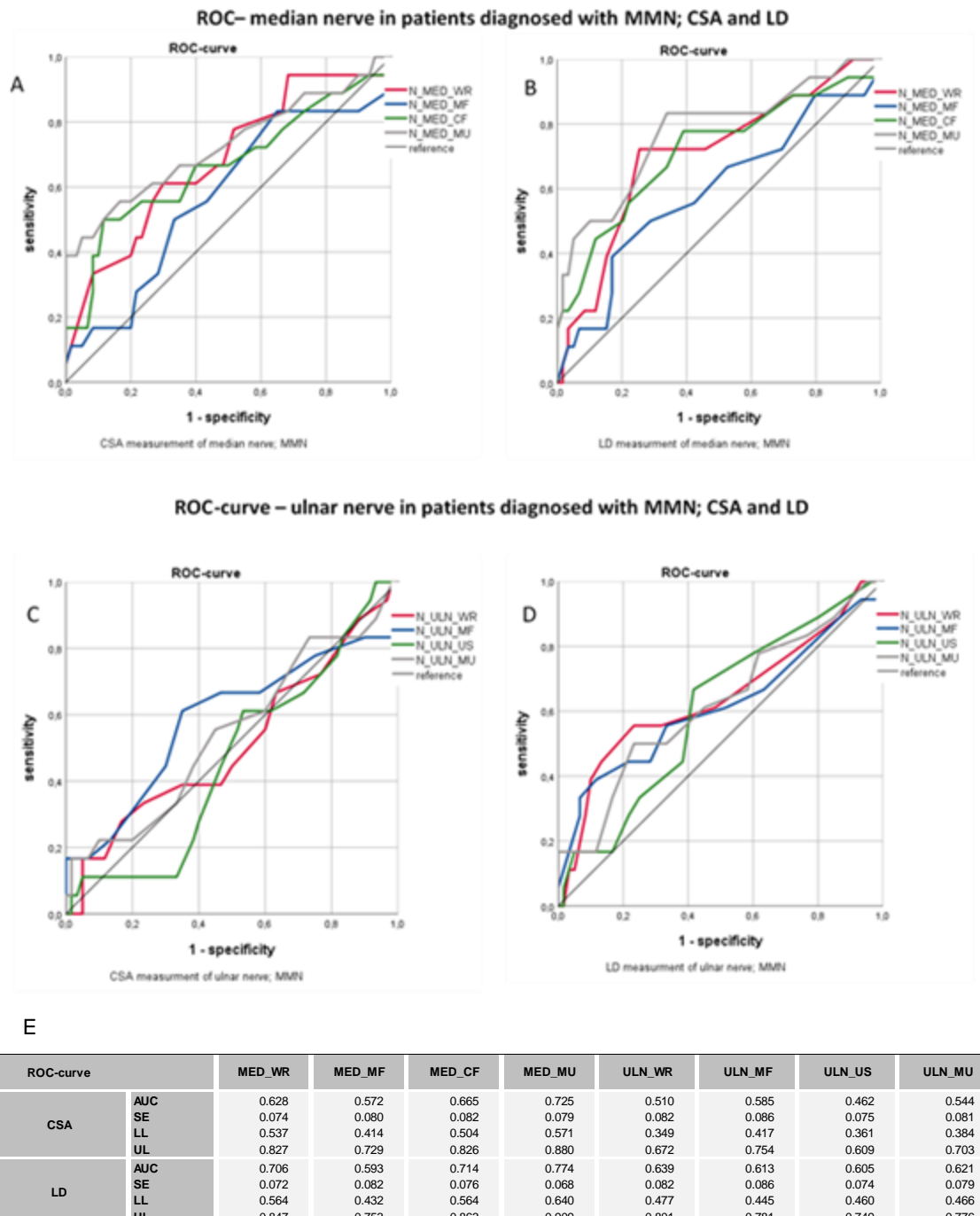


Figure 45: ROC of patients with multifocal motor neuropathy (MMN) – median and ulnar nerve

A) Receiver operating characteristic (ROC) of cross-sectional area (CSA) measurement median nerve in patients with multifocal motor neuropathy (MMN) B) ROC of longitudinal diameter (LD) measurement median nerve in patients with MMN C) ROC of CSA measurement ulnar nerve in patients with MMN D) ROC-curve of CSA measurement median nerve in patients with MMN E) data reference to A-D

Abbreviations: AUC = area under the curve; CSA= cross-sectional area, LD = longitudinal diameter; MED_CF = median nerve, cubital fossa; MED_MF = median nerve, mid forearm; MED_MU = median nerve, mid upper arm; MED_WR = median nerve, wrist; MMN = multifocal motor neuropathy; ROC-curve = receiver operating characteristic-curve; SE = standard error; ULN_MF = ulnar nerve, mid forearm; ULN_MU = ulnar nerve, mid upper arm; ULN_US = ulnar nerve, ulnar sulcus; ULN_WR = ulnar nerve, wrist.

Results

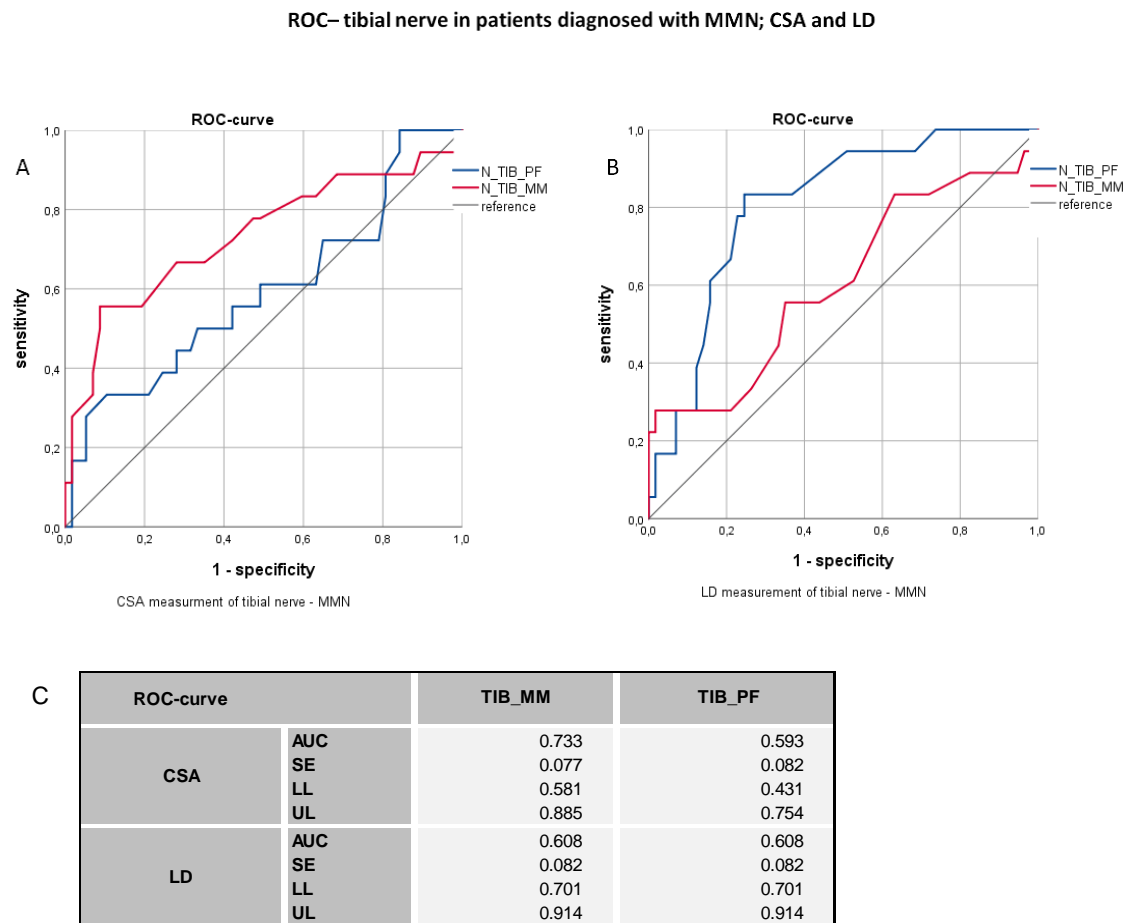


Figure 46: ROC of patients with multifocal motor neuropathy (MMN) – tibial nerve
A) Receiver operating characteristic (ROC) of cross-sectional area (CSA) measurement of tibial nerve in patients with multifocal motor neuropathy (MMN) B) ROC of longitudinal diameter (LD) measurement of tibial nerve in patients with MMN C) data reference to A-B
Abbreviations: AUC = area under the curve; CSA= cross-sectional area, LD = longitudinal diameter; MMN = multifocal motor neuropathy; ROC-curve = receiver operating characteristic-curve; SE = standard error; TIB_MM = tibial nerve, medial malleolus; TIB_PF = tibial nerve, popliteal fossa.

Results

3.3.9 Characterization of the subgroup with ALS

We recruited eight patients diagnosed with ALS. The median disease duration was 3 years (1-4 years). Figure 47A and 47B show a CSA enlargement of peroneal nerve at fibular head in a patient diagnosed with ALS. The white arrow shows one hypoechoic fascicular structure within the cross-section of the nerve. Figure 47C and 47D show the corresponding data of LD. Figure 48 shows results of the measurement of CSA in patients diagnosed with ALS compared to healthy controls. Enlargement of CSA ($p<0.05$) was found at the median and ulnar nerves, and the brachial plexus at the upper extremities. For the lower extremities, enlargement of CSA was found at the peroneal, tibial, and sciatic nerves. Figure 49 shows the results of LD data compared to healthy controls. Enlargement of LD was found for peroneal, tibial and sciatic nerves ($p<0.05$ each). Figure 50 shows supraclavicular plexus of a patient diagnosed with ALS, although CSA is not enlarged intrinsic fascicular structures can be seen. Figures 51-53 show ROCs of median, ulnar, and tibial nerve. AUC was >0.5 at most but not on all analyzed measuring sites.

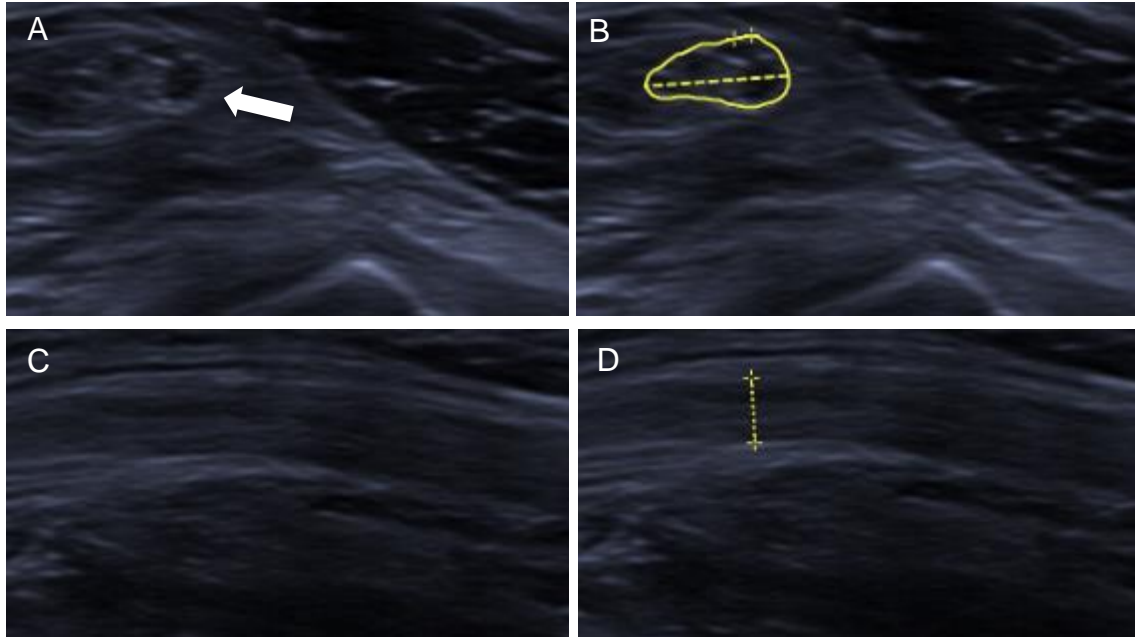


Figure 47: Peroneal nerve of patient with amyotrophic lateral sclerosis (ALS)

A) Peroneal nerve at fibular head in cross section; patient with amyotrophic lateral sclerosis (ALS) B) Peroneal nerve at fibular head measurement of CSA; patient with ALS; CSA = 11 mm² (healthy control cohort: mean 7.1 mm²; standard deviation 1.9 mm²) C) Peroneal nerve at fibular head in longitudinal section; patient with ALS D) Peroneal nerve at fibular head measurement of longitudinal diameter; patient with ALS; LD = 2,5 mm (healthy control cohort: mean 2 mm; standard deviation 0.4 mm)

Results

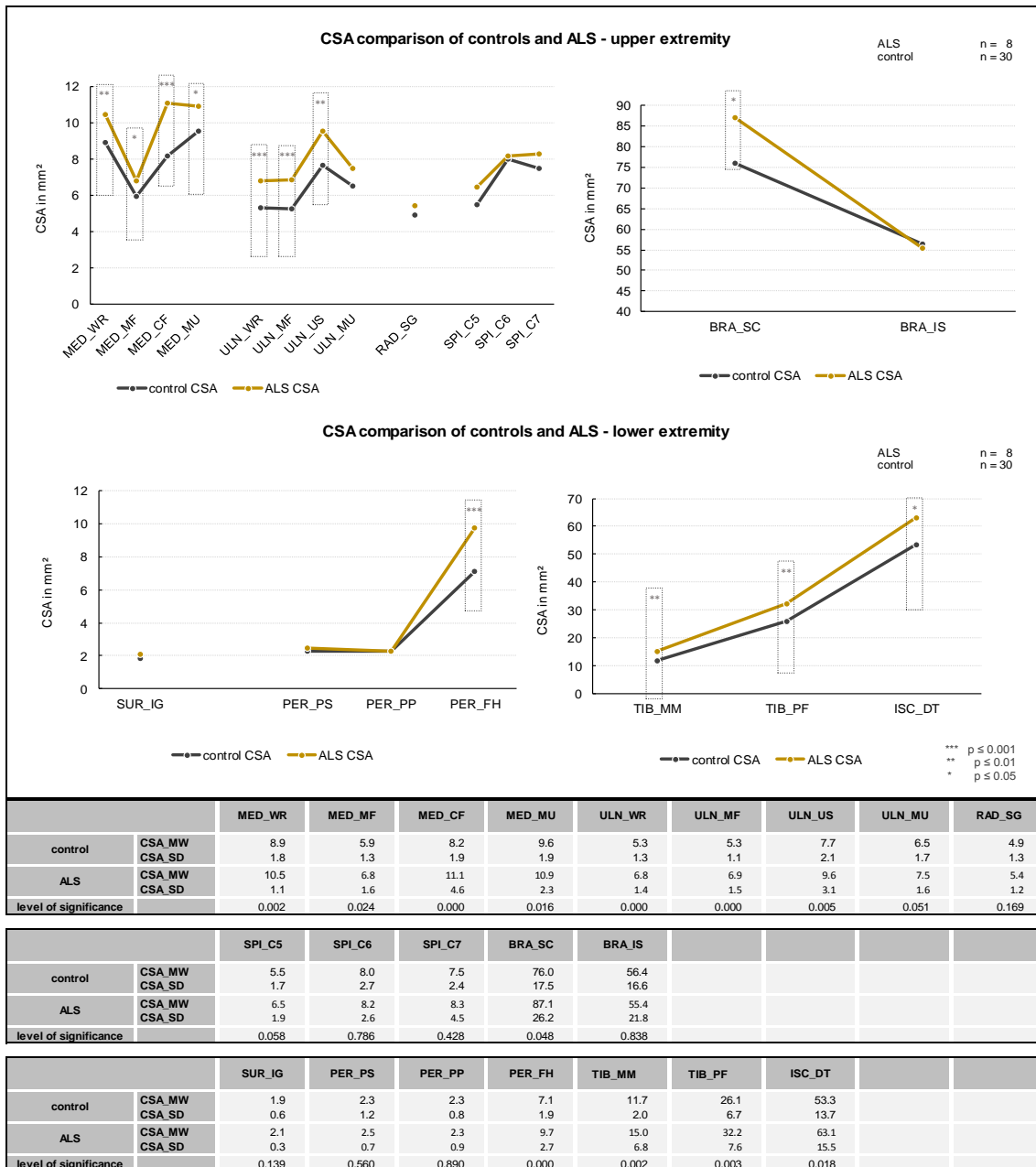


Figure 48: Cross-sectional area (CSA) comparison of healthy control subjects and amyotrophic lateral sclerosis (ALS)

Abbreviations: ALS = amyotrophic lateral sclerosis; BRA_IS = brachial plexus, inter-scalene muscles; BRA_SC = brachial plexus; supra-clavicular; CSA = cross-sectional area; ISC_DT = sciatic nerve, distal thigh; MED_CF = median nerve, cubital fossa; MED_MF = median nerve, mid forearm; MED_MU = median nerve, mid upper arm; MED_WR = median nerve, wrist; PER_FH = peroneal nerve, fibular head; PER_PP = peroneal nerve, profound peroneal nerve; PER_PS = peroneal nerve, superficial peroneal nerve; RAD_SG = radial nerve, spiral groove; SPI_C5 = spinal nerve; SPI_C6 = spinal nerve, sixth cervical nerve; SPI_C7 = spinal nerve, seventh cervical nerve; SUR_IG = sural nerve, inter gastrocnemius muscle; TIB_MM = tibial nerve, medial malleolus; TIB_PF = tibial nerve, popliteal fossa; ULN_MF = ulnar nerve, mid forearm; ULN_MU = ulnar nerve, mid upper arm; ULN_US = ulnar nerve, ulnar sulcus; ULN_WR = ulnar nerve, wrist.

Results

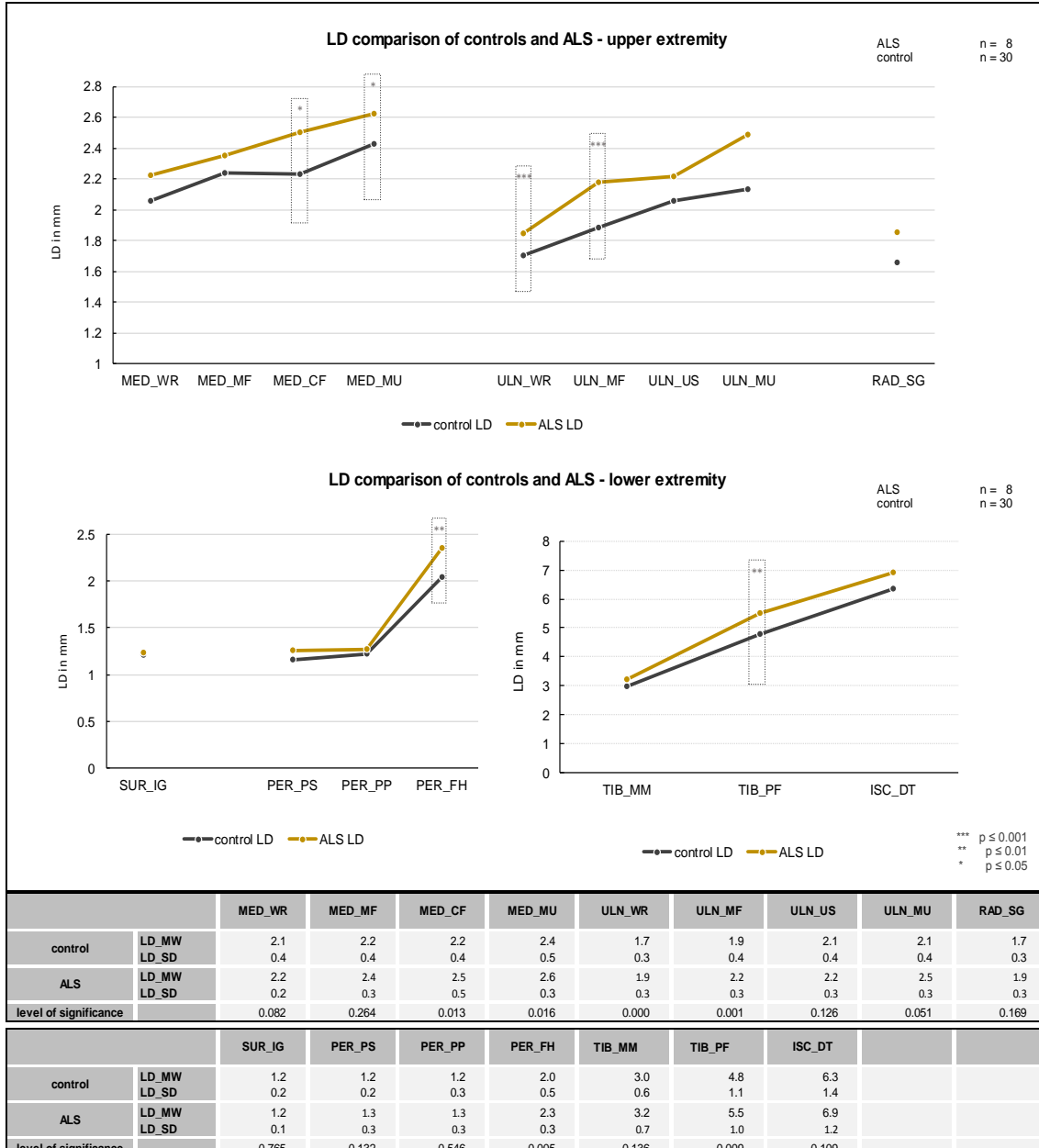


Figure 49: Longitudinal diameter (LD) comparison of healthy control subjects and amyotrophic lateral sclerosis (ALS)

Abbreviations: ALS = amyotrophic lateral sclerosis; ISC_DT = sciatic nerve, distal thigh; LD = longitudinal diameter; MED_CF = median nerve, cubital fossa; MED_MF = median nerve, mid forearm; ; MED_MU = median nerve, mid upper arm; MED_WR = median nerve, wrist; PER_FH = peroneal nerve, fibular head; PER_PP = peroneal nerve, profound peroneal nerve; PER_PS = peroneal nerve, superficial peroneal nerve; RAD_SG = radial nerve, spiral groove; SUR_IG = sural nerve, inter gastrocnemius muscle; TIB_MM = tibial nerve, medial malleolus; TIB_PF = tibial nerve, popliteal fossa; ULN_MF = ulnar nerve, mid forearm; ULN_MU = ulnar nerve, mid upper arm; ULN_US = ulnar nerve, ulnar sulcus; ULN_WR = ulnar nerve, wrist. ; TIB_MM = tibial nerve, medial malleolus; TIB_PF = tibial nerve, popliteal fossa; ULN_MF = ulnar nerve, mid forearm; ULN_MU = ulnar nerve, mid upper arm; ULN_US = ulnar nerve, ulnar sulcus; ULN_WR = ulnar nerve, wrist.

Results

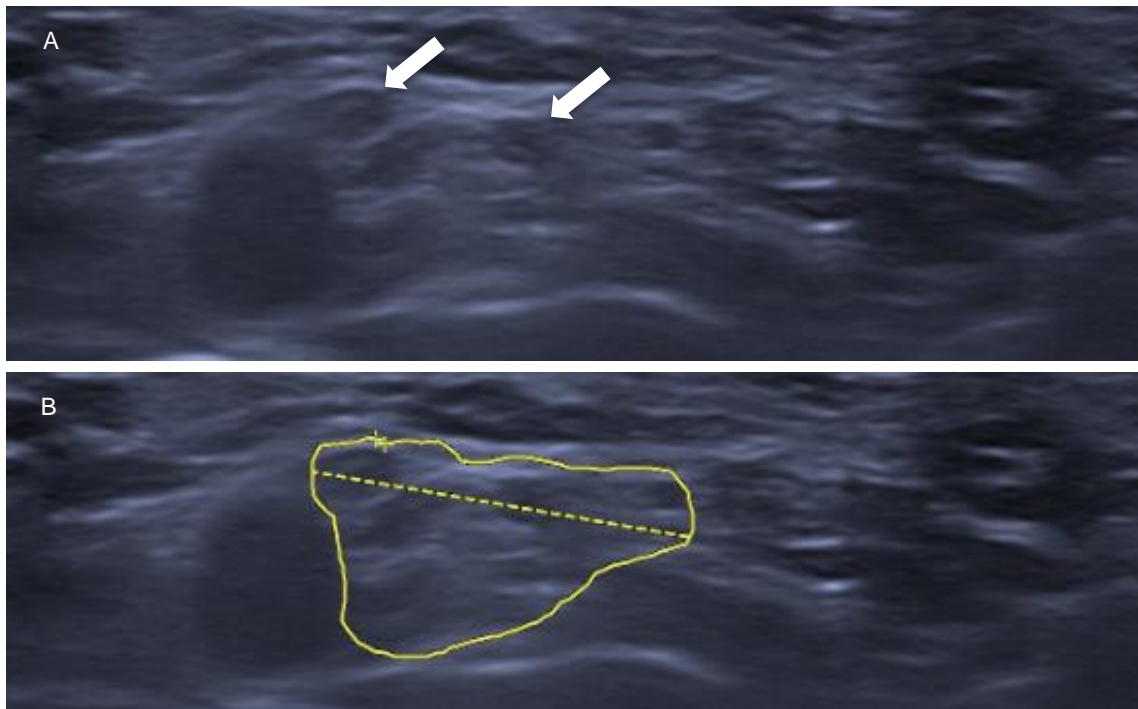


Figure 51: Supraclavicular brachial plexus; patient with amyotrophic lateral sclerosis (ALS)
A) White arrows show hypoechoic fascicular structures within the plexus B) Measurement of cross-sectional area (CSA) = 77 mm² (healthy control cohort: mean 76 mm² standard deviation 17,5 mm)
Abbreviations: MMN = multifocal motor neuropathy; CSA = cross-sectional area; mm = millimeter.

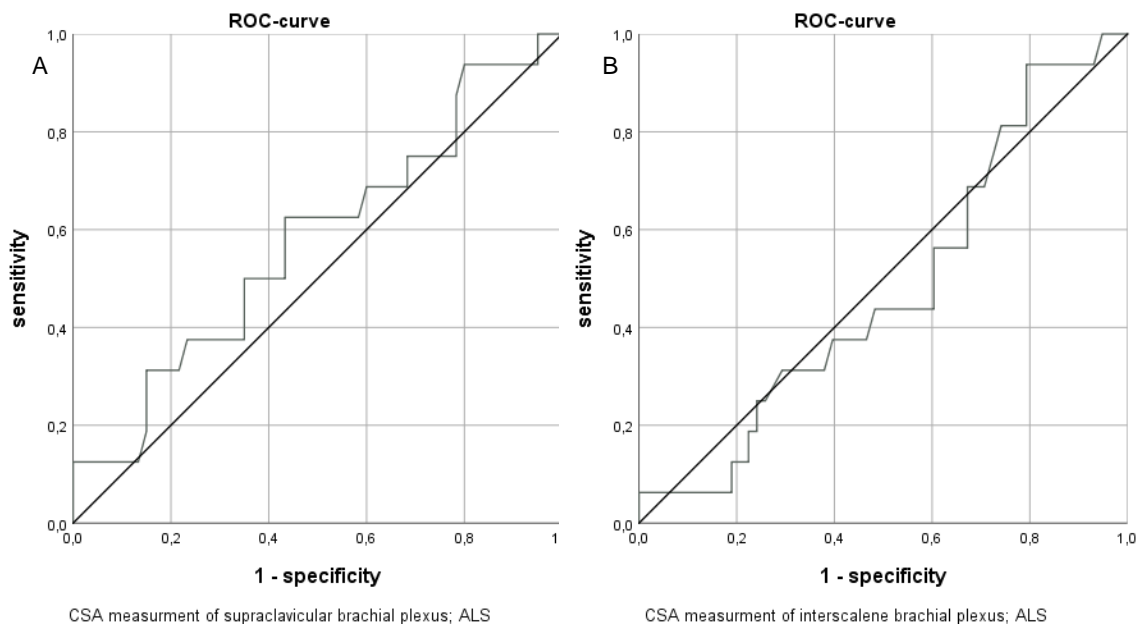


Figure 50: ROC of patients with amyotrophic lateral sclerosis (ALS) – brachial plexus
A) Receiver operating characteristic (ROC) of cross-sectional area (CSA) measurement at supraclavicular brachial plexus. AUC 0.574; standard error 0.083; confidence interval (95%): lower limit 0.412; upper limit 0.736 B) ROC of CSA measurement at interscalene brachial plexus. AUC 0.480; standard error 0.078; confidence interval (95%): lower limit 0.327; upper limit 0.633.
Abbreviations: AUC = area under the curve; ALS = amyotrophic lateral sclerosis; CSA= cross-sectional area; ROC-curve = receiver operating characteristic-curve.

Results

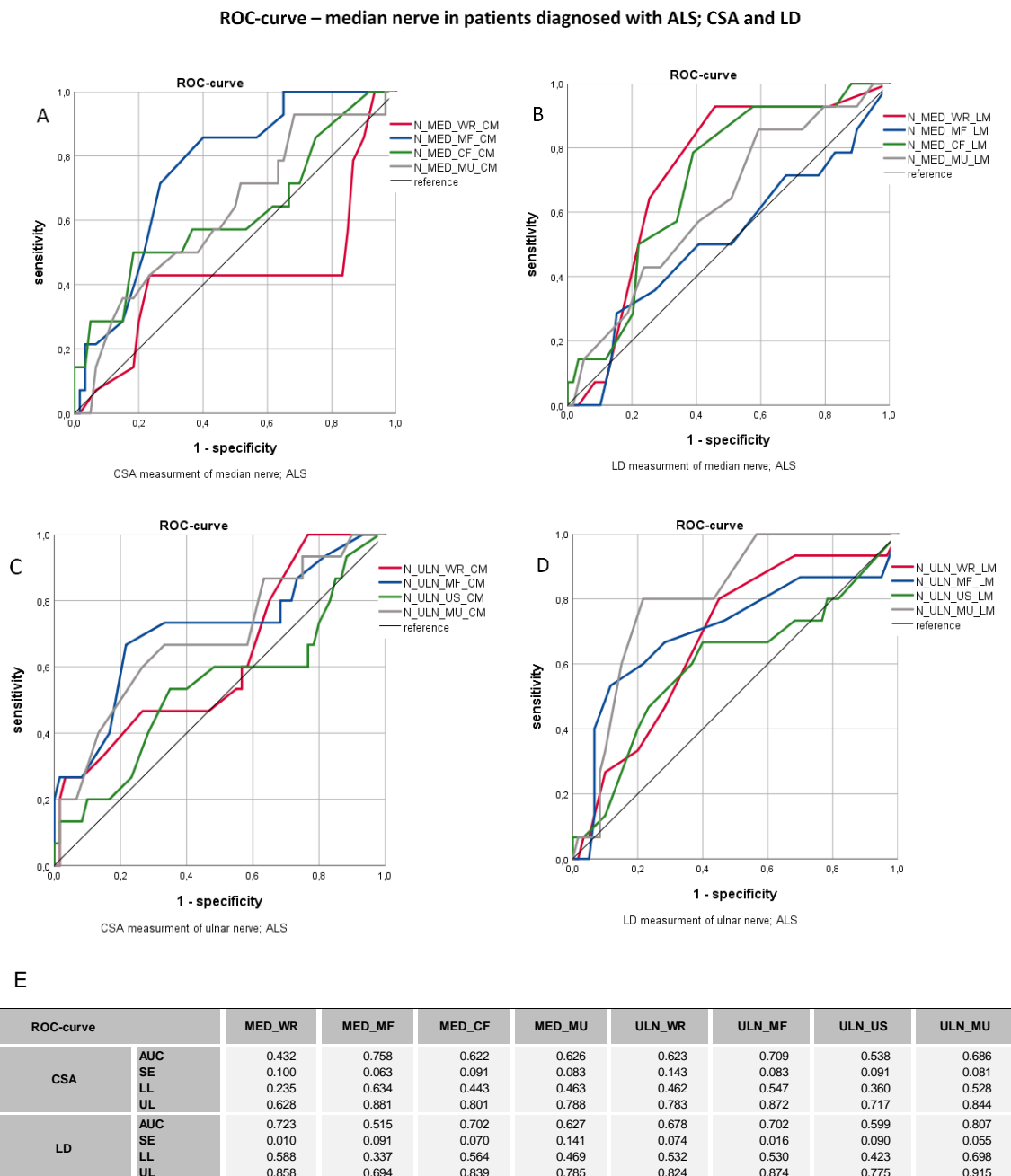


Figure 52: ROC of patients with amyotrophic lateral sclerosis (ALS)– median and ulnar nerve
A) Receiver operating characteristic (ROC) of cross-sectional area (CSA) measurement median nerve in patients with amyotrophic lateral sclerosis (ALS) B) ROC of longitudinal diameter (LD) measurement median nerve in patients with ALS C) ROC of CSA measurement ulnar nerve in patients with ALS D) ROC of CSA measurement median nerve in patients with ALS E) data reference to A-D.

Abbreviations: ALS = amyotrophic lateral sclerosis; AUC = area under the curve; CSA= cross-sectional area, LD = longitudinal diameter; MED_CF = median nerve, cubital fossa; MED_MF = median nerve, mid forearm; MED_MU = median nerve, mid upper arm; MED_WR = median nerve, wrist; ROC-curve = receiver operating characteristic-curve; SE = standard error; ULN_MF = ulnar nerve, mid forearm; ULN_MU = ulnar nerve, mid upper arm; ULN_US = ulnar nerve, ulnar sulcus; ULN_WR = ulnar nerve, wrist.

Results

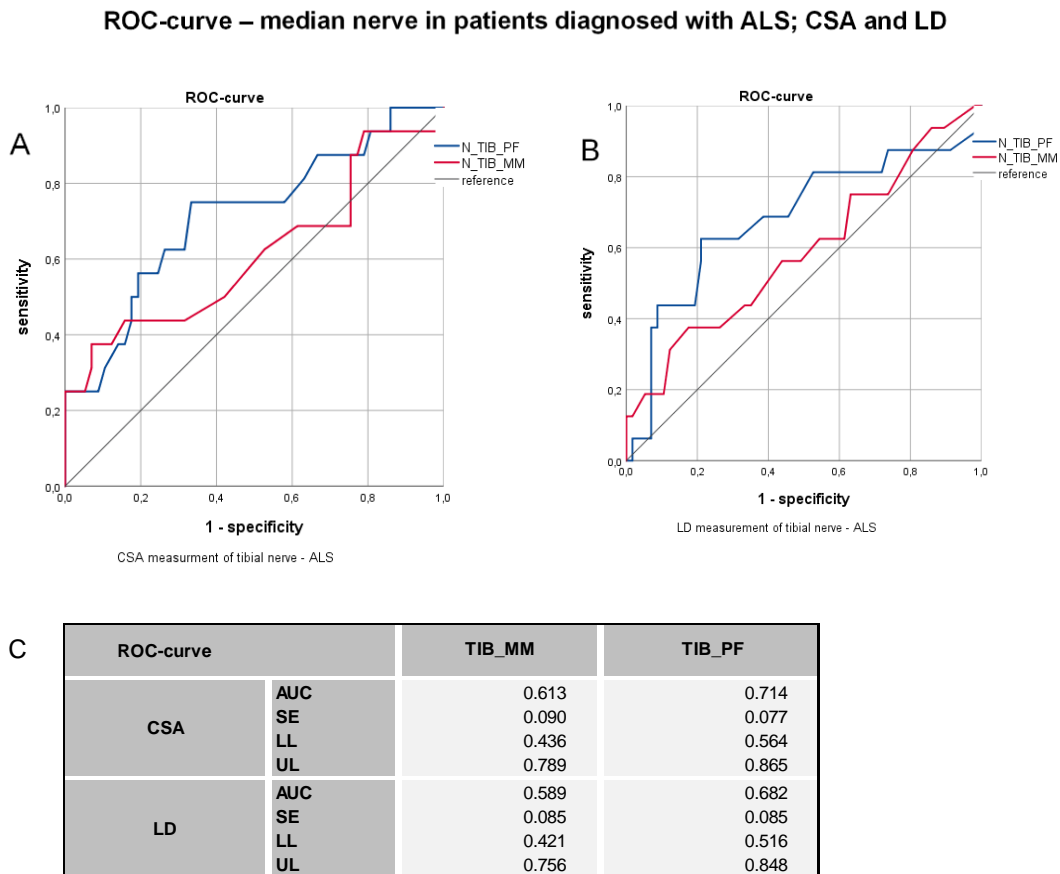


Figure 53: ROC of patients with amyotrophic lateral sclerosis (ALS)– tibial nerve

A) Receiver operating characteristic (ROC) of cross-sectional area (CSA) measurement of tibial nerve in patients with amyotrophic lateral sclerosis (ALS) B) ROC of longitudinal diameter (LD) measurement of tibial nerve in patients with ALS C) data reference to A-B.

Abbreviations: ALS = amyotrophic lateral sclerosis; AUC = area under the curve; CSA= cross-sectional area, LD = longitudinal diameter; MADSAM = multifocal acquired demyelinating polyneuropathy; ROC-curve = receiver operating characteristic-curve; SE = standard error; TIB_MM = tibial nerve, medial malleolus; TIB_PF = tibial nerve, popliteal fossa.

Results

3.3.10 Analysis of the results of nerve biopsy in relation to HRUS data

In 48 patients, a diagnostic nerve biopsy was performed at the sural, radial or ulnar nerve. In one case, nerve biopsy was performed in an external hospital; results of the histological analysis of this patient were not available. 44/48 (92%) patients received a sural nerve biopsy, 3/44 (6%) patients a sensory radial nerve biopsy, and 1/44 (2%) patient a fascicular biopsy of the ulnar nerve. In 36/44 (77%) patients, histological signs of inflammation were found. These patients were diagnosed with CIDP 5/44 (11%), MADSAM 2/44 (5%), MMN 2/44 (5%), PIAN 3/44 (7%), axonal neuropathies 4/44 (9%), NSVN 10/44 (23%), SVN 2/44 (5%), diabetic neuropathy 2/44 (5%), neuropathy, not identified 3/44 (7%), and paraproteinemic neuropathy 1/44 (2%). Results of CSA and LD data of those patients with histological signs of inflammation and those without are shown in Figure 54 and 55. No relevant intergroup difference was found except for single data points such as a larger CSA of the nerve and interscalene brachial plexus of patients with inflammatory neuropathies compared to non-inflammatory neuropathies ($p<0.05$ each). In 17/44 (36%) patients, histological signs of demyelination were found, in 8/44 (17%) patients of these onion-bulb formations were seen. Results of CSA LD comparison of patients with signs of demyelination and those without are shown in Figure 56. The corresponding comparison of the LD of those two groups are shown in Figure 57. For both the CSA and the LD no intergroup differences were found. In 27/44 (57%) patients, signs of nerve edema were found in the histological assessment as described in 2.8. The CSA comparison between patients with and without signs edema is shown in Figure 58. CSA did not differ between groups. Intergroup comparison of the LD is shown in Figure 59. Increased LD was found at the median nerve at mid-forearm and mid-upper arm for the ulnar nerve of patient with edema in nerve biopsy compared to healthy controls ($p<0.05$). In addition, the grade of described edema was quantified. In 14/27 (52 %) of the patients slight grade of edema, in 7/27 (26%) patients medium grade of edema, and in 6/27 (22%) patients high grade edema was found. Results did not change when stratifying the patient groups for the semiquantitative extend of edema (no edema – mild edema – severe edema).

Results

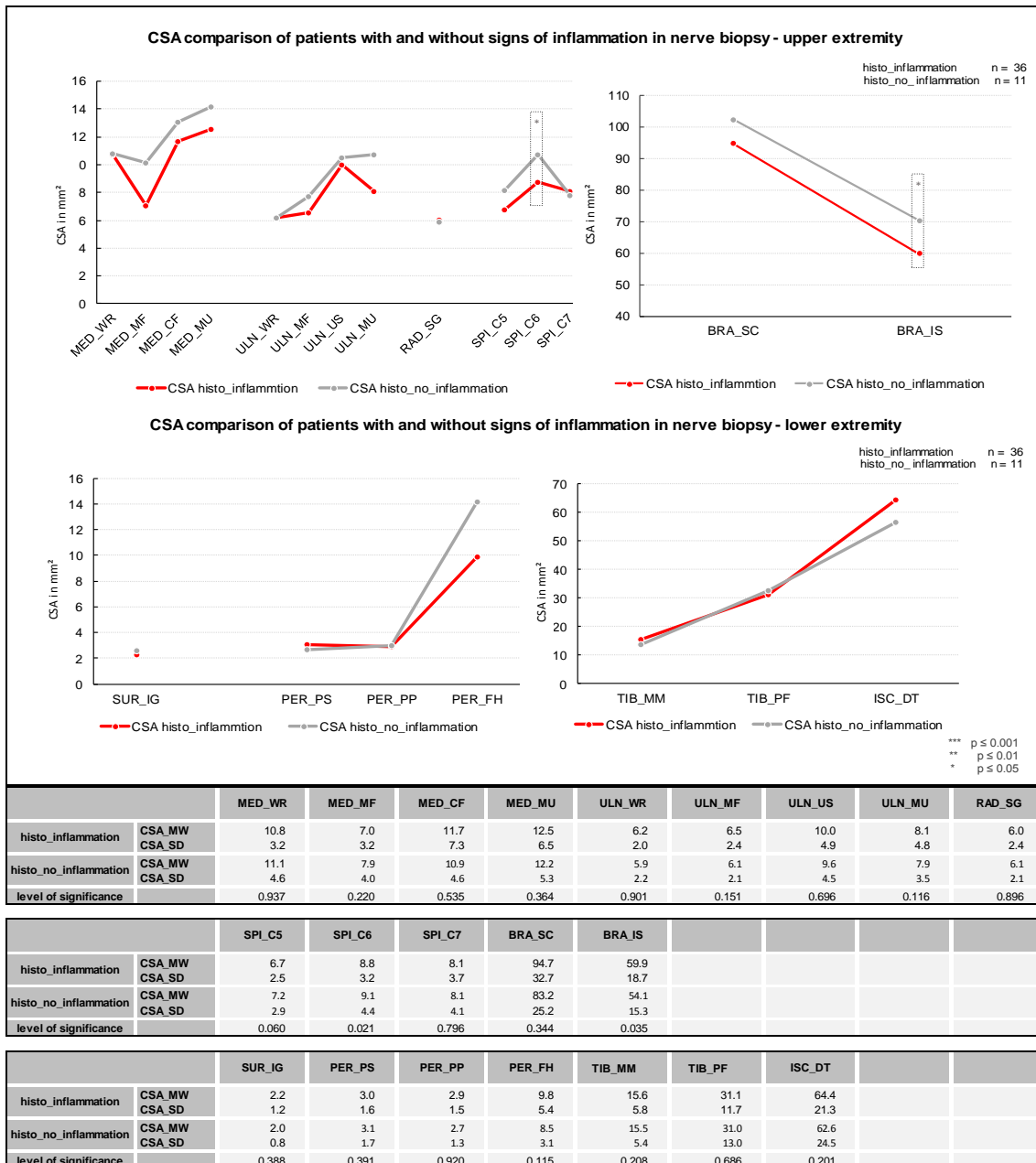


Figure 54: Cross-sectional area (CSA) comparison of patients with and without signs of inflammation in nerve biopsy

Abbreviations: BRA_IS = brachial plexus, inter-scalene muscles; BRA_SC = brachial plexus; supraclavicular; CSA = cross-sectional area; histo_inflammation = patients with signs of inflammation in nerve biopsy; histo_no_inflammation = patients without signs of inflammation in nerve biopsy ISC_DT = sciatic nerve, distal thigh; MED_CF = median nerve, cubital fossa; MED_MF = median nerve, mid forearm; MED_MU = median nerve, mid upper arm; MED_WR = median nerve, wrist; PER_FH = peroneal nerve, fibular head; PER_PP = peroneal nerve, profound peroneal nerve; PER_PS = peroneal nerve, superficial peroneal nerve; RAD SG = radial nerve, spiral groove; SPI_C5 = spinal nerve; SPI_C6 = spinal nerve, sixth cervical nerve; SPI_C7= spinal nerve, seventh cervical nerve; SUR_IG = sural nerve, inter gastrocnemius muscle; TIB_MM = tibial nerve, medial malleolus; TIB_PF = tibial nerve, popliteal fossa; ULN_MF = ulnar nerve, mid forearm; ULN_MU = ulnar nerve, mid upper arm; ULN_US = ulnar nerve, ulnar sulcus; ULN_WR = ulnar nerve, wrist.

Results

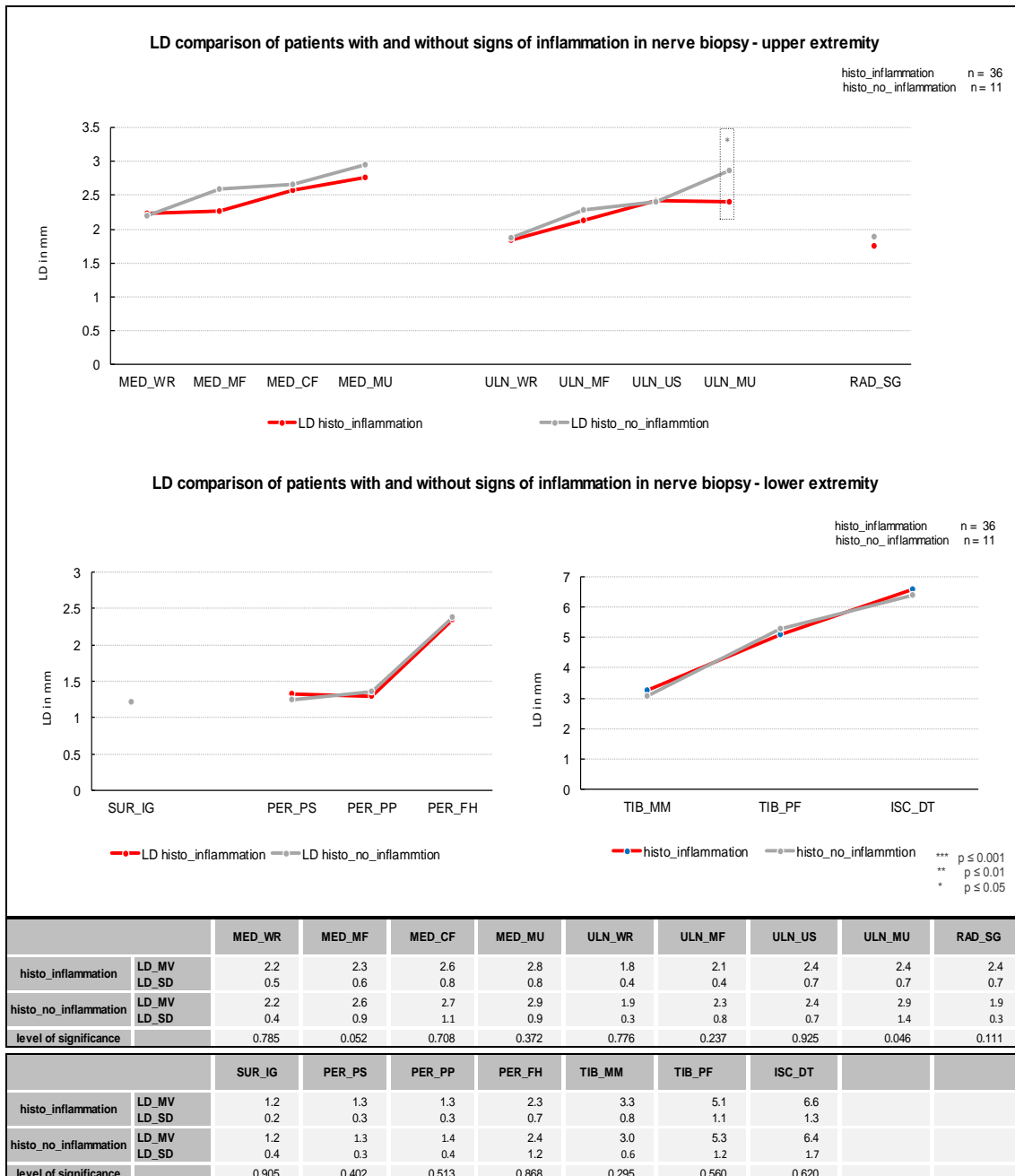


Figure 55: Longitudinal (LD) comparison of patients with and without signs of inflammation in nerve biopsy
Abbreviations: ISC_DT = sciatic nerve, distal thigh; LD = longitudinal diameter; MED_CF = median nerve, cubital fossa; MED_MF = median nerve, mid forearm; MED_MU = median nerve, mid upper arm; MED_WR = median nerve, wrist; PER_FH = peroneal nerve, fibular head; PER_PP = peroneal nerve, profound peroneal nerve; PER_PS = peroneal nerve, superficial peroneal nerve; RAD_SG = radial nerve, spiral groove; SUR_IG = sural nerve, inter gastrocnemius muscle; TIB_MM = tibial nerve, medial malleolus; TIB_PF = tibial nerve, popliteal fossa; ULN_MF = ulnar nerve, mid forearm; ULN_MU = ulnar nerve, mid upper arm; ULN_US = ulnar nerve, ulnar sulcus; ULN_WR = ulnar nerve, wrist.

Results

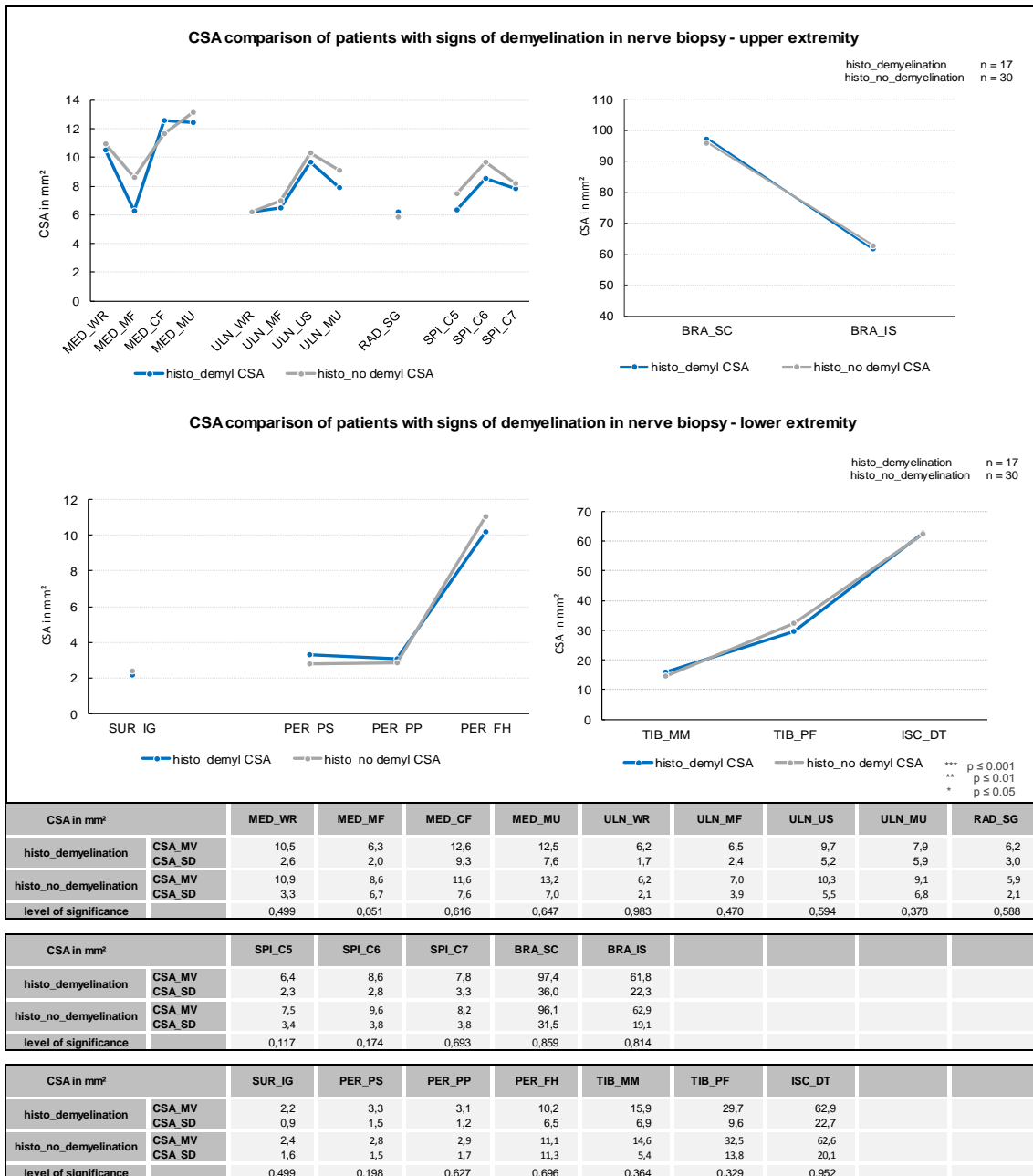


Figure 56: Cross-sectional area (CSA) comparison of patients with signs of demyelination in nerve biopsy

Abbreviations: Abbreviations: BRA_IS = brachial plexus, inter-scalene muscles; BRA_SC = brachial plexus; supra-clavicular; CSA = cross-sectional area; histo_inflammation = patients with signs of inflammation in nerve biopsy; histo_no_inflammation = patients without signs of inflammation in nerve biopsy ISC_DT = sciatic nerve, distal thigh; MED_CF = median nerve, cubital fossa; MED_MF = median nerve, mid forearm; MED_MU = median nerve, mid upper arm; MED_WR = median nerve, wrist; PER_FH = peroneal nerve, fibular head; PER_PP = peroneal nerve, profound peroneal nerve; PER_PS = peroneal nerve, superficial peroneal nerve; RAD_SG = radial nerve, spiral groove; SPI_C5 = spinal nerve; SPI_C6 = spinal nerve, sixth cervical nerve; SPI_C7= spinal nerve, seventh cervical nerve; SUR_IG = sural nerve, inter gastrocnemius muscle; TIB_MM = tibial nerve, medial malleolus; TIB_PF = tibial nerve, popliteal fossa; ULN_MF = ulnar nerve, mid forearm; ULN_MU = ulnar nerve, mid upper arm; ULN_US = ulnar nerve, ulnar sulcus; ULN_WR = ulnar nerve, wrist.

Results

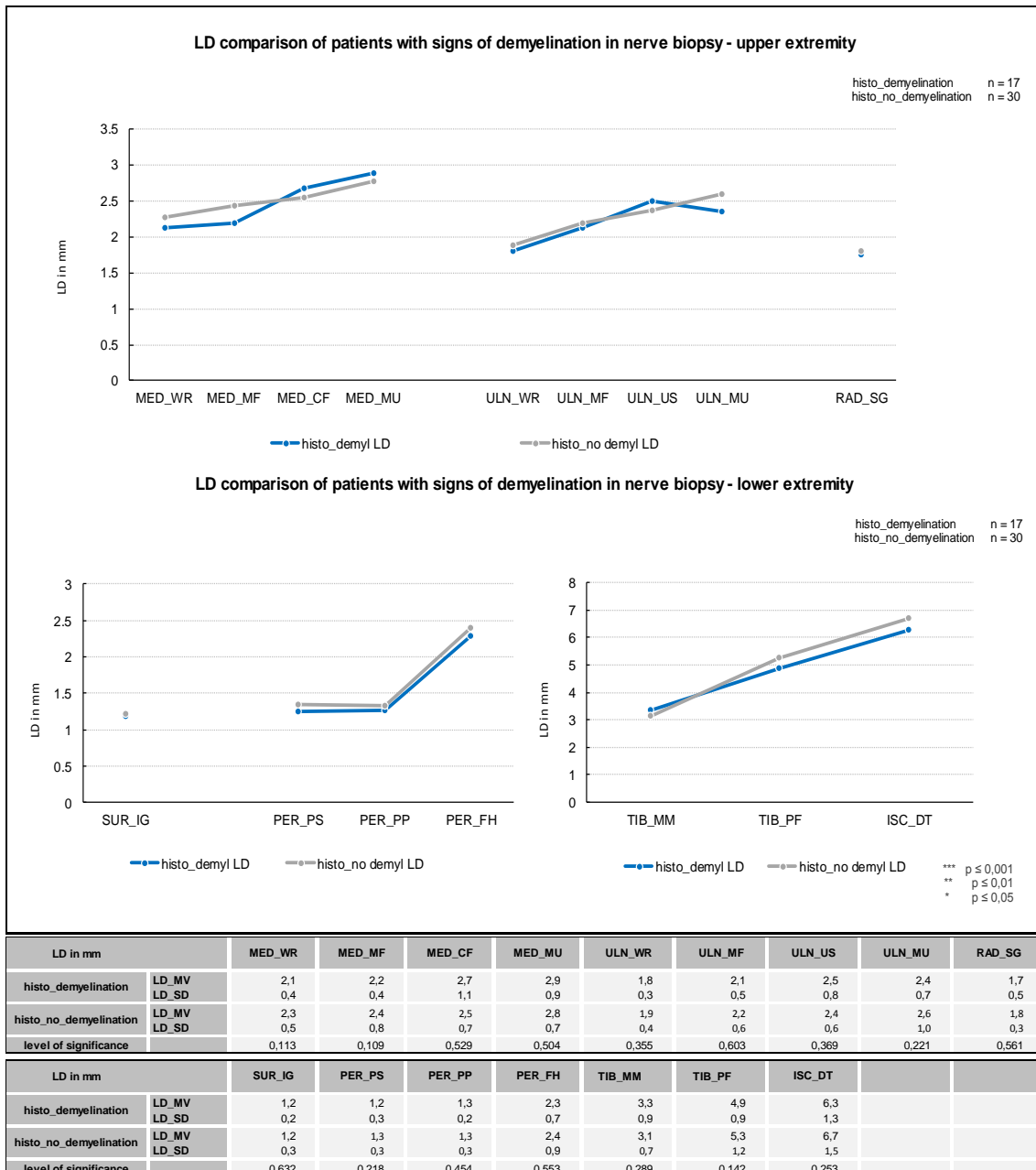


Figure 57: Longitudinal diameter (LD) comparison of patients with signs of demyelination in nerve biopsy
Abbreviations: ISC_DT = sciatic nerve, distal thigh; LD = longitudinal diameter; MED_CF = median nerve, cubital fossa; MED_MF = median nerve, mid forearm; MED_MU = median nerve, mid upper arm; MED_WR = median nerve, wrist; PER_FH = peroneal nerve, fibular head; PER_PP = peroneal nerve, profound peroneal nerve; PER_PS = peroneal nerve, superficial peroneal nerve; RAD_SG = radial nerve, spiral groove; SUR_IG = sural nerve, inter gastrocnemius muscle; TIB_MM = tibial nerve, medial malleolus; TIB_PF = tibial nerve, popliteal fossa; ULN_MF = ulnar nerve, mid forearm; ULN_MU = ulnar nerve, mid upper arm; ULN_US = ulnar nerve, ulnar sulcus; ULN_WR = ulnar nerve, wrist.

Results

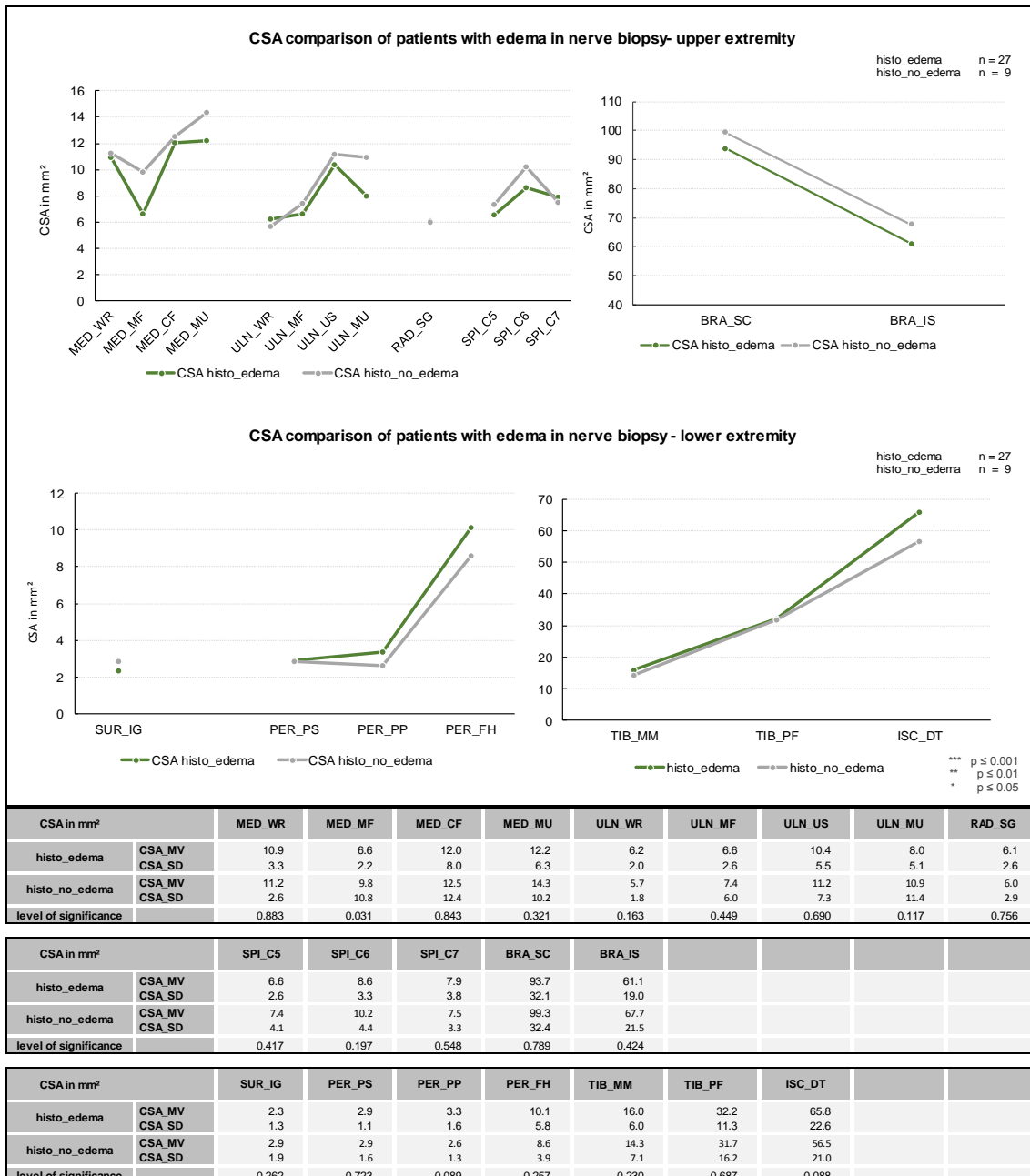


Figure 58: Cross-sectional area (CSA) comparison of patients with edema in nerve biopsy

Abbreviations: BRA_IS = brachial plexus, inter-scalene muscles; BRA_SC = brachial plexus; supra-clavicular; CSA = cross-sectional area; ISC_DT = sciatic nerve, distal thigh; MED_CF = median nerve, cubital fossa; MED_MF = median nerve, mid forearm; MED_MU = median nerve, mid upper arm; MED_WR = median nerve, wrist; PER_FH = peroneal nerve, fibular head; PER_PP = peroneal nerve, profound peroneal nerve; PER_PS = peroneal nerve, superficial peroneal nerve; RAD_SG = radial nerve, spiral groove; SPI_C5 = spinal nerve; SPI_C6 = spinal nerve, sixth cervical nerve; SPI_C7 = spinal nerve, seventh cervical nerve; SUR_IG = sural nerve, inter gastrocnemius muscle; TIB_MM = tibial nerve, medial malleolus; TIB_PF = tibial nerve, popliteal fossa; ULN_MF = ulnar nerve, mid forearm; ULN_MU = ulnar nerve, mid upper arm; ULN_US = ulnar nerve, ulnar sulcus; ULN_WR = ulnar nerve, wrist.

Results

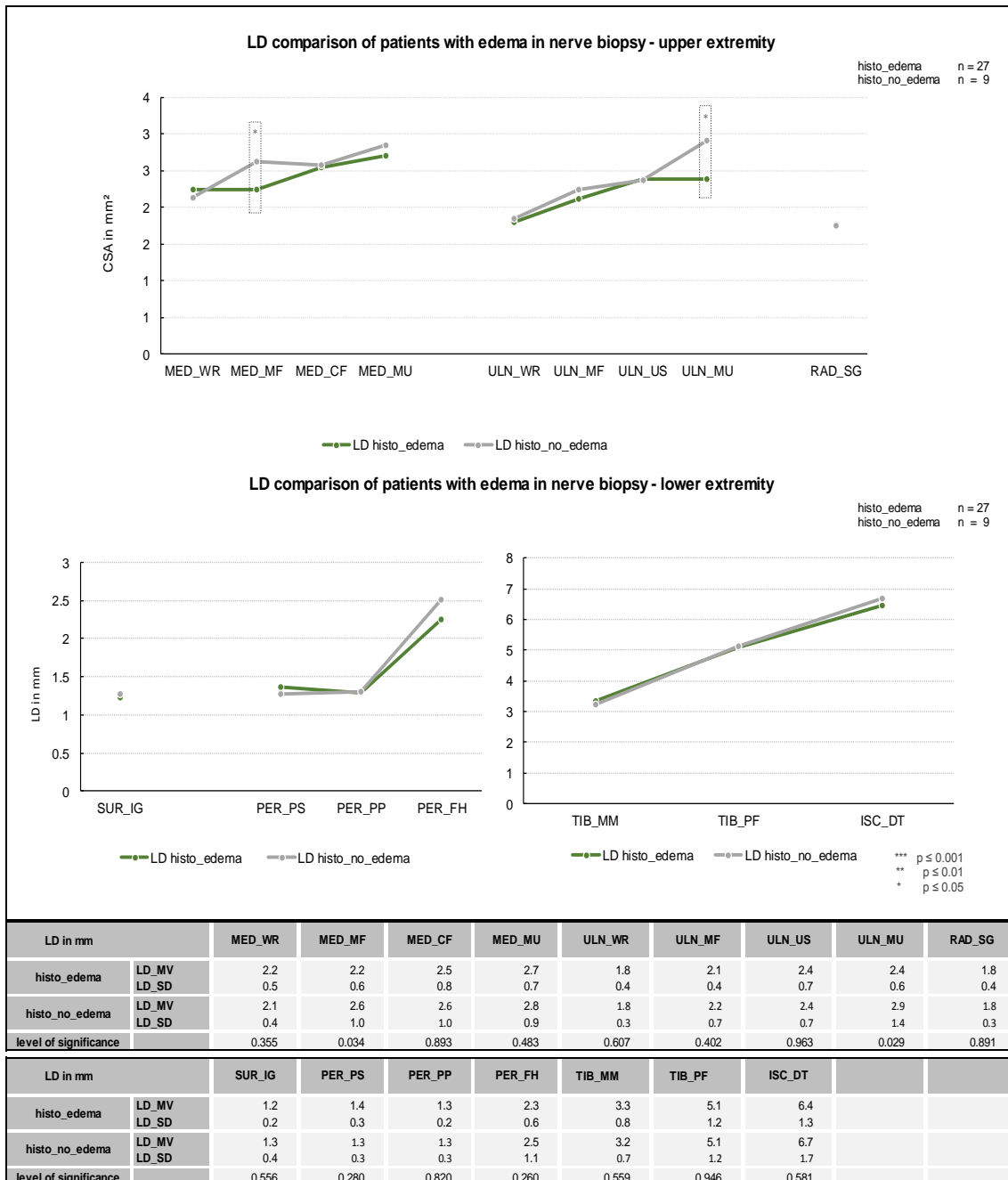


Figure 59: Longitudinal diameter (LD) comparison of patients with edema in nerve biopsy

Abbreviations: ISC_DT = sciatic nerve, distal thigh; LD = longitudinal diameter; MED_CF = median nerve, cubital fossa; MED_MF = median nerve, mid forearm; MED_MU = median nerve, mid upper arm; MED_WR = median nerve, wrist; PER_FH = peroneal nerve, fibular head; PER_PP = peroneal nerve, profound peroneal nerve; PER_PS = peroneal nerve, superficial peroneal nerve; RAD_SG = radial nerve, spiral groove; SUR_IG = sural nerve, inter gastrocnemius muscle; TIB_MM = tibial nerve, medial malleolus; TIB_PF = tibial nerve, popliteal fossa; ULN_MF = ulnar nerve, mid forearm; ULN_MU = ulnar nerve, mid upper arm; ULN_US = ulnar nerve, ulnar sulcus; ULN_WR = ulnar nerve, wrist.

Results

3.3.11 Results of NCS in synopsis with HRUS measurements at sites of electric conduction block (CB)

NCS revealed ten sites with CB in 6/92 (7%) patients. Three of these patients were diagnosed with MMN, one with MADSAM, and one with hereditary neuropathy. The data of NCS in comparison with HRUS measurements (CSA and LD) are shown in Table 4. Normative reference values (mean) with standard deviation are shown below the data point of CSA or LD. If the data point was higher than reference value (mean) plus standard deviation it was marked blue.

In all cases of detected CB associated enlargement of CSA or LD was found.

Table 4: High-resolution nerve ultrasound (HRUS) measurement at sites of conduction block (CB)
 Blue coloration shows enlargement of cross-sectional area (CSA) or longitudinal diameter (LD) above mean in addition with standard deviation (SD). Abbreviations: CB = conduction block; CF = cubital fossa; CMAP = compound muscle action potential; CSA = cross-sectional area; dist. = distal; HRUS = high-resolution nerve ultrasound; MADSAM = multifocal acquired demyelinating sensory and motor neuropathy; hered. NP = hereditary neuropathy; MF = mid forearm; mm = millimeter; MMN = multifocal motor neuropathy; MU = mid-upper arm; mV = millivolt; prox. = proximal; LD = longitudinal diameter; SG = spiral groove; US = ulnar sulcus; WR = wrist.

case 1: MMN		prox. CMAP [mV]	dist. 1 CMAP [mV]	CSA_MU [mm ²]	LD_MU [mm]	CSA_CF [mm ²]	LD_CF [mm]	CSA_MF [mm ²]	LD_MF [mm]
median nerve	right, prox. reference	0,84	2,20	13,0 8,9 (SD 1,8)	4,8 2,4 (SD 0,4)	11,3 8,2 (SD 1,9)	2,7 2,2 (SD 0,3)	5,3 5,9 (SD 1,3)	2,1 2,1 (SD 0,4)
case 2: MMN		prox. CMAP [mV]	dist. 1 CMAP [mV]	CSA_MU [mm ²]	LD_MU [mm]	CSA_CF [mm ²]	LD_CF [mm]	CSA_MF [mm ²]	LD_MF [mm]
median nerve	right, prox. reference	3,07	8,12	19,7 8,9 (SD 1,8)	3,7 2,4 (SD 0,4)	11,0 8,2 (SD 1,9)	3,4 2,2 (SD 0,3)	7,0 5,9 (SD 1,3)	2,0 2,1 (SD 0,4)
case 3: MMN		prox. CMAP [mV]	dist. 1 CMAP [mV]	CSA_MU [mm ²]	LD_MU [mm]	CSA_US [mm ²]	LD_US [mm]	CSA_MF [mm ²]	LD_MF [mm]
ulnar nerve	right, prox. reference	0,77	8,08	6,7 6,5 (SD 1,7)	1,8 2,1 (SD 0,2)	7,7 7,7 (SD 2,1)	2,1 2,1 (SD 0,4)	6,7 5,3 (SD 1,1)	2,0 1,9 (SD 0,3)
case 4: MADSAM		prox. CMAP [mV]	dist. 1 CMAP [mV]	CSA_MU [mm ²]	LD_MU [mm]	CSA_CF [mm ²]	LD_CF [mm]	CSA_MF [mm ²]	LD_MF [mm]
median nerve	right, prox. reference	1,85	4,17	74,7 8,9 (SD 1,8)	9,6 2,4 (SD 0,4)	29,3 8,2 (SD 1,9)	4,0 2,2 (SD 0,3)	4,0 5,9 (SD 1,3)	1,7 2,1 (SD 0,4)
		dist. 1 CMAP [mV]	dist. 2 CMAP [mV]	CSA_CF [mm ²]	LD_CF [mm]	CSA_MF [mm ²]	LD_MF [mm]	CSA_WR [mm ²]	LD_WR [mm]
median nerve	right, dist. reference	4,17	12,38	29,3 8,2 (SD 1,9)	4,0 2,2 (SD 0,3)	4,0 5,9 (SD 1,3)	1,7 2,1 (SD 0,4)	7,3 8,9 (SD 1,8)	1,8 2,1 (SD 0,4)
		prox. CMAP [mV]	dist. 1 CMAP [mV]	CSA_MU [mm ²]	LD_MU [mm]	CSA_US [mm ²]	LD_US [mm]	CSA_MF [mm ²]	LD_MF [mm]
ulnar nerve	right, prox. reference	0,69	2,80	46,7 6,5 (SD 1,7)	7,9 2,1 (SD 0,2)	9,7 7,7 (SD 2,1)	2,4 2,1 (SD 0,4)	14,0 5,3 (SD 1,1)	3,7 1,9 (SD 0,3)
		dist. 1 CMAP [mV]	dist. 2 CMAP [mV]	CSA_US [mm ²]	LD_US [mm]	CSA_MF [mm ²]	LD_MF [mm]	CSA_WR [mm ²]	LD_WR [mm]
ulnar nerve	right, dist. reference	2,80	13,62	9,7 7,7 (SD 2,1)	2,4 2,1 (SD 0,4)	14,0 5,3 (SD 1,1)	3,7 1,9 (SD 0,3)	3,7 5,3 (SD 1,3)	1,6 1,7 (SD 0,3)
		prox. CMAP [mV]	dist. 1 CMAP [mV]	CSA_MU [mm ²]	LD_MU [mm]	CSA_US [mm ²]	LD_US [mm]	CSA_MF [mm ²]	LD_MF [mm]
ulnar nerve	left, prox. reference	2,11	4,69	27,0 6,5 (SD 1,7)	5,2 2,1 (SD 0,2)	12,3 7,7 (SD 2,1)	1,8 2,1 (SD 0,4)	9,3 5,3 (SD 1,1)	2,9 1,9 (SD 0,3)
		dist. 1 CMAP [mV]	dist. 2 CMAP [mV]	CSA_US [mm ²]	LD_US [mm]	CSA_MF [mm ²]	LD_MF [mm]	CSA_WR [mm ²]	LD_WR [mm]
ulnar nerve	left, dist. reference	4,69	13,56	12,3 7,7 (SD 2,1)	1,8 2,1 (SD 0,4)	9,3 5,3 (SD 1,1)	2,9 1,9 (SD 0,3)	10,0 5,3 (SD 1,3)	2,4 1,7 (SD 0,3)
		prox. CMAP [mV]	dist. 1 CMAP [mV]	CSA_SG [mm ²]	LD_SG [mm]				
radial nerve	right, prox. reference	2,58	12,55	12,7 4,9 (SD 1,3)	2,1 1,7 (SD 0,2)				
case 5: hered. NP		prox. CMAP [mV]	dist. 1 CMAP [mV]	CSA_MU [mm ²]	LD_MU [mm]	CSA_US [mm ²]	LD_US [mm]	CSA_MF [mm ²]	LD_MF [mm]
ulnar nerve	right, prox. reference	0,77	1,86	4,0 6,5 (SD 1,7)	2,1 2,1 (SD 0,2)	8,7 7,7 (SD 2,1)	2,1 2,1 (SD 0,4)	7,3 5,3 (SD 1,1)	1,8 1,9 (SD 0,3)

4 Discussion

4.1 Study findings

The objective of our study was to examine the diagnostic utility of HRUS for the differentiation between subtypes of both axonal and demyelinating neuropathies. Additionally, patients with ALS were included.

The first hypothesis was that neuropathy causes enlargement of peripheral nerves compared to healthy controls and that ALS does not cause enlargement of peripheral nerves compared to healthy controls. Our findings were that CSA and LD were enlarged in patients with polyneuropathy at most measured sites. However, nerve enlargement was less frequent in the cohort of patients with ALS – but nerve enlargement was present in ALS as well. Although not systematically examined, morphological alteration of intrinsic nerve structure was found in both patients with polyneuropathy and ALS.

The second hypothesis was that enlargement of peripheral nerves can be detected by measurement of CSA and LD and that both types of measurement deliver comparable results. We found that CSA and LD measurement showed comparable results in most disease groups and groups of stratification. Notable in this context was that nerve enlargement was slightly less frequent than by measurement of LD.

The third hypothesis was that axonal and demyelinating neuropathies show distinctive patterns of nerve enlargement. The subtypes of axonal and demyelinating neuropathies can be identified by HRUS. Comparison between diagnose-defined subgroups of axonal and demyelinating polyneuropathies and healthy controls showed a stronger nerve enlargement with additional enhancement of proximal nerve segments of upper extremities in patients with demyelinating neuropathies compared to patients with axonal neuropathies. Stratification for inflammatory and non-inflammatory neuropathies did only show low enlargement at few sites for the inflammatory subgroup. Defined subtypes of inflammatory neuropathies (NSVN, CIDP, MADSAM, MMN) showed partly strong nerve enlargement. In this study, only slight differences between a defined subgroup of painful and painless neuropathy was found with mild nerve

Discussion

enlargement at some measuring sites. In regional connection to sites of conduction block, nerve enlargement was detected.

The fourth hypothesis was that histological findings show corresponding measurement alterations in HRUS. Stratification for specific characteristics in nerve biopsy did not lead to constructive differences in comparison between groups.

4.1.1 Healthy control cohort and normative values

In a first step, healthy controls were systematically examined to create site-specific normative values. This is obligatory since normal values of nerve size vary between laboratories and examiners (Telleman et al. 2018).

A substantial difference between the left and the right body side was not found in this study. Established data concerning this question partly contradicts this finding – a slight skew to the right body side has been described (Cartwright et al. 2008), whereas other authors found similar CSA at the left and the right side (Zaidman et al. 2009). No systematic positive or negative correlation was found to subcohort specifications such as height, weight or BMI. Zaidman et. al found a correlation between height and average CSA and in a lower extent with weight (Zaidman et al. 2009). Cartwright et al. found a correlation of CSA with weight (Cartwright et al. 2008). However, the direct comparison of the male and female subcohort revealed few, but remarkable differences: the CSA of ulnar nerve at mid forearm and at mid upper arm showed higher CSA values in the male group than in the female subgroup. Similarly, this was found similar for the supraclavicular brachial plexus – at this site the absolute difference between the subgroups was about 10 mm². LD was found to be enlarged for the median nerve at cubital fossa.

With these conflicting data, future studies with larger cohorts of healthy controls are needed to clarify the potential influence of epidemiological data on reference values.

4.1.2 Patients with neuropathy

The comparison of all patients with neuropathy to the healthy control cohort showed increased CSA and LD at most of measuring sides, which suggests that

Discussion

neuropathy causes morphological alteration at peripheral nerves in the sense of enlargement visible with HRUS. The comparison of axonal and demyelinating neuropathies showed higher CSA and LD values at more measuring sites in patients with demyelinating neuropathies compared to patients with axonal polyneuropathies. A different pattern between demyelinating and axonal neuropathies in comparison to controls was already described: demyelinating neuropathies showed stronger nerve thickening in cervical nerve roots and in proximal upper limb nerves compared to axonal neuropathies (Scheidl et al. 2014). We reproduced this finding for proximal median and proximal radial nerve, the C5 nerve root, and the brachial plexus.

The direct comparison of patients with and without inflammatory neuropathy showed a CSA enlargement of brachial plexus and distal ulnar nerves for the subgroup of inflammatory neuropathy. Evidence on this topic is rare, since some studies did recruit patients with axonal neuropathies, but there is a lack of studies with a specific selection of patients with axonal neuropathies with and without signs of inflammation. The comparison patients with painful and painless neuropathy showed just slight CSA enlargement for the painful subgroup at ulnar, tibial, peroneal, and sixth spinal nerve. It remains unclear, if this was due to higher disease activity or higher disease severity.

The subgroup diagnosed with NSVN showed nerve enlargement at the upper and lower extremity compared to healthy controls for the CSA. LD enlargement was found at the upper extremity and to a lower degree in the lower extremity as well. Although not systematically examined in this study, at prescribed sites nerve enlargement appeared to be more focal than in other inflammatory neuropathies. Literature gives corresponding results with focal CSA enlargement in one or more nerves in patients with NSVN. However, strongest nerve enlargement was found for tibial and peroneal nerves (Grimm et al. 2014). In our study, level of significance reached strongest values for several sites of median and ulnar nerve, brachial plexus at supraclavicular site, even the C5 nerve root, distal tibial nerve and peroneal nerve. We also confirmed the finding of a strong LD enlargement of the superficial peroneal nerve in patients with NSVN (Üçeyler et al. 2016). The CIDP-subgroup showed nerve enlargement at most measuring sites for CSA and

Discussion

LD. Enlargement for CSA was present at all measuring sites with exception of the C7 nerve root. Enlargement of the LD was found at all sites with exception of the median nerve at mid forearm and tibial and sural nerve. Recent findings attest HRUS a higher sensitivity but lower specificity than NCS for the detection of CIDP (Herraets et al. 2020). This underlines the importance of HRUS in terms of this potential treatable disease.

In the patients diagnosed with MADSAM, nerve enlargement was seen for CSA and LD at most sites as well. Especially radial nerve and proximal parts of median and ulnar nerve, along with the brachial plexus at the supraclavicular showed the highest nerve enlargement of all neuropathies. Furthermore, a CSA “crescendo” from distal to proximal parts of median and ulnar nerve was remarkable, which could be confirmed by LD measurement. The nerve enlargement in MADSAM was described earlier. In one study nerve enlargement correlated strongly with CB –our data underlines this correlation (Scheidl et al. 2012). In the subgroup diagnosed with MMN, nerve enlargement was present to a lower extent. Ulnar nerve showed no enlargement for the CSA and just slight enlargement for the LD. Radial nerve showed enlargement for both measuring parameters. The nerve enlargement of median nerve was accentuated proximal. Brachial plexus showed CSA enlargement for both measuring sites. Former study results already described multifocal nerve enlargement in patients diagnosed with MMN. Nerve enlargement was found at sites without conduction abnormalities as well and at sites where clinically no sonographic abnormality was suspected (Beekman et al. 2005). A case series additional even identified patients with clinical symptoms compatible with CIDP and MMN with abnormal peripheral ultrasound findings but without electrodiagnostic features of demyelination. These patients responded positively to therapy with intravenous immunoglobulin (Goedee et al. 2019).

The correlation of HRUS findings with nerve conduction studies detected conduction block showed enlargement of CSA and/or LD in associated nerve regions. In some cases, this alteration of the nerve caliber was slight, whereas in some cases enlargement was prominent. This finding corresponds to preexisting literature, which postulates the correlation of conduction block and nerve enlargement (Granata et al. 2009, Scheidl et al. 2012).

Discussion

Hypoechoic fascicular structure did not only occur in CIDP, MADSAM, MMN, NSVN, axonal neuropathy, and ALS. Extent and distribution of these structures were not specifically recorded. Previously, a larger size of nerve fascicles was reported in CIDP, MADSAM, and MMN than in axonal neuropathies at the fibular, ulnar and median nerve (Goedee et al. 2016). It was assumed that nerve enlargement could relate to focal inflammatory demyelinating with swelling of the nerve sheaths (Grimm et al. 2014). As fluid appears hypoechoic in ultrasound investigation, this could be deducted to the partial correlation of nerve enlargement and the presence of hypoechogenic fascicular structure. This suggests that endoneurial fluid contributes to nerve enlargement. But enlargement of CSA was not only present in association with hypoechogenic fascicular structure, but also with hyperechoic intraneuronal alteration shown in Figure 32.

The subgroup analysis after stratification for histological features such as inflammation, demyelination, or edema did not show relevant differences between the group of patients with the respective finding in nerve biopsy and without. This leads to the conclusion that HRUS cannot replace a histological examination. Especially HRUS investigation of sural nerve did not give evidence about histological characteristics in our study. In contrast, ultra-high-frequency ultrasound (linear array transducer, 50-70 MHz) revealed that hyperechogenicity of sural nerve correlates with inflammatory infiltrates in nerve biopsy of patients with progressive neuropathies. (Puma et al. 2021).

4.1.3 Patients with ALS

We found both enlargement of the CSA and the LD at the upper and lower extremities in patients with ALS compared to the healthy control cohort. Median and ulnar nerves showed enlargement for the CSA and to a lower extent for the LD at both entrapment and non-entrapment sites. Brachial plexus showed enlargement at the supraclavicular site. At the lower extremities, the peroneal nerve showed enlargement. It is notable that the nerve enlargement at the proximal parts of the upper extremities (median, ulnar, radial nerve and brachial plexus) occurred to a much lower extend than in inflammatory neuropathies. Remarkable in this context was, that the AUC of ROCs for the investigated

Discussion

inflammatory neuropathies (NSVN, CIDP, MADSAM, MMN) were above 0.5, whereas the AUC of ROCs of the brachial plexus in patients with ALS was close to 0.5.

The spinal nerves showed no enlargement in the cohort of patients with ALS. The easily accessible C5 nerve root differed strongest between inflammatory neuropathies (NSVN, CIDP, MADSAM, MMN) in which enlargement was visible compared to ALS in which no CSA enlargement was present. Hence, this site might help in clinical differentiation between diseases. Literature about this issue is controversial. Previous studies reported a larger CSA in controls than in patients with ALS (Cartwright et al. 2011, Schreiber et al. 2015), but single nerve enlargement was also found in patients with ALS (Grimm et al. 2015).

4.2 Limitations of this study

Our study has some limitations. Firstly, the study was executed as a single HRUS-investigator study, which implies that the interrater reliability could not be classified, and systematic error could not be eliminated. The investigator was not blinded for diagnosis, clinical parameters, and medical history due to recruitment process. Secondly, although the primary group of all recruited patients with neuropathy was large ($n = 84$), the subgroups remained small. Therefore, the statistical power of the results is limited. Lastly, patients were recruited in different stages of disease with and without immunomodulatory therapy, which might had an impact on nerve size. As for CIDP, a smaller nerve size was reported under treatment (Zaidman and Pestronk 2014). This was considered in other studies, which recruited treatment negative patients (Goedee et al. 2016).

Graphical illustration of CSA and LD values shows connecting lines between measuring sites of one nerve or few nerves. This presentation was chosen for reasons of easier comprehension of the Figures.

4.3 Strengths of this study

We performed repetitive HRUS measurements at many sites to guarantee highest possible quality of obtained data.

Discussion

Although HRUS measurement results differ between investigators and center specific reference values need to be defined, our measuring results show good correlation to reference data published (Boehm et al. 2014).

Further, we recruited a large group of patients with different types of neuropathies, which was mandatory for the generation of subgroups to analyze the diagnostic accuracy of HRUS, while only few studies included patients with relevant reference and healthy control groups, in particular axonal neuropathies and ALS (Goedee et al. 2016).

In an early stage of neuropathy, diagnostic accuracy may be limited. Therefore, a longer course of disease may secure the final diagnosis. This might be crucial in differentiating MMN and ALS, which might reveal the true entity only in late course. Most of our patients were diagnosed one year or more and diagnoses were repetitively cross-checked by senior neurologists.

4.4 Perspective

Structural nerve alteration and enlargement of nerves in peripheral nerve disorders is present and can be detected by HRUS, yet its origins and pathophysiological formation are not yet understood. We do not know, if peripheral nerve enlargement in neuropathies is due to inflammatory processes, the endoneurial inclusion of fluid, processes of demyelination and remyelination, a combination or none of that. Further, it must be considered different pathophysiological causes play a role, which are only partly understood. Therefore, the combination of different methods such as electrophysiology, MRI, laboratory tests and nerve biopsy are necessary when diagnosing neuropathies. Recent scientific consideration engages for example in the assessment of the diagnostic performance of nerve ultrasound in comparison with qualitative and (semi-)quantitative MRI and in order to distinguish MMN and CIDP from segmental spinal muscular atrophy (Oudeman et al. 2020).

The capability of HRUS will evolve with technical development and may reveal new aspects and insights in nerve assessment. New findings may open new sights on the previous established knowledge and thus must continually be reviewed and discussed. To our mind, HRUS should continue its path into routine diagnostics with patients in suspicion of neuropathy and ALS.

5 Summary

Neuropathies are a group of potentially treatable diseases with an often disabling and restricting course. ALS is a lethal disease without causal treatment possibilities. The objective of this study was to examine the diagnostic utility of HRUS for the differentiation of subtypes of axonal and demyelinating neuropathies and to investigate its utility for the sonological differentiation of ALS. The hypothetical statement that neuropathy causes enlargement of peripheral nerves compared to healthy controls proved to be right, but the adjunctive assumption that ALS does not cause enlargement of peripheral nerves proved to be wrong – in patients with ALS slight enlargement of peripheral nerves was visible as well. The statement that nerve enlargement can be detected by measurement of CSA and LD with comparable results proved to be right, but the enlargement was slightly less present by measurement of the LD. The statement that axonal and demyelinating neuropathies show distinct patterns of nerve enlargement must be answered differentiated: The comparison between axonal and demyelinating neuropathies showed a stronger nerve enlargement in patients with demyelinating neuropathies than in patients with axonal neuropathies at proximal nerve segments of upper extremities. In the comparison of diagnose-defined subgroups of inflammatory demyelinating neuropathies a respective specific pattern of nerve enlargement was visible. However, remarkable in this context was the strong nerve enlargement found in patients with NSVN, which is classified as axonal neuropathy. Stratification for specific findings in nerve biopsy did not lead to constructive differences in comparison between the different groups. To sum up, HRUS showed to provide a useful contribution in the diagnostic process of neuropathies and ALS but needs to be integrated in a multimodal diagnostic approach.

5 Zusammenfassung

Neuropathien stellen eine Gruppe potenziell behandelbarer Erkrankungen mit häufig behinderndem und einschränkendem Verlauf dar. Die amyotrophe Lateralsklerose ist eine tödliche Erkrankung ohne Möglichkeiten der kausalen Behandlung. Das Ziel dieser Studie war es, den diagnostischen Nutzen von hochauflösendem Ultraschall für die Differenzierung von Subtypen axonaler und demyelinisierender Neuropathien, sowie der amyotrophen Lateralsklerose zu untersuchen. Die hypothetische Aussage, dass durch Neuropathien eine Vergrößerung von peripheren Nerven im Vergleich zu gesunden Kontrollen nachgewiesen werden kann, erwies sich als richtig. Entgegen der hiermit verknüpften Aussage, dass es bei amyotropher Lateralsklerose zu keiner Größenzunahme peripherer Nerven kommt, konnte bei diesen Patienten ebenfalls eine leichte Kaliberzunahme der Nerven nachgewiesen werden. Die Aussage, dass eine Nervenvergrößerung durch die Messung von Querschnittsfläche und longitudinalem Durchmesser mit vergleichbaren Ergebnissen erfolgen kann, erwies sich als richtig, jedoch zeigte sich die Nervenvergrößerung bei der Messung des longitudinalen Durchmessers etwas geringer ausgeprägt. Die Aussage, dass axonale und demyelinisierende Neuropathien unterschiedliche Muster der Nervenvergrößerung aufweisen, muss differenziert beantwortet werden: Der Vergleich axonalen und demyelinisierenden Neuropathien zeigte bei Patienten mit demyelinisierenden Neuropathien, insbesondere an proximalen Nervensegmenten der oberen Extremitäten, eine stärkere Nervenvergrößerung als bei Patienten mit axonalen Neuropathien. Im Vergleich diagnose-definierter Subgruppen demyelinisierender Neuropathien zeigte sich ein jeweils spezifisches Verteilungsmuster der Nervenvergrößerung. In diesem Zusammenhang bemerkenswert war jedoch die starke Nervenvergrößerung bei Patienten mit nicht-systemischer vaskulitischer Polyneuropathie, welche als axonale Neuropathie klassifiziert wird. Die Stratifikation nach spezifischen Befunden in der Nervenbiopsie führte nicht zu konstruktiven Unterschieden im Vergleich der Untergruppen. Zusammenfassend zeigte sich, dass der hochauflösende Nervenultraschall einen nützlichen Beitrag im diagnostischen Prozess von Neuropathien und ALS leisten kann, jedoch in eine multimodale diagnostische Herangehensweise integriert werden muss.

6 Bibliography

- Alshami, A. M., C. W. Cairns, B. K. Wylie, T. Souvlis and M. W. Coppieters (2009). "Reliability and size of the measurement error when determining the cross-sectional area of the tibial nerve at the tarsal tunnel with ultrasonography." *Ultrasound Med Biol* 35(7): 1098-1102.
- Beekman, R., L. H. van den Berg, H. Franssen, L. H. Visser, J. T. van Asseldonk and J. H. Wokke (2005). "Ultrasonography shows extensive nerve enlargements in multifocal motor neuropathy." *Neurology* 65(2): 305-307.
- Boehm, J., E. Scheidl, D. Bereczki, T. Schelle and Z. Aranyi (2014). "High-resolution ultrasonography of peripheral nerves: measurements on 14 nerve segments in 56 healthy subjects and reliability assessments." *Ultraschall Med* 35(5): 459-467.
- Bouhassira, D., N. Attal, J. Fermanian, H. Alchaar, M. Gautron, E. Masquelier, S. Rostaing, M. Lanteri-Minet, E. Collin, J. Grisart and F. Boureau (2004). "Development and validation of the Neuropathic Pain Symptom Inventory." *Pain* 108(3): 248-257.
- Bril, V., S. Tomioka, R. A. Buchanan, B. A. Perkins and T. S. G. m (2009). "Reliability and validity of the modified Toronto Clinical Neuropathy Score in diabetic sensorimotor polyneuropathy." *Diabet Med* 26(3): 240-246.
- Brooks, B. R., R. G. Miller, M. Swash and T. L. Munsat (2000). "El Escorial revisited: revised criteria for the diagnosis of amyotrophic lateral sclerosis." *Amyotroph Lateral Scler Other Motor Neuron Disord* 1(5): 293-299.
- Brown, R. H. and A. Al-Chalabi (2017). "Amyotrophic Lateral Sclerosis." *N Engl J Med* 377(2): 162-172.
- Callaghan, B. C., H. T. Cheng, C. L. Stables, A. L. Smith and E. L. Feldman (2012). "Diabetic neuropathy: clinical manifestations and current treatments." *Lancet Neurol* 11(6): 521-534.
- Cartwright, M. S., M. E. Brown, P. Eulitt, F. O. Walker, V. H. Lawson and J. B. Caress (2009). "Diagnostic nerve ultrasound in Charcot-Marie-Tooth disease type 1B." *Muscle Nerve* 40(1): 98-102.
- Cartwright, M. S., L. V. Passmore, J. S. Yoon, M. E. Brown, J. B. Caress and F. O. Walker (2008). "Cross-sectional area reference values for nerve ultrasonography." *Muscle Nerve* 37(5): 566-571.
- Cartwright, M. S., F. O. Walker, L. P. Griffin and J. B. Caress (2011). "Peripheral nerve and muscle ultrasound in amyotrophic lateral sclerosis." *Muscle Nerve* 44(3): 346-351.
- Collins, M. P., P. J. Dyck, G. S. Gronseth, L. Guillemin, R. D. Hadden, D. Heuss, J. M. Leger, N. C. Notermans, J. D. Pollard, G. Said, G. Sobue, A. F. Vrancken and J. T. Kissel (2010). "Peripheral Nerve Society Guideline

Bibliography

- on the classification, diagnosis, investigation, and immunosuppressive therapy of non-systemic vasculitic neuropathy: executive summary." *J Peripher Nerv Syst* 15(3): 176-184.
- Collins, M. P. and R. D. Hadden (2017). "The nonsystemic vasculitic neuropathies." *Nat Rev Neurol* 13(5): 302-316.
- de Carvalho, M., R. Dengler, A. Eisen, J. D. England, R. Kaji, J. Kimura, K. Mills, H. Mitsumoto, H. Nodera, J. Shefner and M. Swash (2008). "Electrodiagnostic criteria for diagnosis of ALS." *Clin Neurophysiol* 119(3): 497-503.
- Decard, B. F., M. Pham and A. Grimm (2018). "Ultrasound and MRI of nerves for monitoring disease activity and treatment effects in chronic dysimmune neuropathies - Current concepts and future directions." *Clin Neurophysiol* 129(1): 155-167.
- Devigili, G., N. Uceyler, M. Beck, K. Reiners, G. Stoll, K. V. Toyka and C. Sommer (2011). "Vasculitis-like neuropathy in amyotrophic lateral sclerosis unresponsive to treatment." *Acta Neuropathol* 122(3): 343-352.
- Di Pasquale, A., S. Morino, S. Loreti, E. Bucci, N. Vanacore and G. Antonini (2015). "Peripheral nerve ultrasound changes in CIDP and correlations with nerve conduction velocity." *Neurology* 84(8): 803-809.
- Dyck, P. J. B. and J. A. Tracy (2018). "History, Diagnosis, and Management of Chronic Inflammatory Demyelinating Polyradiculoneuropathy." *Mayo Clin Proc* 93(6): 777-793.
- England, J. D. and A. K. Asbury (2004). "Peripheral neuropathy." *The Lancet* 363(9427): 2151-2161.
- Feasby, T. E., W. F. Brown, J. J. Gilbert and A. F. Hahn (1985). "The pathological basis of conduction block in human neuropathies." *J Neurol Neurosurg Psychiatry* 48(3): 239-244.
- Feasby, T. E., A. F. Hahn, W. F. Brown, C. F. Bolton, J. J. Gilbert and W. J. Koopman (1993). "Severe axonal degeneration in acute Guillain-Barre syndrome: evidence of two different mechanisms?" *J Neurol Sci* 116(2): 185-192.
- Goedee, v. d. Pol, J. T. van Asseldonk and N. C. Notermans (2016). "<vandenBerg_PNP_ALS.pdf>." *Neurology*.
- Goedee, H. S., G. J. Brekelmans, J. T. van Asseldonk, R. Beekman, W. H. Mess and L. H. Visser (2013). "High resolution sonography in the evaluation of the peripheral nervous system in polyneuropathy--a review of the literature." *Eur J Neurol* 20(10): 1342-1351.
- Goedee, H. S., I. J. T. Herraets, L. H. Visser, H. Franssen, J. H. van Asseldonk, W. L. van der Pol and L. H. van den Berg (2019). "Nerve ultrasound can identify treatment-responsive chronic neuropathies without electrodiagnostic features of demyelination." *Muscle Nerve* 60(4): 415-419.

Bibliography

- Goedee, H. S., W. L. van der Pol, J. H. van Asseldonk, A. Vrancken, N. C. Notermans, L. H. Visser and L. H. van den Berg (2016). "Nerve sonography to detect peripheral nerve involvement in vasculitis syndromes." *Neurol Clin Pract* 6(4): 293-303.
- Granata, G., C. Pazzaglia, P. Calandro, M. Luigetti, C. Martinoli, M. Sabatelli and L. Padua (2009). "Ultrasound visualization of nerve morphological alteration at the site of conduction block." *Muscle Nerve* 40(6): 1068-1070.
- Grimm, A., B. F. Decard, I. Athanasopoulou, K. Schweikert, M. Sinnreich and H. Axer (2015). "Nerve ultrasound for differentiation between amyotrophic lateral sclerosis and multifocal motor neuropathy." *J Neurol* 262(4): 870-880.
- Grimm, A., B. F. Décard and H. Axer (2014). "Ultrasonography of the peripheral nervous system in the early stage of Guillain-Barré syndrome." *J Peripher Nerv Syst* 19(3): 234-241.
- Grimm, A., B. F. Decard, A. Bischof and H. Axer (2014). "Ultrasound of the peripheral nerves in systemic vasculitic neuropathies." *J Neurol Sci* 347(1-2): 44-49.
- Grimm, A., B. Heiling, U. Schumacher, O. W. Witte and H. Axer (2014). "Ultrasound differentiation of axonal and demyelinating neuropathies." *Muscle Nerve* 50(6): 976-983.
- Gwathmey, K. G., T. M. Burns, M. P. Collins and P. J. B. Dyck (2014). "Vasculitic neuropathies." *The Lancet Neurology* 13(1): 67-82.
- Hadden, R. D., E. Nobile-Orazio and C. Sommer (2010). "European Federation of Neurological Societies/Peripheral Nerve Society Guideline on management of paraproteinemic demyelinating neuropathies. Report of a Joint Task Force of the European Federation of Neurological Societies and the Peripheral Nerve Society--first revision." *J Peripher Nerv Syst* 15(3): 185-195.
- Hautzinger M., B. M., Hofmeister, D., Keller F. (2012). "Allgemeine Depressionsskala (ADS) (Vol. 2)." Göttingen: Hogrefe.
- Heinemeyer, O. and C. D. Reimers (1999). "Ultrasound of radial, ulnar, median, and sciatic nerves in healthy subjects and patients with hereditary motor and sensory neuropathies." *Ultrasound Med Biol* 25(3): 481-485.
- Herraets, I. J. T., H. S. Goedee, J. A. Telleman, R. P. A. van Eijk, J. T. van Asseldonk, L. H. Visser, L. H. van den Berg and W. L. van der Pol (2020). "Nerve ultrasound improves detection of treatment-responsive chronic inflammatory neuropathies." *Neurology* 94(14): e1470-e1479.
- Heuß, D., E. Hund, J. Klehmet, I. Kurth, H. Lehmann, C. Sommer, W. Löscher, S. Renaud. (2019). "Diagnostik bei Polyneuropathien", S1 Leitlinie. in: Deutsche Gesellschaft für Neurologie (Hrsg.), Leitlinien für Diagnostik

Bibliography

- und Therapie in der Neurologie. Online: www.dgn.org/leitlinien (abgerufen am 19.12.2020).
- Hufschmidt, A., C. Lücking, S. Rauer, F. X. Glocker (2017). *Neurologie compact*, 7.überarbeitete Auflage, Georg Thieme Verlag (Stuttgart/New York): 563-583.
- Imamura, K., Y. Tajiri, H. Kowa and K. Nakashima (2009). "Peripheral nerve hypertrophy in chronic inflammatory demyelinating polyradiculoneuropathy detected by ultrasonography." *Intern Med* 48(7): 581-582.
- Jang, J. H., C. S. Cho, K. S. Yang, H. Y. Seok and B. J. Kim (2014). "Pattern analysis of nerve enlargement using ultrasonography in chronic inflammatory demyelinating polyneuropathy." *Clin Neurophysiol* 125(9): 1893-1899.
- Jelsing, E. J., J. C. Presley, E. Maida, N. J. Hangiandreou and J. Smith (2015). "The effect of magnification on sonographically measured nerve cross-sectional area." *Muscle Nerve* 51(1): 30-34.
- Kerasnoudis, A., K. Pitarokoili, V. Behrendt, R. Gold and M. S. Yoon (2014). "Nerve ultrasound score in distinguishing chronic from acute inflammatory demyelinating polyneuropathy." *Clin Neurophysiol* 125(3): 635-641.
- Kerasnoudis, A., K. Pitarokoili, V. Behrendt, R. Gold and M. S. Yoon (2015). "Correlation of nerve ultrasound, electrophysiological and clinical findings in chronic inflammatory demyelinating polyneuropathy." *J Neuroimaging* 25(2): 207-216.
- Kiernan, M. C., S. Vucic, B. C. Cheah, M. R. Turner, A. Eisen, O. Hardiman, J. R. Burrell and M. C. Zoing (2011). "Amyotrophic lateral sclerosis." *Lancet* 377(9769): 942-955.
- Kimura, J. (1984). "Principles and pitfalls of nerve conduction studies." *Ann Neurol* 16(4): 415-429.
- Lewis, R. A., A. J. Sumner, M. J. Brown and A. K. Asbury (1982). "Multifocal demyelinating neuropathy with persistent conduction block." *Neurology* 32(9): 958-964.
- Loewenbruck, K. F., J. Liesenberg, M. Dittrich, J. Schafer, B. Patzner, B. Trausch, J. Machetanz, A. Hermann and A. Storch (2016). "Nerve ultrasound in the differentiation of multifocal motor neuropathy (MMN) and amyotrophic lateral sclerosis with predominant lower motor neuron disease (ALS/LMND)." *J Neurol* 263(1): 35-44.
- Ludolph, C., T. Grehl, T. Dengler, M. Hecht, T. Meyer, W. Löscher, S. Petri, M. Weber, J. Weishaupt (2014). "Amyotrophe Lateralsklerose (Motoneuronerkrankungen), S1 Leitlinie. ." in: Deutsche Gesellschaft für Neurologie (Hrsg.), *Leitlinien für Diagnostik und Therapie in der Neurologie*. Online: www.dgn.org/leitlinien (abgerufen am 19.12.2020).

Bibliography

- Martinoli, C., A. Schenone, S. Bianchi, P. Mandich, C. Caponetto, M. Abbruzzese and L. E. Derchi (2002). "Sonography of the median nerve in Charcot-Marie-Tooth disease." *AJR Am J Roentgenol* 178(6): 1553-1556.
- Matsuoka, N., T. Kohriyama, K. Ochi, M. Nishitani, Y. Sueda, Y. Mimori, S. Nakamura and M. Matsumoto (2004). "Detection of cervical nerve root hypertrophy by ultrasonography in chronic inflammatory demyelinating polyradiculoneuropathy." *J Neurol Sci* 219(1-2): 15-21.
- Merkies, I. S., P. I. Schmitz, F. G. van der Meche, J. P. Samijn and P. A. van Doorn (2002). "Clinimetric evaluation of a new overall disability scale in immune mediated polyneuropathies." *J Neurol Neurosurg Psychiatry* 72(5): 596-601.
- Merkies, I. S., P. I. Schmitz, F. G. Van Der Meche and P. A. Van Doorn (2003). "Comparison between impairment and disability scales in immune-mediated polyneuropathies." *Muscle Nerve* 28(1): 93-100.
- Notermans, N. C., J. H. Wokke, H. Franssen, Y. van der Graaf, M. Vermeulen, L. H. van den Berg, P. R. Bär and F. G. Jennekens (1993). "Chronic idiopathic polyneuropathy presenting in middle or old age: a clinical and electrophysiological study of 75 patients." *J Neurol Neurosurg Psychiatry* 56(10): 1066-1071.
- Oudeman, J., F. Eftimov, G. J. Strijkers, J. J. Schneiders, S. D. Roosendaal, M. P. Engbersen, M. Froeling, H. S. Goedee, P. A. van Doorn, M. W. A. Caan, I. N. van Schaik, M. Maas, A. J. Nederveen, M. de Visser and C. Verhamme (2020). "Diagnostic accuracy of MRI and ultrasound in chronic immune-mediated neuropathies." *Neurology* 94(1): e62-e74.
- Padua, L., D. Coraci, M. Lucchetta, I. Paolasso, C. Pazzaglia, G. Granata, M. Cacciavillani, M. Luigetti, F. Manganelli, C. Pisciotta, G. Piscosquito, D. Pareyson and C. Briani (2018). "Different nerve ultrasound patterns in charcot-marie-tooth types and hereditary neuropathy with liability to pressure palsies." *Muscle Nerve* 57(1): E18-e23.
- Padua, L., G. Granata, M. Sabatelli, M. Inghilleri, M. Lucchetta, M. Luigetti, D. Coraci, C. Martinoli and C. Briani (2014). "Heterogeneity of root and nerve ultrasound pattern in CIDP patients." *Clin Neurophysiol* 125(1): 160-165.
- Puma, A., N. Grecu, L. Villa, C. Butori, T. Besson, C. Cambieri, M. Cavalli, N. Azulay, S. Sacconi and C. Raffaelli (2021). "Ultra-high-frequency ultrasound imaging of sural nerve: A comparative study with nerve biopsy in progressive neuropathies." *Muscle Nerve* 63(1): 46-51.
- Rajabally, Y. A. and G. Chavada (2009). "Lewis-sumner syndrome of pure upper-limb onset: diagnostic, prognostic, and therapeutic features." *Muscle Nerve* 39(2): 206-220.
- Rattay, T. W., N. Winter, B. F. Decard, N. M. Dammeier, F. Hartig, M. Ceanga, H. Axer and A. Grimm (2017). "Nerve ultrasound as follow-up tool in treated multifocal motor neuropathy." *Eur J Neurol* 24(9): 1125-1134.

Bibliography

- Reul, C., P. Koberle, N. Uceyler and F. Puppe (2016). "Expectation-Driven Text Extraction from Medical Ultrasound Images." *Stud Health Technol Inform* 228: 712-716.
- Russell, J. W. and L. A. Zilliox (2014). "Diabetic neuropathies." *Continuum (Minneapolis Minn)* 20(5 Peripheral Nervous System Disorders): 1226-1240.
- Sander, H. W. and N. Latov (2003). "Research criteria for defining patients with CIDP." *Neurology* 60(8 Suppl 3): S8-15.
- Scheidl, E., J. Bohm, M. Simo, B. Bereznai, D. Bereczki and Z. Aranyi (2014). "Different patterns of nerve enlargement in polyneuropathy subtypes as detected by ultrasonography." *Ultrasound Med Biol* 40(6): 1138-1145.
- Scheidl, E., J. Bohm, M. Simo, C. Rozsa, B. Bereznai, T. Kovacs and Z. Aranyi (2012). "Ultrasonography of MADSAM neuropathy: focal nerve enlargements at sites of existing and resolved conduction blocks." *Neuromuscul Disord* 22(7): 627-631.
- Schreiber, S., S. Abdulla, G. Debska-Vielhaber, J. Machts, V. Dannhardt-Stieger, H. Feistner, A. Oldag, M. Goertler, S. Petri, K. Kollewe, S. Kropf, F. Schreiber, H. J. Heinze, R. Dengler, P. J. Nestor and S. Vielhaber (2015). "Peripheral nerve ultrasound in amyotrophic lateral sclerosis phenotypes." *Muscle Nerve* 51(5): 669-675.
- Schreiber, S., A. Oldag, C. Kornblum, K. Kollewe, S. Kropf, A. Schoenfeld, H. Feistner, S. Jakubiczka, W. S. Kunz, C. Scherlach, C. Tempelmann, C. Mawrin, R. Dengler, F. Schreiber, M. Goertler and S. Vielhaber (2013). "Sonography of the median nerve in CMT1A, CMT2A, CMTX, and HNPP." *Muscle Nerve* 47(3): 385-395.
- Sommer, C., H. Richter, J. P. Rogausch, J. Frettloh, M. Lungenhausen and C. Maier (2011). "A modified score to identify and discriminate neuropathic pain: a study on the German version of the Neuropathic Pain Symptom Inventory (NPSI)." *BMC Neurol* 11: 104.
- Sommer, C. L., S. Brandner, P. J. Dyck, Y. Harati, C. LaCroix, M. Lammens, L. Magy, S. I. Mellgren, M. Morbin, C. Navarro, H. C. Powell, A. E. Schenone, E. Tan, A. Urtizberea and J. Weis (2010). "Peripheral Nerve Society Guideline on processing and evaluation of nerve biopsies." *J Peripher Nerv Syst* 15(3): 164-175.
- Suk, J. I., F. O. Walker and M. S. Cartwright (2013). "Ultrasonography of peripheral nerves." *Curr Neurol Neurosci Rep* 13(2): 328.
- Telleman, J. A., A. Grimm, S. Goedee, L. H. Visser and C. M. Zaidman (2018). "Nerve ultrasound in polyneuropathies." *Muscle Nerve* 57(5): 716-728.
- Tesfaye, S., A. J. Boulton, P. J. Dyck, R. Freeman, M. Horowitz, P. Kempler, G. Lauria, R. A. Malik, V. Spallone, A. Vinik, L. Bernardi and P. Valensi (2010). "Diabetic neuropathies: update on definitions, diagnostic

Bibliography

- criteria, estimation of severity, and treatments." *Diabetes Care* 33(10): 2285-2293.
- Trojaborg, W. (1998). "Acute and chronic neuropathies: new aspects of Guillain-Barre syndrome and chronic inflammatory demyelinating polyneuropathy, an overview and an update." *Electroencephalogr Clin Neurophysiol* 107(5): 303-316.
- Üçeyler, N., K. A. Schafer, D. Mackenrodt, C. Sommer and W. Mullges (2016). "High-Resolution Ultrasonography of the Superficial Peroneal Motor and Sural Sensory Nerves May Be a Non-invasive Approach to the Diagnosis of Vasculitic Neuropathy." *Front Neurol* 7: 48.
- Van den Bergh, P. Y., R. D. Hadden, P. Bouche, D. R. Cornblath, A. Hahn, I. Illa, C. L. Koski, J. M. Leger, E. Nobile-Orazio, J. Pollard, C. Sommer, P. A. van Doorn and I. N. van Schaik (2010). "European Federation of Neurological Societies/Peripheral Nerve Society guideline on management of chronic inflammatory demyelinating polyradiculoneuropathy: report of a joint task force of the European Federation of Neurological Societies and the Peripheral Nerve Society - first revision." *Eur J Neurol* 17(3): 356-363.
- van Schaik, I. N., P. Bouche, I. Illa, J. M. Léger, P. Van den Bergh, D. R. Cornblath, E. M. Evers, R. D. Hadden, R. A. Hughes, C. L. Koski, E. Nobile-Orazio, J. Pollard, C. Sommer and P. A. van Doorn (2006). "European Federation of Neurological Societies/Peripheral Nerve Society guideline on management of multifocal motor neuropathy." *Eur J Neurol* 13(8): 802-808.
- Von Korff, M., P. Crane, M. Lane, D. L. Miglioretti, G. Simon, K. Saunders, P. Stang, N. Brandenburg and R. Kessler (2005). "Chronic spinal pain and physical-mental comorbidity in the United States: results from the national comorbidity survey replication." *Pain* 113(3): 331-339.
- Vrancken, A. F., N. C. Notermans, G. H. Jansen, J. H. Wokke and G. Said (2004). "Progressive idiopathic axonal neuropathy--a comparative clinical and histopathological study with vasculitic neuropathy." *J Neurol* 251(3): 269-278.
- Watson, J. C. and P. J. Dyck (2015). "Peripheral Neuropathy: A Practical Approach to Diagnosis and Symptom Management." *Mayo Clin Proc* 90(7): 940-951.
- Zaidman, C. M., M. Al-Lozi and A. Pestronk (2009). "Peripheral nerve size in normals and patients with polyneuropathy: an ultrasound study." *Muscle Nerve* 40(6): 960-966.
- Zaidman, C. M. and A. Pestronk (2014). "Nerve size in chronic inflammatory demyelinating neuropathy varies with disease activity and therapy response over time: a retrospective ultrasound study." *Muscle Nerve* 50(5): 733-738.

Appendix

I List of Abbreviation

ADS	"Allgemeine Depressions Skala"
ALS	Amyotrophic lateral sclerosis
AMSAN	Acute motor and sensory axonal neuropathy
ANA	Anti-nuclear antibodies
ANCA	Anti-neutrophil cytoplasmatic autoantibodies
AUC	Area under the curve
BMI	Body mass index
BRA_IS	Brachial plexus, inter-scalene muscles
BRA_SC	Brachial plexus; supra-clavicular
C5/6/7	Fifth/sixth/seventh cervical nerve
CB	conduction block
CES-D-Scale	Center for Epidemiologic Studies Depression Scale
CIAP	Chronic idiopathic axonal polyneuropathy
CIDP	Chronic inflammatory demyelinating polyneuropathy
CMT	Charcot-Marie-Tooth
CSA	Cross-sectional area
DEGUM	"Deutsche Gesellschaft für Ultraschall in der Medizin"
DICOM	Digital Imaging and Communications in Medicine
EFNS	European Federation of Neurological Societies
ENA	Extractable nuclear antigen
GCPS	Graded Chronic Pain Scale
Hb	Hemoglobin
HNPP	Hereditary neuropathy with liability to pressure palsies
HRUS	High-resolution nerve ultrasound
IBM	International Business Machines Corporation
Ig	Immunoglobulin
INCAT	Inflammatory Cause and Treatment
ISC_DT	Sciatic nerve, distal thigh
LD	Longitudinal diameter

I List of Abbreviation

MED_CF	Median nerve, cubital fossa
MED_MF	Median nerve, mid forearm
MED_MU	Median nerve, mid upper arm
MED_WR	Median nerve, wrist
mMRC	Modified Medical Research Council Score
mTCNS	Modified Toronto Clinical Neuropathy Score
MADSAM	Multifocal acquired demyelinating sensory and motor neuropathy
MHz	Mega Hertz
mm	Millimeter
MMN	Multifocal motor neuropathy
N	Basic population
n	Number of cases with one specific attribute
NCS	Nerve conduction studies
NPSI	Neuropathic Pain Symptom Inventory
NP	Neuropathy
NRS	Numeric rating scale
NSVN	Non-systemic vasculitic neuropathy
ODSS	Overall Disability Sum Score
p	Level of significance
PER_FH	Peroneal nerve, fibular head
PER_PP	Peroneal nerve, profound peroneal nerve;
PER_PS	Peroneal nerve, superficial peroneal nerve;
PIAN	Progressive idiopathic axonal neuropathy
PNS	Peripheral Nerve Society
RAD_SG	Radial nerve, spiral groove
ROC	Receiver operating characteristic
SD	Standard deviation
SPI_C5/6/7	Spinal nerve, fifth/sixth/seventh cervical nerve
SPSS	Statistical Package for the Social Sciences
SVN	Systemic vasculitic neuropathy
SUR_IG	Sural nerve, inter gastrocnemius muscle
TIB_MM	Tibial nerve, medial malleolus

I List of Abbreviation

TIB_PF	Tibial nerve, popliteal fossa
ULN_MF	Ulnar nerve, mid forearm
ULN_MU	Ulnar nerve, mid upper arm
ULN_US	Ulnar nerve, ulnar sulcus
ULN_WR	Ulnar nerve, wrist

II List of Figures

Figure 1: Median nerve at wrist of healthy control – cross-section and longitudinal section	4
Figure 2 : Median nerve of healthy control – cross-section and longitudinal section	17
Figure 3: Cross-sectional area (CSA) comparison of male and female control subjects.....	20
Figure 4: Longitudinal diameter (LD) comparison of male and female control subjects.....	21
Figure 5: Distribution of diagnoses and subgroups of polyneuropathy and amyotrophic lateral sclerosis (ALS).....	23
Figure 6: Receiver operating curve (ROC) patients with neuropathy vs. healthy controls – brachial plexus	25
Figure 7: Cross-sectional area (CSA) comparison of patients with neuropathy and control subjects	26
Figure 8: Longitudinal diameter (LD) comparison of patients with neuropathy and control subjects	27
Figure 9: Receiver operating characteristic (ROC) of cross-sectional area (CSA) measurement at brachial plexus.....	28
Figure 10: Cross-sectional area (CSA) comparison of patients with axonal and demyelinating neuropathies	29
Figure 11: Longitudinal diameter (LD) comparison of patients with axonal and demyelinating neuropathies	30
Figure 12: Receiver operating characteristic (ROC)of cross-sectional area (CSA) measurement at brachial plexus.....	31
Figure 13: Cross-sectional area (CSA) comparison of patients with and without inflammatory neuropathy	32
Figure 14: Longitudinal diameter (LD) comparison of patients with and without inflammatory neuropathy	33
Figure 15: ROC of patients with painful and painless neuropathies – brachial plexus.....	34

II List of Figures

Figure 16: Cross-sectional area (CSA) comparison of patients with and with painless neuropathy	35
Figure 17: Longitudinal diameter (LD) comparison of patients with and with painless neuropathy.....	36
Figure 18: Median Nerve of patient with non-systemic vasculitic neuropathy (NSVN) – cross-section and longitudinal section.....	37
Figure 19: Cross-sectional area (CSA) comparison of control subjects and patients with non-systemic vasculitic neuropathy (NSVN).....	38
Figure 20: Longitudinal diameter (LD) comparison of healthy control subjects and patients with non-systemic vasculitic neuropathy (NSVN)	39
Figure 21: Supraclavicular Brachial plexus; patient with non-systemic vasculitic neuropathy (NSVN)	40
Figure 22: ROC of patients with non-systemic-vasculitic neuropathy (NSVN) – brachial plexus.....	40
Figure 23: ROC of patients with non-systemic-vasculitic neuropathy (NSVN) – median and ulnar nerve	41
Figure 24: ROC of patients with non-systemic-vasculitic neuropathy (NSVN) – tibial nerve	42
Figure 25: Median nerve at cubital fossa of a patient with chronic inflammatory demyelinating polyneuropathy (CIDP) – cross-section and longitudinal section	43
Figure 26: Cross-sectional area (CSA) comparison of healthy control subjects and patients with chronic inflammatory demyelinating polyneuropathy (CIDP)	44
Figure 27: Longitudinal diameter (LD) comparison of healthy control subjects and chronic inflammatory neuropathy (CIDP)	45
Figure 28: ROC of patients with chronic inflammatory demyelinating polyneuropathy (CIDP)– brachial plexus.....	46
Figure 29: Supraclavicular Brachial plexus; patient with chronic inflammatory demyelinating polyneuropathy (CIDP) – cross-section	46

II List of Figures

Figure 30: ROC of patients with chronic inflammatory demyelinating polyneuropathy (CIDP) -median and ulnar nerve	47
Figure 31: ROC of patients with chronic inflammatory demyelinating polyneuropathy (CIDP) -tibial nerve	48
Figure 32: Supraclavicular Brachial plexus; patient with multifocal acquired demyelinating and sensory neuropathy (MDASAM)— cross-section	49
Figure 33: Cross-sectional area (CSA) comparison of healthy control subjects and multifocal acquired demyelinating sensory and motor neuropathy (MADSAM)	50
Figure 34: Longitudinal diameter (LD) comparison of healthy control subjects and patients with multifocal acquired demyelinating sensory and motor neuropathy (MADSAM)	51
Figure 35: Supraclavicular brachial plexus; patient with multifocal acquired demyelinating sensory and motor neuropathy (MADSAM)	52
Figure 36: ROC of patients with multifocal acquired demyelinating sensory and motor neuropathy (MADSAM) -tibial nerve.....	52
Figure 37: ROC of patients with multifocal acquired demyelinating sensory and motor neuropathy (MADSAM) -median and ulnar nerve.....	53
Figure 38: ROC of patients with multifocal acquired demyelinating sensory and motor neuropathy (MADSAM) – tibial nerve	54
Figure 39 Radial nerve of patient with multifocal motor neuropathy (MMN)	55
Figure 40: Radial nerve of second patient with multifocal motor neuropathy (MMN)	55
Figure 41: Cross-sectional area (CSA) comparison of healthy control subjects and multifocal motor neuropathy (MMN)	56
Figure 42: Longitudinal diameter (LD) comparison of healthy control subjects and patients with multifocal motor neuropathy (MMN)	57
Figure 43 Supraclavicular brachial plexus; patient with multifocal motor neuropathy (MMN)	58
Figure 44: ROC of patients with multifocal motor neuropathy (MMN) - brachial plexus.....	58

II List of Figures

Figure 45: ROC of patients with multifocal motor neuropathy (MMN) – median and ulnar nerve	59
Figure 46: ROC of patients with multifocal motor neuropathy (MMN) – tibial nerve	60
Figure 47: Peroneal nerve of patient with amyotrophic lateral sclerosis (ALS)	61
Figure 48: Cross-sectional area (CSA) comparison of healthy control subjects and amyotrophic lateral sclerosis (ALS)	62
Figure 49: Longitudinal diameter (LD) comparison of healthy control subjects and amyotrophic lateral sclerosis (ALS)	63
Figure 50: ROC of patients with amyotrophic lateral sclerosis (ALS)– brachial plexus.....	64
Figure 51: Supraclavicular brachial plexus; patient with amyotrophic lateral sclerosis (ALS)	64
Figure 52: ROC of patients with amyotrophic lateral sclerosis (ALS)– median and ulnar nerve	65
Figure 53: ROC of patients with amyotrophic lateral sclerosis (ALS)– tibial nerve	66
Figure 54: Cross-sectional area (CSA) comparison of patients with and without signs of inflammation in nerve biopsy	68
Figure 55: Longitudinal (LD) comparison of patients with and without signs of inflammation in nerve biopsy.....	69
Figure 56: Cross-sectional area (CSA) comparison of patients with signs of demyelination in nerve biopsy	70
Figure 57: Longitudinal diameter (LD) comparison of patients with signs of demyelination in nerve biopsy	71
Figure 58: Cross-sectional area (CSA) comparison of patients with edema in nerve biopsy	72
Figure 59: Longitudinal diameter (LD) comparison of patients with edema in nerve biopsy	73

III List of Tables

III List of Tables	
Table 1: Correlation of cross-sectional area (CSA) and longitudinal diameter (LD) with height, weight, and body-mass-index (BMI)	19
Table 2: Normative values for cross-sectional area (CSA) and longitudinal diameter (LD) of upper and lower extremities	22
Table 3: A) Results of neuropathy scores B) Results of questionnaires stratified for axonal and demyelinating neuropathies.	24
Table 4: High-resolution nerve ultrasound (HRUS) measurement at sites of conduction block (CB).....	74

IV Danksagung

IV Danksagung

Mein besonderer Dank gilt folgenden Personen:

- Frau Univ. Prof. Dr. Nurcan Üçeyler für die Möglichkeit zur Promotion in ihrer Arbeitsgruppe, die Vergabe des Dissertationsthemas, die kontinuierliche und gewissenhafte Ausbildung, das Mentoring, die Supervision und Korrektur dieser Dissertation.
- Frau Univ.-Prof. Dr. Claudia Sommer für die gewissenhafte und vertrauensvolle Unterstützung in allen Phasen des Promotionsprozesses.
- Herrn Univ. Prof. Dr. Frank Puppe und Herrn Christian Reul (Lehrstuhl für Informatik IV der Universität Würzburg) für die gute Zusammenarbeit bei der Erstellung einer Software zum Bildtransfer im Rahmen dieser Studie.
- Meiner Kollegin Frau Anna Hirschmann für die gute Zusammenarbeit bei der Rekrutierung der Patienten dieser Studie.
- Allen Mitgliedern der Arbeitsgruppen Sommer und Üçeyler für die Unterstützung und Lösungsfindung zu allen denkbaren Fragen im Rahmen eines sehr guten Arbeitsumfeldes.
- Meiner Familie und meinen Freunden für die Unterstützung und Begleitung während des Promotionsprozesses.

V Curriculum vitae

V Curriculum vitae

Philipp Andreas Köberle

Address: Universitätsklinikum Würzburg, Neurologische Klinik und Poliklinik
Josef-Schneider-Str.11, 97080 Würzburg

birth: March 6th, 1990 in Crailsheim

denomination: Roman Catholic

marital status: unmarried

Academic education

1997-2001 Eichendorffschule Crailsheim (elementary school)

2001-2010 Albert-Schweizer-Gymnasium Crailsheim (secondary school)

Civilian Service

2010 – 2011 German Red Cross; Crailsheim – emergency medical service

Academic studies

2011 – 2017 Julius-Maximilians-Universität; Würzburg – human medicine

2013 First section of medical examination

2014 Sapienza Università di Roma – study detention

2014 to date Scientific work about “High-resolution ultrasound for the identification of pathological patterns in patients with polyneuropathies and amyotrophic lateral sclerosis”
- Scientific working group Prof. Üçeyler

2016 Second section of medical examination

2016 – 2017 Medical practical year - Universitätsklinikum Würzburg

2017 Third section of medical examination

2018 Approbation as physician

Work activities

2014 – 2015 University of Würzburg - computer science

2014 – 2016 University of Würzburg - anaesthesiology; emergency medicine

2018 to date Resident physician - Universitätsklinikum Würzburg

Languages English – fluently; Spanish and Italian – elementary knowledge

Würzburg, December 30th, 2020

signed, Philipp Andreas Köberle

V Lebenslauf

V Lebenslauf

Philipp Andreas Köberle

Anschrift: Universitätsklinikum Würzburg, Neurologische Klinik und Poliklinik
Josef-Schneider-Str.11, 97080 Würzburg

geboren: 06.03.1990 in Crailsheim

Konfession: römisch-katholisch

Familienstand: ledig

Schulische Ausbildung

1997-2001 Eichendorffschule Crailsheim (Grundschule)

2001-2010 Albert-Schweizer-Gymnasium Crailsheim

Zivildienst

2010 – 2011 Deutsches Rotes Kreuz Crailsheim – Rettungsdienst

Studium

2011 – 2017 Julius-Maximilians-Universität Würzburg; Humanmedizin

2013 Erster Abschnitt der Ärztlichen Prüfung

2014 Sapienza Università di Roma – Studienaufenthalt

2014 – heute Wissenschaftliche Arbeit zu „Hochauflösender Ultraschall zur Identifizierung von pathologischen Mustern bei Patienten mit Polyneuropathien und amyotropher Lateralsklerose“
- wissenschaftlich Arbeitsgruppe Prof. Üçeyler

2016 Zweiter Abschnitt der Ärztlichen Prüfung

2016 – 2017 medizinisch-praktisches Jahr am Universitätsklinikum Würzburg

2017 Dritter Abschnitt der Ärztlichen Prüfung

2018 Approbation zum Arzt

Tätigkeiten

2014 – 2015 Universität Würzburg – Informatik

2014 – 2016 Universität Würzburg – Anästhesiologie; Notfallmedizin

2018 – heute Assistenzarzt Neurologische Universitätsklinik Würzburg

Sprachen Englisch – fließend; Spanisch und Italienisch – Grundkenntnisse

Würzburg, 30.12.2020

gez. Philipp Andreas Köberle

VI Publication & Congress participation

Publication

Reul, C., P. Koberle, N. Uceyler and F. Puppe (2016). "Expectation-Driven Text Extraction from Medical Ultrasound Images." Stud Health Technol Inform 228: 712-716.

Congress participation

Koeberle, P., A. Hirschmann, C. Reul, F. Puppe, C. Sommer, and N. Üçeyler (2018). "Hochauflösender Nervenultraschall bei Patienten mit histologisch gesicherter nicht-systemischer vaskulitischer Neuropathie". DGN (Deutsche Gesellschaft für Neurologie) Congress, Berlin. Poster presentation.